Article

Cell Reports

The IL-17F/IL-17RC Axis Promotes Respiratory Allergy in the Proximal Airways

Graphical Abstract

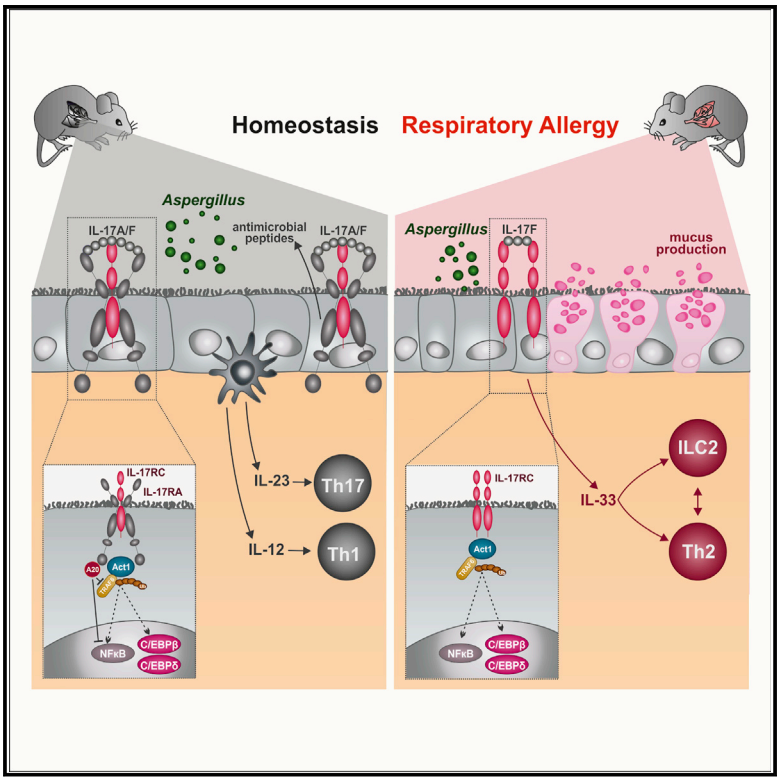

Highlights

- The IL-17F/IL-17RC axis is functional under conditions of IL-17RA deficiency
- Dysregulated signaling via IL-17RC exacerbates *Aspergillus* airway inflammation
- IL-17RC may be useful as a therapeutic target for treating respiratory allergy

Authors

Antonella De Luca, Marilena Pariano, Barbara Cellini, ..., Luigi Maiuri, Jan Fric, Teresa Zelante

Correspondence

teresa.zelante@unipg.it

In Brief

De Luca et al. reveal the complexity of IL-17 signaling in *Aspergillus* lung infection and fungal allergy. The authors describe a pathogenic loop under conditions of IL-17RA disruption and pave the way for therapeutic strategies selectively targeting the IL-17F/IL-17RC axis.

De Luca et al., 2017, Cell Reports *20*, 1667–1680
August 15, 2017 © 2017 The Author(s).
http://dx.doi.org/10.1016/j.celrep.2017.07.063

Cell Reports
Article

OPEN ACCESS
CellPress

The IL-17F/IL-17RC Axis Promotes Respiratory Allergy in the Proximal Airways

Antonella De Luca,[1] Marilena Pariano,[1] Barbara Cellini,[1] Claudio Costantini,[1] Valeria Rachela Villella,[2] Shyam Sushama Jose,[3] Melissa Palmieri,[1] Monica Borghi,[1] Claudia Galosi,[1] Giuseppe Paolicelli,[1] Luigi Maiuri,[2,4] Jan Fric,[3] and Teresa Zelante[1,5,*]
[1]Department of Experimental Medicine, University of Perugia, 06132 Perugia, Italy
[2]European Institute for Research in Cystic Fibrosis, San Raffaele Scientific Institute, Milan, Italy
[3]Center for Translational Medicine, International Clinical Research Center, St. Anne's University Hospital Brno, Czech Republic
[4]Department of Health Sciences, University of Eastern Piedmont, Novara, Italy
[5]Lead Contact
*Correspondence: teresa.zelante@unipg.it
http://dx.doi.org/10.1016/j.celrep.2017.07.063

SUMMARY

The interleukin 17 (IL-17) cytokine and receptor family is central to antimicrobial resistance and inflammation in the lung. Mice lacking IL-17A, IL-17F, or the IL-17RA subunit were compared with wild-type mice for susceptibility to airway inflammation in models of infection and allergy. Signaling through IL-17RA was required for efficient microbial clearance and prevention of allergy; in the absence of IL-17RA, signaling through IL-17RC on epithelial cells, predominantly by IL-17F, significantly exacerbated lower airway *Aspergillus* or *Pseudomonas* infection and allergic airway inflammation. In contrast, following infection with the upper respiratory pathogen *Staphylococcus aureus*, the IL-17F/IL-17RC axis mediated protection. Thus, IL-17A and IL-17F exert distinct biological effects during pulmonary infection; the IL-17F/IL-17RC signaling axis has the potential to significantly worsen pathogen-associated inflammation of the lower respiratory tract in particular, and should be investigated further as a therapeutic target for treating pathological inflammation in the lung.

INTRODUCTION

The interleukin 17 (IL-17) cytokine family is a critical component of inflammatory responses, acting on diverse cell types to induce production of pro-inflammatory cytokines, chemokines, and prostaglandins (Patel and Kuchroo, 2015). On the basis of sequence homology, a total of six IL-17 members have been described: IL-17A, IL-17B, IL-17C, IL-17D, IL-17E (also known as IL-25), and IL-17F. Of the six, IL-17A and IL-17F are best studied and most closely related. In both humans and mice, IL-17A and IL-17F can form homodimers or heterodimers (IL-17A/F) capable of ligating IL-17R subunits (Wright et al., 2007; Chang and Dong, 2007).

Signaling through IL-17R by IL-17 family members is regulated at multiple levels. The IL-17R exists as a heteromer of IL-17RA-E subunits (Moseley et al., 2003), which possess distinct biological properties and differential affinities for IL-17-family cytokines: in humans, IL-17RA binds to IL-17A with a high affinity, while IL-17RC has a high affinity for IL-17F but can also bind IL-17A (Patel and Kuchroo, 2015); in mice, IL-17RA binds both IL-17A and IL-17F, while IL-17RC binds only IL-17F (Toy et al., 2006; Krstic et al., 2015; Kuestner et al., 2007); despite having only 22% sequence homology (Haudenschild et al., 2002), the IL-17RA and IL-17RC subunits share a common ability to mediate IL-17 signaling, but disentangling the effects of signaling through each subunit has proved challenging. There is some evidence from in vitro studies that murine IL-17RA requires IL-17RC to realize its signaling potential (Toy et al., 2006), though the extent to which this is true in vivo and whether IL-17RC has a reciprocal requirement for IL-17RA remains unclear. Recent data have also uncovered a role for the intracellular ubiquitin-specific protease USP25 in negative regulation of IL-17A-mediated signaling and inflammation (Zhong et al., 2012; Ma, 2012), while earlier work found that ubiquitination of the IL-17R was triggered by IL-17F only (Rong et al., 2007). In addition, though inflammatory downstream IL-17RA signaling has been described (Conti et al., 2009), few studies have examined the potential role of IL-17RC. Thus, what is clear is that the activation of IL-17R subunits is tightly regulated; what remains unclear is how this regulation translates into significant biological effects in vivo.

The downstream effects of interactions between IL-17 and IL-17R family members are especially important for immune responses at the body's mucosal barriers: regulation of IL-17 responses is central to resolution of *Candida albicans* infection in the gut (Zelante et al., 2007; Conti and Gaffen, 2015), as well as in combating pulmonary and nasal infections (Archer et al., 2016; Rathore and Wang, 2016). However, dysregulation of the IL-17/IL-17R axis contributes to pathogenic inflammatory reactions against commensals or environmental fungi (Zelante et al., 2007), as well as to auto-immune and auto-inflammatory conditions, including asthma, psoriasis, and obesity (Endo et al., 2016; Cosmi et al., 2016; Sakkas and Bogdanos, 2016; Patel and Kuchroo, 2015), and perhaps also to cystic fibrosis (Alivand et al., 2016; McAllister et al., 2005). Of particular interest and pressing concern is the role of IL-17-mediated responses at the intersection of respiratory disease and fungal infection, such as in allergic broncho-pulmonary aspergillosis (ABPA).

This is an open access article under the CC BY-NC-ND license (http://creativecommons.org/licenses/by-nc-nd/4.0/).

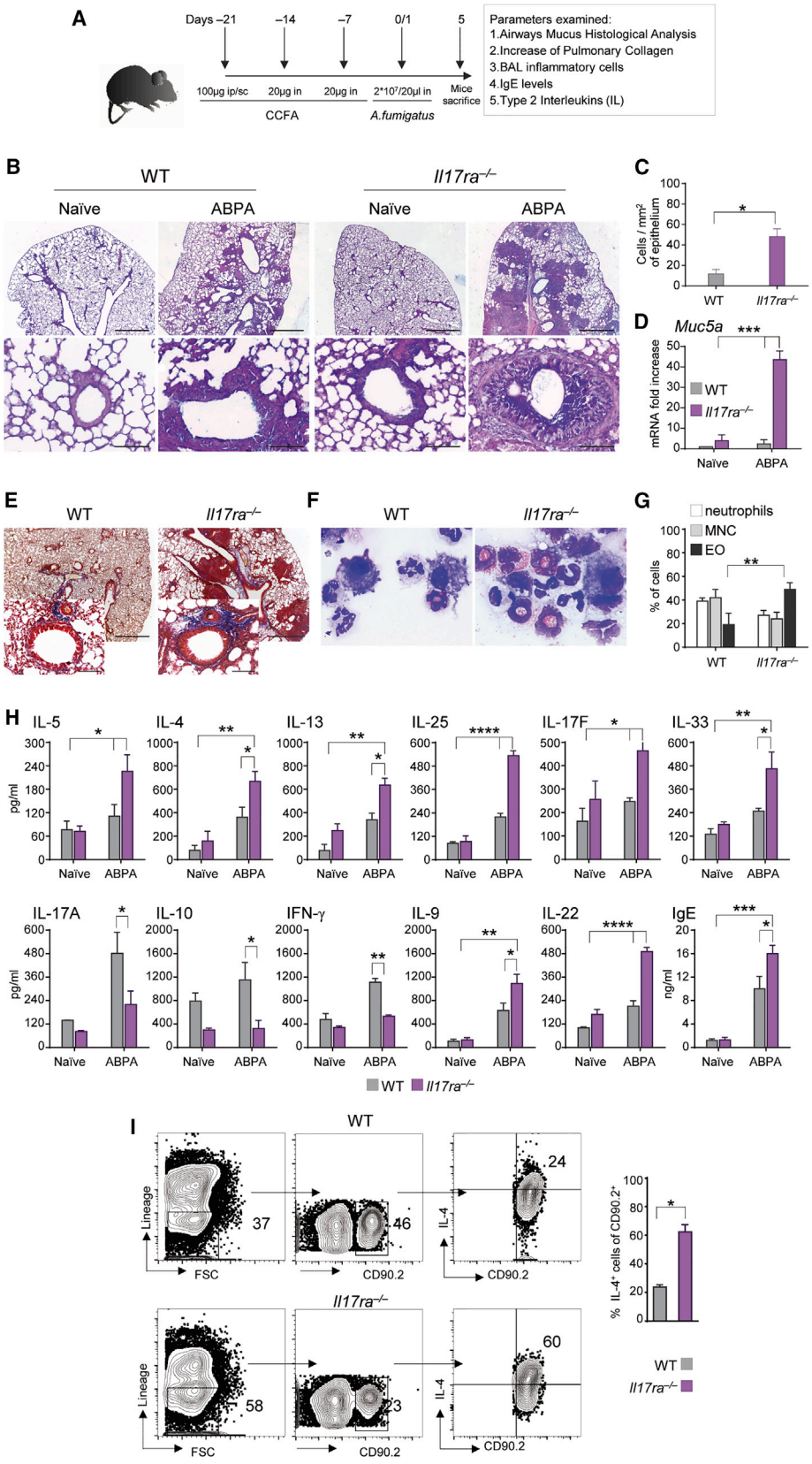

(legend on next page)

ABPA affects approximately 5 million people worldwide, causing serious recurrent respiratory impairment in immune-compromised individuals and significant exacerbations in asthma and cystic fibrosis patients (Burgel et al., 2016).

Asthma is a complex and heterogeneous disease of allergy and inflammation affecting lung functions, and there is compelling evidence for a role of the IL-17/IL-17R axis in the pathology of specific subtypes of the condition. The presence of IL-17 in asthmatic airways is significantly related to asthma severity; engineered overexpression of IL-17F results in increased inflammatory cytokine and chemokine expression and exacerbated antigen-induced goblet cell hyperplasia and pulmonary inflammation in the airways of mice (Oda et al., 2005), both hallmarks of asthma. There is also evidence that asthmatic patients express higher levels of IL-17F cytokine in the epithelial compartment compared with healthy subjects (Ota et al., 2014). A sub-group of patients with severe steroid-dependent or steroid-resistant asthma exhibit marked neutrophil recruitment and T helper 17 (Th17)-chemokine overexpression in bronchial biopsies (Fahy, 2009) and bronchoalveolar lavage (BAL) fluid (Chesné et al., 2014), sometimes with evidence of concurrent Th2 involvement (Cosmi et al., 2016). Where high levels of IL-17F, in particular, are present in the bronchial and nasal lamina propria, there is a strong association with poor lung function (Sorbello et al., 2015), but the underlying mechanisms driving IL-17-mediated exacerbation of airway inflammation remain unclear, and what, if any, role is played by IL-17 in concurrent fungal infection of these patients is unknown.

In the present study, we used genetically modified mice and models of pulmonary infection and allergy to unravel the contribution of the IL-17A/IL-17F/IL-17R pathways to microbial resistance and allergy in the lung. We found that signaling through IL-17RA was required for efficient microbial clearance and prevention of microbe-induced allergy; however, in mice lacking IL-17RA, the interaction of IL-17F with IL-17RC on epithelial cells in the upper airways contributed to inflammatory allergy, despite providing protection against local colonizers. These data shed light on the distinct roles of IL-17A and IL-17F cytokines during infection and inflammation of the lung in vivo and identify differential IL-17R subunit expression patterns within and across mucosal tissues as a potentially significant mediator of protection and pathology. Moreover, we reveal that the IL-17F/IL-17RC axis warrants further investigation as a therapeutic target for treatment of allergic inflammation of the airways.

RESULTS

Mice Lacking IL-17RA Are More Susceptible to *A. fumigatus* Infection and Allergic Inflammation

To elucidate the contribution of IL-17A or IL-17F in *Aspergillus*-induced allergic airway inflammation, we subjected wild-type (WT) and *Il17ra*$^{-/-}$ mice to experimentally induced ABPA (Figure 1A). Mice were first sensitized by injecting an adjuvanted, non-infectious mixture of *A. fumigatus* proteins and glycoproteins (crude culture filtrate antigen [CCFA]), which leads to an allergic reaction to subsequent infection with live *A. fumigatus* (Figure 1A). Alcian blue staining of lung sections indicated significant mucous cell hyperplasia in *Il17ra*$^{-/-}$ ABPA mice (Figures 1B and 1C), alongside significantly higher transcript abundance of *Muc5a* mRNA, which is associated with mucus over-production during inflammation, in *Il17ra*$^{-/-}$ ABPA mice compared with WT mice with ABPA (Figure 1D). Relative to WT mice, *Il17ra*$^{-/-}$ mice exhibited massive peri-bronchial collagen deposition (Figure 1E), significantly more BAL eosinophils (Figures 1F and 1G), and significantly higher levels of IgE protein in lung homogenates following ABPA induction (Figure 1H). Expression of type 2 cytokines (IL-5, IL-4, IL-13, IL-25, IL-33, and IL-9) and type 17 cytokines (IL-17F and IL-22) was markedly elevated in *Il17ra*$^{-/-}$ mice with ABPA compared with their naive counterparts and with WT mice as measured by ELISA (Figure 1H). Type 1 cytokine IFN-γ was downregulated in *Il17ra*$^{-/-}$ mice with ABPA as well as IL-10 (Figure 1H). Because both innate lymphoid cells type 2 (ILC2) and Th cells can expand in response to IL-33 during fungus-induced inflammation of the airways (Piehler et al., 2016), we measured the relative abundance of both these cell populations within total lung cells (Figures 1I and S1A). Lungs of *Il17ra*$^{-/-}$ mice contained higher frequencies of IL-4^{+}ILC2 (Figure 1I), IL-4^{+}CD3^{+}CD69^{+}, and IL-4^{+}CD3^{+}CD69^{-} (Figure S1A) cells during ABPA than did those of WT mice. The expansion of Th2 cells and ILC2 in the lung was further confirmed by the significantly higher abundance of *Gata3* mRNA in thoracic lymph nodes (TLNs) from *Il17ra*$^{-/-}$ mice with ABPA than in WT animals (Figure S1B). These data are consistent with published work showing that preferential expansion of IL-4^{+}ILC2 in the early phases of inflammatory responses is required to support later Th2 differentiation that is typical of asthma (Pelly et al., 2016). As expected, mRNA expression of the Th1 cytokine IFN-γ and transcription factor *Tbet* was significantly lower in *Il17ra*$^{-/-}$ mice with ABPA compared with WT; similarly, the regulatory

Figure 1. IL-17RA Deficiency Results in Higher Susceptibility to ABPA

(A) Schematic representation of ABPA model. ABPA was induced by repeated injection of mice with *A. fumigatus* culture filtrate extract dissolved in Freund's incomplete adjuvant followed by intranasal infection with resting conidia 1 week after the last injection.

(B) WT and *Il17ra*$^{-/-}$ asthmatic mice assessed for lung histology (Alcian blue staining; the scale bar represents 1 mm or 100 μm).

(C) Individual counts of lung goblet cells.

(D) Expression of *Muc5a* gene (RT-PCR) in the lung.

(E) Lung histology (Masson trichrome staining; the scale bar represents 1 mm or 100 μm in inset).

(F and G) BAL morphometry (original magnification, 100×) (F) and the differential cell count of mononuclear cells (MNC), neutrophils, and eosinophils (EO) (G) was determined on May-Grunwald Giemsa staining.

(H) IgE levels and cytokine production (ELISA) in lung homogenates.

(I) Intracellular IL-4 cytokine production was examined using flow cytometry. Flow gates indicate the percentage of CD90.2 cells producing IL-4. Pre-gate was done on total lung leukocytes; lineage marker includes anti-CD5, CD11b, CD45R, anti-7-4, anti-GR1, and anti-TER-119.

Assays were done at 5 days post-infection (dpi). Data pooled from three independent experiments (n = 6 mice per group); mean ± SD. *$p < 0.05$, **$p < 0.01$, ***$p < 0.001$, and ****$p < 0.0001$. Two-way ANOVA, Bonferroni post hoc test. Two-tailed Student's t test, nonparametric Mann-Whitney U test.

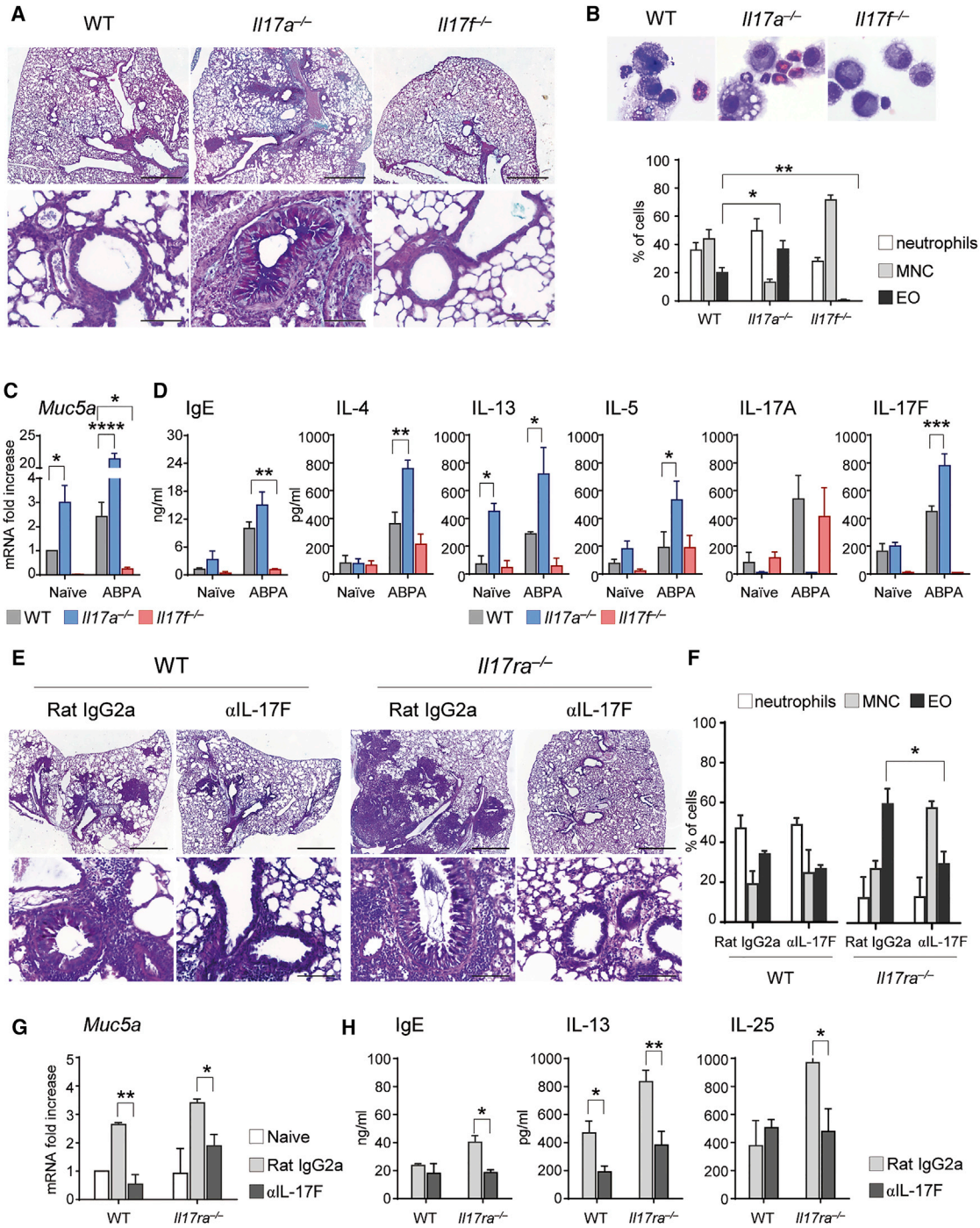

Figure 2. In ABPA, IL-17F Contributes to the Development of Allergy in IL-17RA Deficiency

(A) WT, *Il17a*$^{-/-}$, and *Il17f*$^{-/-}$ mice were sensitized and challenged with *A. fumigatus* conidia and assessed for histological analysis of Alcian blue-stained lung section (the scale bar represents 1 mm or 100 μm).

(B) BAL morphometry and differential cell count of MNC, neutrophils, and EO was determined by May-Grunwald Giemsa staining (original magnification, 100×).

(C) Expression of *Muc5a* gene (RT-PCR) in the lung.

(D) IgE levels and cytokine production (ELISA) in lung homogenates.

(E) Lung histology (Alcian blue staining; the scale bar represents 1 mm or 100 μm) of WT and *Il17ra*$^{-/-}$ asthmatic mice treated with isotype control monoclonal antibody (mAb) or IL-17F neutralizing mAb.

(F) BAL morphometry expressed as a cell percentage of mice treated as in (E).

(legend continued on next page)

cytokine IL-10 and transcription factor *Foxp3* were less abundant in *Il17ra*$^{-/-}$ mice, as was IL-17A (Figures 1H and S1B). However, despite the lack of IL-17RA, expression of genes previously identified as activated by IL-17R signaling (Conti et al., 2009) was upregulated in lung homogenates following ABPA induction (Figure S1C), although *Rorc* was not differentially expressed in *Il17ra*$^{-/-}$ mice (Figure S1B).

In summary, these data show that mice lacking the IL-17RA subunit exhibit exacerbated inflammatory responses in the lung following allergic sensitization and exposure to *A. fumigatus*; this response is characterized by excessive mucus production, aberrant collagen deposition, and the production of Th2-associated cytokines. Intriguingly, the absence of IL-17RA was associated with increased expression of IL-17R-downstream genes in ABPA. Therefore, IL-17RA is required for restraining allergic reactivity upon exposure to *A. fumigatus*, but in the absence of IL-17RA and in the context of the resultant exacerbated allergic reactivity, there is evidence of retained IL-17R signaling in these mice.

We then asked whether IL-17RA played a similar role during fungal infection of the lung as in ABPA. We previously showed that high and/or deregulated levels of IL-17A are detrimental during fungal infection (Romani et al., 2008); here we asked specifically whether mice lacking IL-17RA exhibited differential susceptibility to *Aspergillus* infection compared with WT mice. We intranasally infected *Il17ra*$^{-/-}$ mice with live *A. fumigatus* conidia and evaluated parameters of infection, inflammation and Th immunity (Figure S2A). Lungs from *Il17ra*$^{-/-}$ mice had significantly higher fungal burdens compared with WT (Figure S2B), which was associated with diffuse lung inflammation and goblet cell hyperplasia (Figure S2C), significantly higher neutrophil frequencies in BAL fluid cytospins (Figure S2D), increased mRNA expression of *Cxcl1* and *Cxcl2* in lung cells (Figure S2E), and increased MPO production from lung homogenates (Figure S2F), relative to *A. fumigatus*-infected WT mice. Protein levels of the pro-inflammatory cytokines TNF-α and IL-1β (Figure S2G), as well as IL-17F, IL-22, and IL-25, but not IL-17A (Figure S2H), were significantly more elevated in lung homogenates of *Il17ra*$^{-/-}$ mice than WT in response to *A. fumigatus* infection. In addition, type 2 cytokine and IL-9 production and *Gata3* transcription, but not *Tbet* and *Foxp3* transcription were also significantly more elevated in the lungs and TLNs, respectively, of infected IL-17RA-deficient mice (Figures S2I and S2J); taken together with the increased goblet cell mucus production (Figure S2C, inset), these findings suggesting the development of type 2 inflammation, typically characterized by Th2 adaptive response, in the airways of *Il17ra*$^{-/-}$ mice infected with *A. fumigatus*.

Considering the *A. fumigatus* infection and allergic inflammation models together, IL-17RA clearly contributes to protective antifungal responses while restraining the development of allergic lung reactivity. Mice lacking IL-17RA were also predisposed toward the production of higher levels of IL-17F and IL-25 during both ABPA (Figure 1H) and aspergillosis (Figure S2H); we therefore went on to ask what roles were played by these IL-17R-binding cytokines in experimental murine *Aspergillus* diseases.

IL-17F Contributes to Susceptibility to Infection and Allergy

Because both IL-17A and IL-17F are capable of binding to IL-17RA (Krstic et al., 2015), we used *Il17a*$^{-/-}$ and *Il17f*$^{-/-}$ mice to determine the relative contribution of each cytokine to protective IL-17RA signaling in ABPA and aspergillosis. Mice lacking IL-17A were more susceptible to ABPA, while mice lacking IL-17F were more resistant, compared with WT mice. Lung sections from *Il17a*$^{-/-}$ mice exhibited greater mucin production by goblet cells than either WT or *Il17f*$^{-/-}$ mice (Figure 2A); BAL cytospins revealed significantly higher frequencies of eosinophils in *Il17a*$^{-/-}$ mice (Figure 2B), accompanied by significantly higher spontaneous and ABPA-induced *Muc5a* mRNA expression (Figure 2C), and significantly greater production of type 2- and type 17-associated cytokines (Figure 2D) than in WT animals. In aspergillosis, we found exacerbated lung inflammatory pathology in *Il17a*$^{-/-}$ mice, compared with WT or *Il17f*$^{-/-}$ mice (Figure S3A). Accordingly, significantly greater fungal burdens were present in the lungs of *Il17a*$^{-/-}$ than in WT mice (Figure S3B), consistent with the observed attenuation in Th1-associated cytokine (IFNγ and IL-12p70) production (Figure S3C).

These results seemed to suggest that IL-17A is restraining both resistance to *Aspergillus* infection and *Aspergillus*-induced allergic responses. However, the engineered absence of IL-17A also induced significant upregulation of IL-17F expression during ABPA, while the levels of IL-17A were comparable in *Il17f*$^{-/-}$ and WT mice (Figure 2D). The same pattern was evident in aspergillosis (Figure S3D). These findings posed the question: was it the absence of IL-17A per se in *Il17a*$^{-/-}$ mice, or rather the increased levels of IL-17F, that was responsible for their increased susceptibility to *Aspergillus* diseases? We thus treated WT and *Il17ra*$^{-/-}$ mice bearing ABPA or WT and *Il17a*$^{-/-}$ bearing *Aspergillus* infection with IL-17F-neutralizing or isotype-matched control antibodies; neutralization of IL-17F induced significant reductions across all signs of mouse respiratory allergy (Figures 2E–2H), lung inflammation, and fungal colonization (Figures S3E and S3F) in infection, indicative of a pathogenic role for IL-17F in these models of *Aspergillus* allergy and infection. However, despite the high susceptibility of *Il17a*$^{-/-}$ mice to *A. fumigatus*, IL-17A administration greatly increased, while its ablation decreased, the susceptibility of WT mice to the infection (Figures S3G and S3H); conversely, the administration of IL-17F greatly exacerbated pathogenesis in WT and *Il17f*$^{-/-}$ mice bearing ABPA (Figures 3A–3D).

Taken together these findings confirm both that deregulated IL-17A production can contribute to pathology during infection (Romani et al., 2008) and that, consistent with the association of the *Il17f* gene with asthma and chronic obstructive pulmonary

(G) Expression of *Muc5a* gene (RT-PCR) in the lung.

(H) IgE levels and cytokines production (ELISA) in lung homogenates.

Assays were done at 5 dpi. Data pooled from three independent experiments (A–D, n = 6 mice per group; E–H, n = 3 mice per group); mean ± SD. *$p < 0.05$, **$p < 0.01$, ***$p < 0.001$, and ****$p < 0.0001$. Two-way ANOVA, Bonferroni post hoc test.

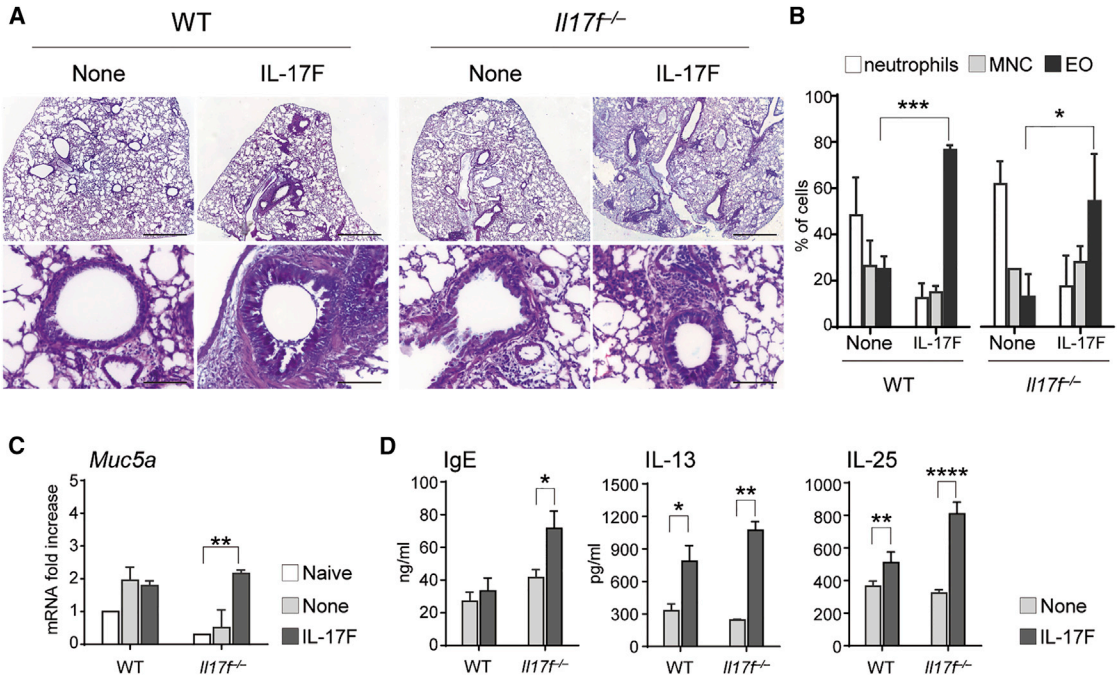

Figure 3. IL-17F Administration Exacerbates Respiratory Allergy in a Mouse Model of ABPA

(A) WT and *Il17f*$^{-/-}$ asthmatic mice were treated with murine recombinant IL-17F and assessed for histological analysis of Alcian blue-stained lung section (the scale bar represents 1 mm or 100 μm).

(B) BAL differential cell count of MNC, neutrophils, and EO.

(C) Expression of *Muc5a* gene (RT-PCR) in the lung.

(D) IgE levels and cytokines production (ELISA) in lung.

Assays were done at 5 dpi. Data pooled from three independent experiments (n = 3 mice per group); mean ± SD. *$p < 0.05$, **$p < 0.01$, ***$p < 0.001$, and ****$p < 0.0001$. Two-way ANOVA, Bonferroni post hoc test.

disease in humans (Hizawa et al., 2006), IL-17F plays a major role in driving pathological inflammation and allergy in response to *Aspergillus* in the murine lung.

IL-17F Provides Antibacterial Resistance in the Upper Airways against *S. aureus*

IL-17R signaling is also critical for pulmonary neutrophil recruitment and host defense against bacteria (Tsai et al., 2013; Gu et al., 2013); therefore to understand the broader context of our findings on the roles of the IL-17/IL-17R axis in pulmonary infections we extended our investigation to include exposure to two common bacterial pathogens. We first exposed murine lung epithelial cells from *Il17ra*$^{-/-}$ and WT mice to the upper respiratory tract colonizer *S. aureus* or the lower respiratory tract colonizers *P. aeruginosa* or *A. fumigatus* in vitro (Figure 4A). Comparative gene expression analysis revealed that the pathogens induced different levels of *Il17a* and *Il17f* transcription in both WT and *Il17ra*$^{-/-}$ epithelial cells; of particular interest, in the absence of IL-17RA, significantly higher levels of IL-17A are induced by *A. fumigatus* and *P. aeruginosa* than by *S. aureus* (Figure 4A). In contrast, significantly higher levels of IL-17F are induced by pathogens of the upper airway in *Il17ra*$^{-/-}$ lung epithelial cells. We then intranasally infected WT, *Il17f*$^{-/-}$, and *Il17ra*$^{-/-}$ mice with *S. aureus* (Figures 4B–4E) or *P. aeruginosa* (Figures 4F–4I) and measured infectious and inflammatory outcomes. These data showed that *Il17ra*$^{-/-}$ mice were as resistant as WT mice to *S. aureus* infection, as shown by lung colonization and histopathology, while in contrast, susceptibility to *S. aureus* infection was significantly higher in *Il17f*$^{-/-}$ mice (Figures 4C–4E) (lung colonization mean ± SD [log colony-forming units (CFU)]: 2.7 ± 0.24 in WT mice and 3.3 ± 0.32 in *Il17f*$^{-/-}$ mice); thus, it seems that despite its exacerbatory role in *Aspergillus* diseases, IL-17F confers antimicrobial resistance to this upper airway pathogen. This is also explained by the increased expression of IL-17F in WT epithelial cells as physiological immune protective response against *S. aureus* (Figure 4A). Conversely, and similar to our observations with *A. fumigatus* infection, *Il17ra*$^{-/-}$ mice were more susceptible to *P. aeruginosa* intranasal infection than were WT animals, exhibiting significantly higher bacterial loads in the lung (Figure 4G), significantly higher frequencies of polymorphonuclear neutrophils in BAL fluid (Figures 4H and 4I), and marked histological signs of interstitial allergic inflammation (Figure 4I). *Il17f*$^{-/-}$ mice were as resistant as WT to *P. aeruginosa* colonization (Figure 4G), neutrophil recruitment (Figures 4H and 4I), and inflammation (Figure 4I). Thus, those pathogens (*A. fumigatus* and *P. aeruginosa*) that naturally induce lower levels of *Il17f* transcription seem to become more virulent in conditions in which IL-17F release is extremely high, as seen in *Il17ra*$^{-/-}$ mice during allergic or inflammatory responses, and less virulent when IL-17F is

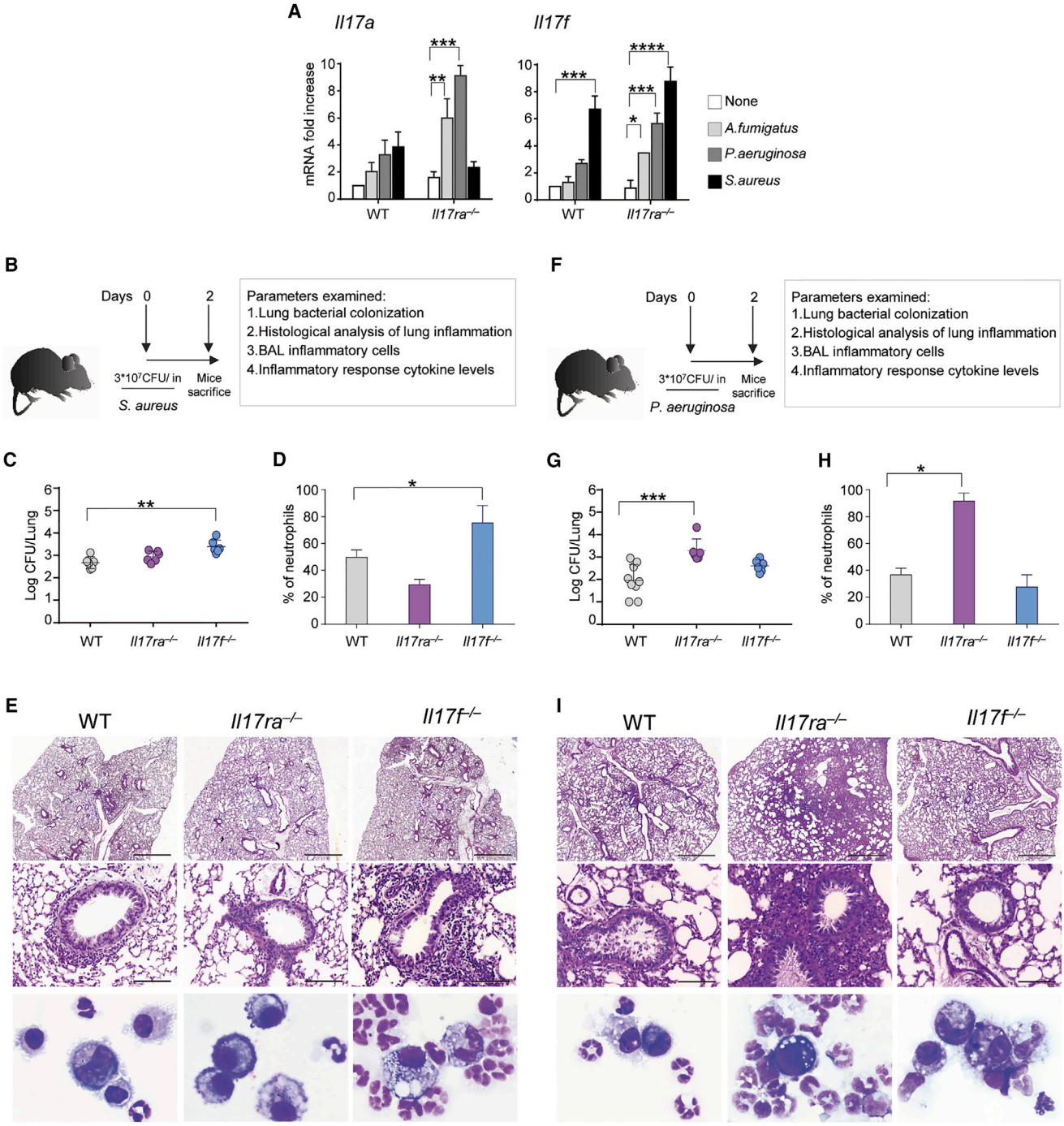

Figure 4. The IL-17F/IL17RC Pathway Provides Antibacterial Resistance in the Upper Airways

(A) Expression of *Il17a* and *Il17f* gene (RT-PCR) in WT and *Il17ra*$^{-/-}$ murine lung epithelial cells naive stimulated with live *A. fumigatus* conidia (1:1, cells/fungi), *P. aeruginosa*, or *S. aureus* (1:100, cells/bacteria) for 8 hr at 37°C.

(B) Schematic representation of *S. aureus* infection model.

(C) WT, *Il17ra*$^{-/-}$, and *Il17f*$^{-/-}$ mice were infected intranasally with live *S. aureus* and assessed for bacterial growth (log CFU).

(D) BAL morphometry, expressed as a percentage of neutrophils.

(E) Lung histology (PAS; the scale bar represents 1 mm or 100 μm) and BAL May-Grunwald Giemsa staining (original magnification, 100×).

(F) Schematic representation of *P. aeruginosa* infection model.

(G) WT, *Il17ra*$^{-/-}$, and *Il17f*$^{-/-}$ mice were infected intranasally with live *P. aeruginosa* and assessed for bacterial growth (log CFU).

(legend continued on next page)

absent, as in *Il17f*$^{-/-}$ mice. In contrast, *S. aureus*, which induces abundant *Il17f* transcription in IL-17F-competent lung epithelial cells in vitro, is rendered more virulent in the absence of IL-17F in vivo.

The IL-17F/IL-17RC Pathway in Lung Epithelial Cells Mediates Respiratory Allergy to *A. fumigatus*

The biological effects of IL-17F observed in *Il17ra*$^{-/-}$ mice led us to ask which signaling pathway was being engaged by IL-17F. Published studies show that IL-17RA only forms homodimers in the unliganded state (Kramer et al., 2006) and that both IL-17RA and IL-17RC are involved in ligand-bound IL-17R complexes (Ho et al., 2010). Given that IL-17F has a higher binding affinity for IL-17RC than IL-17RA in mice (Hu et al., 2010), we first assessed whether IL-17RC signaling was capable of mediating the downstream effects of IL-17F in conditions of IL-17RA deficiency. Comparing expression of IL-17RC protein and mRNA in epithelial cells from *A. fumigatus*-infected WT and *Il17ra*$^{-/-}$ mice revealed significant upregulation of IL-17RC in *Il17ra*$^{-/-}$ lung cells during *Aspergillus* intranasal infection (Figures 5A and 5B). In vitro, IL-17RC expression significantly increased in lung epithelial cells isolated from in *Il17ra*$^{-/-}$ mice following exposure to *A. fumigatus* and not to *P. aeruginosa* (Figure 5C), suggesting that pathogen- or fungus-specific mechanisms might be involved in driving upregulated IL-17RC expression. In addition, among the pathogens tested, only exposure to *A. fumigatus* significantly increased transcript abundance of the IL-17A or IL-17F downstream gene *Cxcl2* in *Il17ra*$^{-/-}$ epithelial cells, relative to untreated controls (Figure 5D). We also obtained a similar pattern of cytokine/cytokine receptor expression by using two different more physiological system of culture: air-liquid interface (ALI) (Figures S4A and S4B) and 3D lung organoid system of culture (Figure S4C). Further evidence that IL-17RC expressed in the context of IL-17RA deficiency was able to activate downstream signaling pathways came from detection of NF-κB phosphorylation following treatment of lung epithelial cells with IL-17A, IL-17F, or IL-17A and IL-17F (Figure 5E). In addition, a protein array analysis of murine lung epithelial cells showed that exposure to IL-17F resulted in TRAF-6-dependent phosphorylation of the IL-17R proximal signaling molecules AKT and IκBα (Figures 5F and S4D). IL-17F exposure of epithelial cells isolated from either WT or *Il17ra*$^{-/-}$ mice also resulted in significantly increased IL-33 (Figure 5G) production and of *Il17rc* expression in *Il17ra*$^{-/-}$ cells (Figure 5H). Last, in addition to NF-κB signaling IL-17RC-dependent expression of proximal signaling molecules as *Cepbβ* and *Cepbδ* transcription factors (Gaffen, 2009), which act downstream of IL-17RA proximal signaling, was evident both in vitro (Figure 5I) and in vivo (Figure 5J). These data support that following the disruption of the IL-17RA function, the remaining part of the receptor (IL-17RC) is still functional, being already demonstrated that IL-17RC may form heterodimers or homotrimers upon ligand binding (Ely et al., 2009; You et al., 2006). In this particular condition, in which IL-17RC is the only available subunit, and its expression is particularly high (Figures 5A–5C) homodimerization may eventually be favored. Therefore, we investigated whether IL-17RC, as it is lacking the distal signaling component of IL-17RA, which is essential for the activation of regulatory partners such as A20 (Garg and Gaffen, 2013), triggers a dysregulated signaling response. Thus, we exposed lung epithelial cells to IL-17A, IL-17F, or IL-17A and IL-17F (Figures 5K and 5L), and we measured *A20* expression as well as *Il33*. The results showed that only IL-17A in WT mice is able to trigger *A20* expression, while only IL-17F triggers IL-33 in IL-17RA deficiency (Figure 5L).

Thus, activation of the IL17F/IL17RC axis leadings to a positive loop because *Aspergillus* increases IL-17F expression (Figure 4A), which induces the expression of IL-33 and IL-17RC on epithelial cells, especially in IL-17RA deficiency (Figures 5G, 5H, and 5L), where A20-mediated regulation is absent (Figure 5K). In addition, IL-33 signaling is known (Hatta et al., 2017) to increase IL-17F transcription. The persistent activation of this loop may be the direct consequence of the absence of A20 induction by the IL-17RA subunits (Figure 5K).

The importance of signaling through IL-17RC in vivo was evident in both WT and *Il17ra*$^{-/-}$ mice treated with IL-17RC-specific small interfering RNA (siRNA) during ABPA induction: fungal burden (Figure 6A), inflammatory pathology (Figure 6B), eosinophil frequency in BAL fluid (Figure 6C), expression of *Il17f* and *Muc5a* (Figure 6D), production of IgE, and expression of type 2 cytokines (Figure 6E) were all markedly lower following treatment with *Il-17rc* siRNA, where a significant reduction of *Il17rc* expression was measured (Figure 6F). Similarly, use of IL-17RC=neutralizing antibody showed a reduction of ABPA pathogenesis (Figures S5A–S5C). Parallel reductions in severity of infection and inflammatory pathology upon IL-17RC siRNA treatment were also observed during *A. fumigatus* infections in vivo (Figures S5D–S5H). Interestingly, the reduction of *Il17f* with siRNA of IL-17RC suggests the existence of a positive loop of expression between IL-17RC and IL-17F (Figures 6D and S5G).

IL-17RC expression and IL-17F was increased on isolated tracheal cells compared with total lung cells and in naive or infected mice (Figure S6A) in IL-17RA deficiency, further confirming the preferential IL-17RC expression on epithelial cells. Interestingly, the tracheas of *Il17ra*$^{-/-}$ mice express higher levels of *Il17rc* then WT (Figure S6B).

Of interest, *Il17f* expression and *Il17rc* were also contingent upon the route of infection, with a higher degree in the intranasal than the intratracheal route of infection, particularly in *Il17ra*$^{-/-}$ mice (Figure S6C). In fact, although intratracheal infected WT mice showed a similar fungal load compared with the intranasal model of infection (Figures S2D and S6D), *Il17ra*$^{-/-}$ mice were more resistant upon intratracheal infection with *A. fumigatus* (Figures S6D and S6E) compared with the intranasal route (Figure S2D). Altogether, these results indicate that the expression of the IL-17F/IL-17RC axis in the upper airways may be contingent upon pathogen exposure. In the case of *Aspergillus*, the

(H) BAL morphometry, expressed as a percentage of neutrophils.

(I) Lung histology (PAS; the scale bar represents 1 mm or 100 μm) and BAL May-Grunwald Giemsa staining (original magnification, 100×).

Assays were done at 2 dpi. Data pooled from three independent experiments (n = 6 mice per group); mean ± SD. *$p < 0.05$, **$p < 0.01$, ***$p < 0.001$, and ****$p < 0.0001$. Two-way ANOVA, Bonferroni post hoc test.

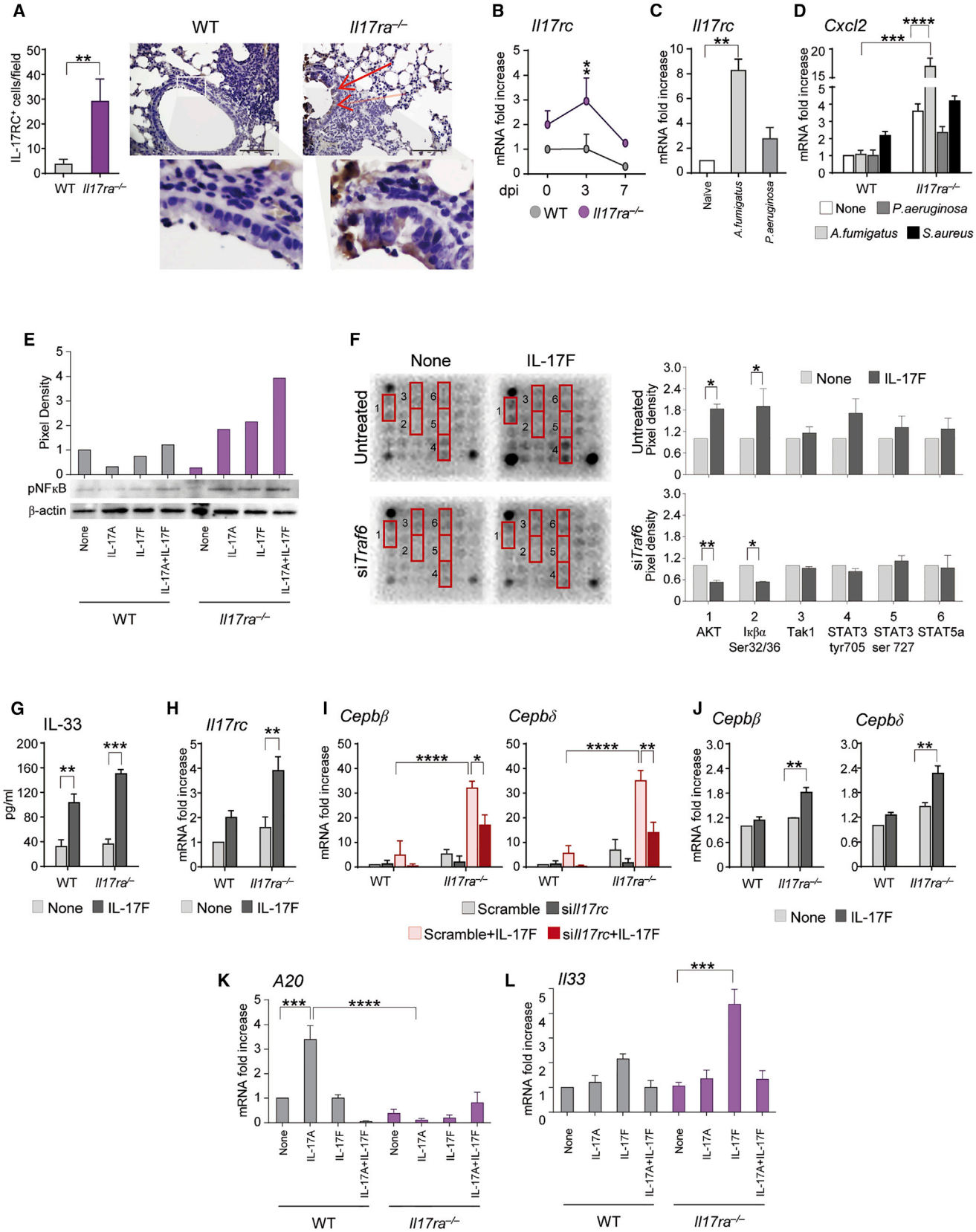

(legend on next page)

simultaneous induction of IL-17RC and IL-17F expression, the latter apparently reinforcing IL-17RC expression, points to the existence of a positive loop amplifying the allergic response to the fungus.

DISCUSSION

The complexity of the IL-17 cytokine family and its receptors shows the existence of multiple levels of regulation across space and time, designed to enable effective immunity while minimizing the risk of auto-inflammation and allergy; however, disentangling the effects of specific family members and their receptors in infection and pathologic inflammation has so far been difficult. IL-17A and IL-17F have been extensively studied in pulmonary diseases as well as in allergy (Lu et al., 2015; Fujita et al., 2012); in the case of IL-17F, there is now robust evidence of its involvement in asthma (Ota et al., 2014), with mechanistic studies uncovering induction of IL-17F production by epithelial cells in response to the Th2 cytokine IL-33, which is abundant in the asthmatic airway (Fujita et al., 2012). Our study goes on to show a plausible mechanism underlying the allergenic potential of IL-17F. By studying *Il17ra*$^{-/-}$ mice, we uncovered a pathogenic loop based on the activation of the IL-17F/IL-17RC pathway during *A. fumigatus*-linked allergy and infection; our data indicate that IL-17RA contributes to protective antifungal responses while restraining the development of allergic lung reactivity during infection; in contrast, the IL-17F/IL-17RC axis comes to predominate in conditions of IL-17RA deficiency and promotes allergy during *A. fumigatus* infection. Importantly, we have shown that exacerbation of lung pathology and allergy promotion in IL-17RA deficiency was not spontaneously developed, as the IL-17F/IL-17RC axis is induced only upon infection with specific pathogens. In addition, it can be excluded that gut or lung dysbiosis contributes to the susceptibility of *Il17ra*$^{-/-}$ mice to aspergillosis or ABPA, as naive mice do not display any spontaneous type 2 inflammation, different from atopic dermatitis as shown in double-deficient *filaggrin/Il17ra*$^{-/-}$ mice or in acute versus graft disease (Floudas et al., 2017; Varelias et al., 2017). We also observed pathogen-specific patterns of IL-17F/IL-17RC axis expression in the upper airways; *Aspergillus* and *Pseudomonas* in conditions of IL-17RA deficiency induced the simultaneous expression of IL-17RC and IL-17F, the latter apparently reinforcing IL-17RC expression, a finding highlighting the important contribution of pathogens to the generation of a positive loop amplifying the allergic response during microbial colonization and/or infection. It seems that the relative expression levels of IL-17RA and IL-17RC are key determinants of the function and overall biological activity of these cytokines in the lung: complete loss of *Il17f* resulted here in greater resistance to *A. fumigatus* infection and ABPA; likewise, silencing of IL-17RC reduced the immunopathology present in IL-17RA deficiency. These data support previous findings showing that IL-17F-deficient mice are highly resistant to acute allergic inflammation upon intranasal challenge of fungal proteinases derived from *A. oryzae* (Cheung et al., 2008). Therefore, hyperactivity of the IL-17F/IL-17RC axis can mediate allergic asthmatic disease when disruption of *Il17ra* deficiency also occurs, consistent with the increased susceptibility to fungal and bacterial infections seen in conditions of human genetic deficiency in either IL-17RA or IL-17F (Huppler et al., 2012).

It is known that IL-17RA acts as a common receptor subunit for multiple members of the IL-17 family (Ho and Gaffen, 2010), while IL-17RC recognizes only IL-17A and IL-7F (Toy et al., 2006); however, there have not been any studies on IL-17RC signaling in the absence of IL-17RA. Using *Il17ra*$^{-/-}$ mice, we provide evidence for biologically relevant IL-17RA-indepedent signaling through IL-17RC on lung epithelial cells in response to IL-17F. In our model, in infected *Il17ra*$^{-/-}$ mice, IL-17RC signaling may be due to the homodimerization of the remaining IL-17R subunit (IL-17RC), which may occur because of the increased expression of the IL-17RC subunit upon infection as well as of its ligand IL-17F. We also highlighted the potential

Figure 5. The IL-17F/IL-17RC Pathway Was Functional in IL-17RA Deficiency

(A) IL-17RC expression (stained brown) was evaluated in whole-lung tissue sections from WT and *Il17ra*$^{-/-}$ mice bearing *Aspergillus* infection at 3 dpi using immunohistochemistry. Red arrows indicate lung IL-17RC^{+} cells, quantified by individual counting at BX51 microscope (Olympus). Briefly, images were captured using bright field microscopy at 40× microscopic magnification, and the number of lung IL-17RC^{+} cells was measured in each section (n = 6 sections from ten mice per group) by an observer blinded to the treatment groups. Cell nuclei were counterstained with hematoxylin. (The scale bar represents 100 μm or 12.5 μm in insert).

(B and C) Expression of *Il17rc* gene (RT-PCR) in lung infected at 3 and 7 dpi (B) and murine lung epithelial cells, isolated from *Il17ra*$^{-/-}$ mice, stimulated with live *A. fumigatus* conidia (1:1, cells/fungi) or *P. aeruginosa* (1:100, cells/bacteria) for 8 hr at 37°C (C).

(D) Expression of *Cxcl2* gene (RT-PCR) in murine lung epithelial cells stimulated with live *A. fumigatus* conidia (1:1, cells/fungi), *P. aeruginosa*, or *S. aureus* (1:100, cells/bacteria) for 8 hr at 37°C.

(E) Phospho(p)NF-κB protein expression in murine lung epithelial cells stimulated with recombinant IL-17A and/or IL-17F. Expression of pNF-κB was normalized against the corresponding β-actin.

(F) Activation of distinct intracellular kinases in murine lung epithelial cells from naive *Il17ra*$^{-/-}$ mice using the PathScan immune cell signaling antibody array kit, exposed to 100 ng/ml IL-17F for 15 min and pretreated with specific siRNA for *Traf6*.

(G and H) ELISA of IL-33 (G) and expression of *Il17rc* gene (H) (RT-PCR) under exposure of 100 ng of IL-17F for 8 hr on murine lung epithelial cells.

(I) Expression of *Cepbβ* and *Cepbδ* genes (RT-PCR) in murine lung epithelial cells from naive WT and *Il17ra*$^{-/-}$ mice exposed to 100 ng/ml IL-17F for 8 hr and pretreated with specific siRNA for *Il17rc* or scrambled siRNA.

(J) WT and *Il17ra*$^{-/-}$ asthmatic mice were treated with murine recombinant IL-17F and assessed for expression of *Cepbβ* and *Cepbδ* genes (RT-PCR) in murine lung cells.

(K and L) Expression of *A20* (K) and *Il33* (L) genes (RT-PCR) in murine lung epithelial cells from naive WT and *Il17ra*$^{-/-}$ mice stimulated with recombinant IL-17A and/or IL-17F for 8 hr at 37°C.

Data pooled from three independent experiments (n = 6 mice per group); mean ± SD. *$p < 0.05$, **$p < 0.01$, ***$p < 0.001$, and ****$p < 0.0001$. One-way and two-way ANOVA, Bonferroni post hoc test.

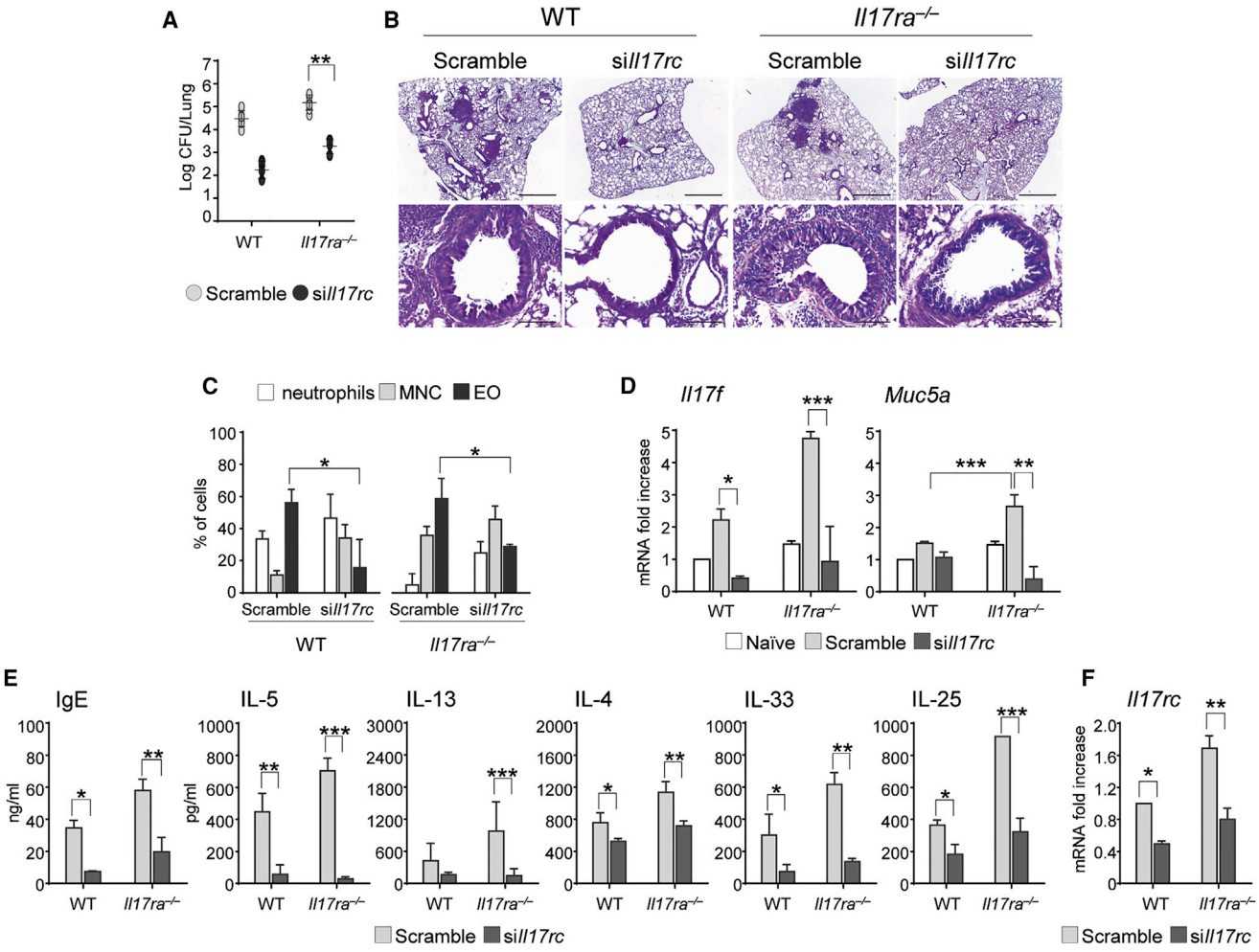

Figure 6. The IL-17F/IL-17RC Pathway Mediates Allergic Response in ABPA

(A) WT and *Il17ra*$^{-/-}$ asthmatic mice were given *Il17rc* siRNA or scrambled siRNA intranasally 1 day before and 1 and 3 days after the infection and assessed for fungal growth (log CFU).

(B) Lung histology (Alcian blue; the scale bar represents 1 mm or 100 μm).

(C) BAL morphometry expressed as percentages of MNC, neutrophils, and EO.

(D) Expression of *Il17f* and *Muc5a* genes (RT-PCR) in the lung.

(E) IgE levels and cytokines production (ELISA) in lung homogenates.

(F) Expression of *Il17rc* gene (RT-PCR) in the lung.

Assays were done at 5 dpi. Data pooled from three independent experiments (n = 3 mice per group); mean ± SD. *$p < 0.05$, **$p < 0.01$, and ***$p < 0.001$. Two-way ANOVA, Bonferroni post hoc test.

significance of compartmentalized expression of IL-17R subunits in the airways, finding indications that the IL-17F/IL-17RC axis is more active in the upper airways rather than the lower. This may also partly explain the relative pathogen specificity of IL-17F/IL-17RC expression; it is plausibly adaptive that the IL-17F/IL-17RC pathway was both more highly induced and overtly protective against *S. aureus,* an upper respiratory tract pathogen, while the IL-17A/IL-17RA pathway was both more stimulated by, and required for protection from, *Aspergillus* diseases of the lower airways. It will be interesting in future studies to understand whether the same pattern is generalized to other pathogens of specific regions of the airways and indeed to other mucosal sites. In addition, the discovery of a pathogenic loop in conditions of IL-17RA disruption may eventually pave the way for therapeutic strategies based on the use of neutralizing antibodies. Interestingly, the most direct evidence for a role in Th17 immunity in human fungal infections comes from cases of IL-17RA or IL-17RC mutations (Ling et al., 2015; Puel et al., 2011).

Moreover, hyperexpression of *Il-17f* gene in the airway of mice has been demonstrated to increase airway neutrophilia, airway hyperreactivity, and mucus hypersecretion (Kawaguchi et al., 2009). Therefore, the use of antibodies against IL-17RC or IL-17F may have important therapeutic implications in asthma. Importantly, targeting IL-17 is an effective therapy for several specific conditions, although the clinical use revealed different

essential aspects of Th17 to be considered in therapy. Indeed, clinical trial using antibodies targeting IL-17RA (brodalumab [anti-IL-17RA]) in Crohn's disease were terminated early because of exacerbation of the disease in the treatment group (Targan et al., 2016). Also, in the context of persistent asthma, it has been demonstrated a failure in the treatment of patient with brodalumab (Busse et al., 2013). In this regard, our study highlights an important aspect of IL-17R biology, which may eventually explain the failure of targeted therapy following neutralization of IL-17RA proteins. Definitively, neutralization of IL-17RA may have a strong impact on IL-17RC signaling dysregulation.

In conclusion, IL-17F/IL-17RC axis dysregulation predisposing to allergic inflammation, as highlighted here, would argue against these therapeutics in the context of asthma, while antibodies neutralizing IL-17F may represent a better option in the future.

EXPERIMENTAL PROCEDURES

Animals

Female C57BL/6 8- to 10-week-old mice were purchased from Charles River. Homozygous female 8- to 10-week-old *Il17ra*$^{-/-}$, *Il17a*$^{-/-}$, and *Il17f*$^{-/-}$ mice on a C57BL/6 background were bred under specific pathogen-free conditions in the animal facility at the University of Perugia. The animal studies described here were performed in accordance with the Italian Approved Animal Welfare Authorization 360/2015-PR and Legislative Decree #26/2014, which provided ad hoc clearance by the Italian Ministry of Health over a 5-year period (2015–2020). Animals were assessed twice daily for physical conditions and behavior. Animals ranked as moribund were humanely euthanized by CO_2 asphyxiation.

siRNA Design and Delivery

The Integrated DNA Technologies pool duplexes of predesigned siRNA IL-17RC (MMC.RNAI.N134159.12.1) were purchased from Integrated DNA Technologies (IDT, TEMA Ricerca) and siRNA against TRAF6 from Eurofins. For in vivo studies, each mouse was lightly anesthetized by inhaled ether, then given unmodified siRNA (10 mg/kg), or equivalent doses of nonspecific control siRNA duplex, intranasally in a volume of 20 μl of duplex buffer (IDT, TEMA Ricerca). This procedure was repeated four times 1 day before the infection and on days 1, 3, and 5 after infection in the infection model; in ABPA 1 day before the infection and on days 1 and 3. For in vitro studies, specific predesigned siRNA targeting TRAF6 was transfected into murine lung epithelial cells using Lipofectamine 2000 (Invitrogen) before incubation for 24 hr at 37°C in 5% CO_2. The efficiency of gene silencing was assessed by RT-PCR at 48 hr after the last siRNA injection in total lung cells, for in vitro studies after 24 hr of culture.

Cell Signaling Array

Murine lung epithelial cells were exposed to 100 ng/ml of IL-17F for 15 min. The detection of 18 well-characterized signaling molecules when phosphorylated or cleaved was performed using the PathScan Intracellular Signaling Array Kit (Chemiluminescent Readout; Cell Signaling): cell lysate was incubated on the slide followed by application of a biotinylated detection antibody cocktail; streptavidin-conjugated HRP and LumiGLO reagent were then used to visualize the bound detection antibody by chemiluminescence. Images of the slides were captured with either a digital imaging system using ChemiDoc XRS, or the Bio-Rad imaging system (Bio-Rad) and quantification achieved by densitometry image analysis using Image Lab 3.1.1 software (Bio-Rad).

Statistical Analysis

Data are expressed as mean ± SD. Horizontal bars in figures indicate means. Statistical significance was calculated using one- or two-way ANOVA (Bonferroni post hoc test) for multiple comparisons and using a two-tailed Student's t test for single comparison. The data reported either are from one representative experiment out of three to five independent experiments (western blotting) or are pooled from three to five experiments. The in vivo groups consisted of three to six mice per group. Statistical analysis was performed with Prism 6 software (GraphPad Software).

ACCESSION NUMBERS

The accession numbers for flow cytometry data reported in this paper are Flow Repository: FR-FCM-ZY83 and FR-FCM-ZY85.

SUPPLEMENTAL INFORMATION

Supplemental Information includes Supplemental Experimental Procedures and six figures and can be found with this article online at http://dx.doi.org/10.1016/j.celrep.2017.07.063.

AUTHOR CONTRIBUTIONS

A.D.L. conducted, designed, and analyzed experiments. M. Pariano did immunohistochemistry and western blotting. B.C. and C.C. revised the manuscript and performed data analysis. V.R.V. and L.M. performed and designed ALI experiments. S.S.J. and J.F. designed and performed experiments with lung organoids. M. Palmieri conducted bacterial infection experiments. M.B. performed histological analysis. C.G. and G.P. analyzed qPCR data. T.Z. wrote the manuscript and coordinated the project.

ACKNOWLEDGMENTS

This study was supported by an Italian grant funded by the Italian Cystic Fibrosis Research Foundation (Research Project FFC#22/2014), the Specific Targeted Research Project FunMeta (ERC-2011-AdG-293714), Italian grant "Programma per Giovani Ricercatori—Rita Levi Montalcini 2013," the European Social Fund, the European Regional Development Fund, Project MAGNET (CZ.02.1.01/0.0/0.0/15_003/0000492), and the European Regional Development Fund for the project Kompetenzzentrum MechanoBiologie (ATCZ133) in the Interreg V-A Austria–Czech Republic program. We thank Dr. Lucy Robinson of Insight Editing London for her assistance in the preparation of the text and Dr. Cristina Massi-Benedetti for digital art and editorial assistance.

Received: March 6, 2017
Revised: June 17, 2017
Accepted: July 23, 2017
Published: August 15, 2017

REFERENCES

Alivand, M.R., Sabouni, F., and Soheili, Z.S. (2016). Probable chemical hypoxia effects on progress of CNV through induction of promoter CpG demethylation and overexpression of IL17RC in human RPE cells. Curr. Eye Res. *41*, 1245–1254.

Archer, N.K., Adappa, N.D., Palmer, J.N., Cohen, N.A., Harro, J.M., Lee, S.K., Miller, L.S., and Shirtliff, M.E. (2016). IL-17A and IL-17F are critical for antimicrobial peptide production and clearance of *Staphylococcus aureus* nasal colonization. Infect. Immun. *84*, 3575–3583.

Burgel, P.R., Paugam, A., Hubert, D., and Martin, C. (2016). *Aspergillus fumigatus* in the cystic fibrosis lung: pros and cons of azole therapy. Infect. Drug Resist. *9*, 229–238.

Busse, W.W., Holgate, S., Kerwin, E., Chon, Y., Feng, J., Lin, J., and Lin, S.L. (2013). Randomized, double-blind, placebo-controlled study of brodalumab, a human anti-IL-17 receptor monoclonal antibody, in moderate to severe asthma. Am. J. Respir. Crit. Care Med. *188*, 1294–1302.

Chang, S.H., and Dong, C. (2007). A novel heterodimeric cytokine consisting of IL-17 and IL-17F regulates inflammatory responses. Cell Res. *17*, 435–440.

Chesné, J., Braza, F., Mahay, G., Brouard, S., Aronica, M., and Magnan, A. (2014). IL-17 in severe asthma. Where do we stand? Am. J. Respir. Crit. Care Med. *190*, 1094–1101.

Cheung, P.F., Wong, C.K., and Lam, C.W. (2008). Molecular mechanisms of cytokine and chemokine release from eosinophils activated by IL-17A, IL-17F, and IL-23: implication for Th17 lymphocytes-mediated allergic inflammation. J. Immunol. *180*, 5625–5635.

Conti, H.R., and Gaffen, S.L. (2015). IL-17-mediated immunity to the opportunistic fungal pathogen *Candida albicans*. J. Immunol. *195*, 780–788.

Conti, H.R., Shen, F., Nayyar, N., Stocum, E., Sun, J.N., Lindemann, M.J., Ho, A.W., Hai, J.H., Yu, J.J., Jung, J.W., et al. (2009). Th17 cells and IL-17 receptor signaling are essential for mucosal host defense against oral candidiasis. J. Exp. Med. *206*, 299–311.

Cosmi, L., Liotta, F., and Annunziato, F. (2016). Th17 regulating lower airway disease. Curr. Opin. Allergy Clin. Immunol. *16*, 1–6.

Ely, L.K., Fischer, S., and Garcia, K.C. (2009). Structural basis of receptor sharing by interleukin 17 cytokines. Nat. Immunol. *10*, 1245–1251.

Endo, Y., Yokote, K., and Nakayama, T. (2016). The obesity-related pathology and Th17 cells. Cell. Mol. Life Sci. *74*, 1231–1245.

Fahy, J.V. (2009). Eosinophilic and neutrophilic inflammation in asthma: insights from clinical studies. Proc. Am. Thorac. Soc. *6*, 256–259.

Floudas, A., Saunders, S.P., Moran, T., Schwartz, C., Hams, E., Fitzgerald, D.C., Johnston, J.A., Ogg, G.S., Mckenzie, A.N., Walsh, P.T., and Fallon, P.G. (2017). IL-17 receptor A maintains and protects the skin barrier to prevent allergic skin inflammation. J. Immunol. *199*, 707–717.

Fujita, J., Kawaguchi, M., Kokubu, F., Ohara, G., Ota, K., Huang, S.K., Morishima, Y., Ishii, Y., Satoh, H., Sakamoto, T., and Hizawa, N. (2012). Interleukin-33 induces interleukin-17F in bronchial epithelial cells. Allergy *67*, 744–750.

Gaffen, S.L. (2009). Structure and signalling in the IL-17 receptor family. Nat. Rev. Immunol. *9*, 556–567.

Garg, A.V., and Gaffen, S.L. (2013). IL-17 signaling and A20: a balancing act. Cell Cycle *12*, 3459–3460.

Gu, C., Wu, L., and Li, X. (2013). IL-17 family: cytokines, receptors and signaling. Cytokine *64*, 477–485.

Hatta, M., Surachmanto, E.E., Islam, A.A., and Wahid, S. (2017). Expression of mRNA IL-17F and sIL-17F in atopic asthma patients. BMC Res. Notes *10*, 202.

Haudenschild, D., Moseley, T., Rose, L., and Reddi, A.H. (2002). Soluble and transmembrane isoforms of novel interleukin-17 receptor-like protein by RNA splicing and expression in prostate cancer. J. Biol. Chem. *277*, 4309–4316.

Hizawa, N., Kawaguchi, M., Huang, S.K., and Nishimura, M. (2006). Role of interleukin-17F in chronic inflammatory and allergic lung disease. Clin. Exp. Allergy *36*, 1109–1114.

Ho, A.W., and Gaffen, S.L. (2010). IL-17RC: a partner in IL-17 signaling and beyond. Semin. Immunopathol. *32*, 33–42.

Ho, A.W., Shen, F., Conti, H.R., Patel, N., Childs, E.E., Peterson, A.C., Hernández-Santos, N., Kolls, J.K., Kane, L.P., Ouyang, W., and Gaffen, S.L. (2010). IL-17RC is required for immune signaling via an extended SEF/IL-17R signaling domain in the cytoplasmic tail. J. Immunol. *185*, 1063–1070.

Hu, Y., Ota, N., Peng, I., Refino, C.J., Danilenko, D.M., Caplazi, P., and Ouyang, W. (2010). IL-17RC is required for IL-17A- and IL-17F-dependent signaling and the pathogenesis of experimental autoimmune encephalomyelitis. J. Immunol. *184*, 4307–4316.

Huppler, A.R., Bishu, S., and Gaffen, S.L. (2012). Mucocutaneous candidiasis: the IL-17 pathway and implications for targeted immunotherapy. Arthritis Res. Ther. *14*, 217.

Kawaguchi, M., Kokubu, F., Fujita, J., Huang, S.K., and Hizawa, N. (2009). Role of interleukin-17F in asthma. Inflamm. Allergy Drug Targets *8*, 383–389.

Kramer, J.M., Yi, L., Shen, F., Maitra, A., Jiao, X., Jin, T., and Gaffen, S.L. (2006). Evidence for ligand-independent multimerization of the IL-17 receptor. J. Immunol. *176*, 711–715.

Krstic, J., Obradovic, H., Kukolj, T., Mojsilovic, S., Okic-Dordevic, I., Bugarski, D., and Santibanez, J.F. (2015). An overview of interleukin-17A and interleukin-17 receptor A structure, interaction and signaling. Protein Pept. Lett. *22*, 570–578.

Kuestner, R.E., Taft, D.W., Haran, A., Brandt, C.S., Brender, T., Lum, K., Harder, B., Okada, S., Ostrander, C.D., Kreindler, J.L., et al. (2007). Identification of the IL-17 receptor related molecule IL-17RC as the receptor for IL-17F. J. Immunol. *179*, 5462–5473.

Ling, Y., Cypowyj, S., Aytekin, C., Galicchio, M., Camcioglu, Y., Nepesov, S., Ikinciogullari, A., Dogu, F., Belkadi, A., Levy, R., et al. (2015). Inherited IL-17RC deficiency in patients with chronic mucocutaneous candidiasis. J. Exp. Med. *212*, 619–631.

Lu, S., Li, H., Gao, R., Gao, X., Xu, F., Wang, Q., Lu, G., Xia, D., and Zhou, J. (2015). IL-17A, but not IL-17F, is indispensable for airway vascular remodeling induced by exaggerated Th17 cell responses in prolonged ovalbumin-challenged mice. J. Immunol. *194*, 3557–3566.

Ma, A.I. (2012). The ubiquitous nature of IL-17. Nat. Immunol. *13*, 1034–1035.

McAllister, F., Henry, A., Kreindler, J.L., Dubin, P.J., Ulrich, L., Steele, C., Finder, J.D., Pilewski, J.M., Carreno, B.M., Goldman, S.J., et al. (2005). Role of IL-17A, IL-17F, and the IL-17 receptor in regulating growth-related oncogene-alpha and granulocyte colony-stimulating factor in bronchial epithelium: implications for airway inflammation in cystic fibrosis. J. Immunol. *175*, 404–412.

Moseley, T.A., Haudenschild, D.R., Rose, L., and Reddi, A.H. (2003). Interleukin-17 family and IL-17 receptors. Cytokine Growth Factor Rev. *14*, 155–174.

Oda, N., Canelos, P.B., Essayan, D.M., Plunkett, B.A., Myers, A.C., and Huang, S.K. (2005). Interleukin-17F induces pulmonary neutrophilia and amplifies antigen-induced allergic response. Am. J. Respir. Crit. Care Med. *171*, 12–18.

Ota, K., Kawaguchi, M., Matsukura, S., Kurokawa, M., Kokubu, F., Fujita, J., Morishima, Y., Huang, S.K., Ishii, Y., Satoh, H., and Hizawa, N. (2014). Potential involvement of IL-17F in asthma. J. Immunol. Res. *2014*, 602846.

Patel, D.D., and Kuchroo, V.K. (2015). Th17 cell pathway in human immunity: lessons from genetics and therapeutic interventions. Immunity *43*, 1040–1051.

Pelly, V.S., Kannan, Y., Coomes, S.M., Entwistle, L.J., Rückerl, D., Seddon, B., MacDonald, A.S., McKenzie, A., and Wilson, M.S. (2016). IL-4-producing ILC2s are required for the differentiation of TH2 cells following Heligmosomoides polygyrus infection. Mucosal Immunol. *9*, 1407–1417.

Piehler, D., Eschke, M., Schulze, B., Protschka, M., Müller, U., Grahnert, A., Richter, T., Heyen, L., Köhler, G., Brombacher, F., and Alber, G. (2016). The IL-33 receptor (ST2) regulates early IL-13 production in fungus-induced allergic airway inflammation. Mucosal Immunol. *9*, 937–949.

Puel, A., Cypowyj, S., Bustamante, J., Wright, J.F., Liu, L., Lim, H.K., Migaud, M., Israel, L., Chrabieh, M., Audry, M., et al. (2011). Chronic mucocutaneous candidiasis in humans with inborn errors of interleukin-17 immunity. Science *332*, 65–68.

Rathore, J.S., and Wang, Y. (2016). Protective role of Th17 cells in pulmonary infection. Vaccine *34*, 1504–1514.

Romani, L., Fallarino, F., De Luca, A., Montagnoli, C., D'Angelo, C., Zelante, T., Vacca, C., Bistoni, F., Fioretti, M.C., Grohmann, U., et al. (2008). Defective tryptophan catabolism underlies inflammation in mouse chronic granulomatous disease. Nature *451*, 211–215.

Rong, Z., Cheng, L., Ren, Y., Li, Z., Li, Y., Li, X., Li, H., Fu, X.Y., and Chang, Z. (2007). Interleukin-17F signaling requires ubiquitination of interleukin-17 receptor via TRAF6. Cell. Signal. *19*, 1514–1520.

Sakkas, L.I., and Bogdanos, D.P. (2016). Are psoriasis and psoriatic arthritis the same disease? The IL-23/IL-17 axis data. Autoimmun. Rev. *16*, 10–15.

Sorbello, V., Ciprandi, G., Di Stefano, A., Massaglia, G.M., Favatà, G., Conticello, S., Malerba, M., Folkerts, G., Profita, M., Rolla, G., and Ricciardolo, F.L. (2015). Nasal IL-17F is related to bronchial IL-17F/neutrophilia and exacerbations in stable atopic severe asthma. Allergy *70*, 236–240.

Targan, S.R., Feagan, B., Vermeire, S., Panaccione, R., Melmed, G.Y., Landers, C., Li, D., Russell, C., Newmark, R., Zhang, N., et al. (2016). A randomized, double-blind, placebo-controlled phase 2 study of brodalumab in

patients with moderate-to-severe Crohn's disease. Am. J. Gastroenterol. *111*, 1599–1607.

Toy, D., Kugler, D., Wolfson, M., Vanden Bos, T., Gurgel, J., Derry, J., Tocker, J., and Peschon, J. (2006). Cutting edge: interleukin 17 signals through a heteromeric receptor complex. J. Immunol. *177*, 36–39.

Tsai, H.C., Velichko, S., Hung, L.Y., and Wu, R. (2013). IL-17A and Th17 cells in lung inflammation: an update on the role of Th17 cell differentiation and IL-17R signaling in host defense against infection. Clin. Dev. Immunol. *2013*, 267971.

Varelias, A., Ormerod, K.L., Bunting, M.D., Koyama, M., Gartlan, K.H., Kuns, R.D., Lachner, N., Locke, K.R., Lim, C.Y., Henden, A.S., et al. (2017). Acute graft-versus-host disease is regulated by an IL-17-sensitive microbiome. Blood *129*, 2172–2185.

Wright, J.F., Guo, Y., Quazi, A., Luxenberg, D.P., Bennett, F., Ross, J.F., Qiu, Y., Whitters, M.J., Tomkinson, K.N., Dunussi-Joannopoulos, K., et al. (2007). Identification of an interleukin 17F/17A heterodimer in activated human CD4+ T cells. J. Biol. Chem. *282*, 13447–13455.

You, Z., Shi, X.B., DuRaine, G., Haudenschild, D., Tepper, C.G., Lo, S.H., Gandour-Edwards, R., de Vere White, R.W., and Reddi, A.H. (2006). Interleukin-17 receptor-like gene is a novel antiapoptotic gene highly expressed in androgen-independent prostate cancer. Cancer Res. *66*, 175–183.

Zelante, T., De Luca, A., Bonifazi, P., Montagnoli, C., Bozza, S., Moretti, S., Belladonna, M.L., Vacca, C., Conte, C., Mosci, P., et al. (2007). IL-23 and the Th17 pathway promote inflammation and impair antifungal immune resistance. Eur. J. Immunol. *37*, 2695–2706.

Zhong, B., Liu, X., Wang, X., Chang, S.H., Liu, X., Wang, A., Reynolds, J.M., and Dong, C. (2012). Negative regulation of IL-17-mediated signaling and inflammation by the ubiquitin-specific protease USP25. Nat. Immunol. *13*, 1110–1117.

Cell Reports, Volume *20*

Supplemental Information

The IL-17F/IL-17RC Axis Promotes Respiratory Allergy in the Proximal Airways

Antonella De Luca, Marilena Pariano, Barbara Cellini, Claudio Costantini, Valeria Rachela Villella, Shyam Sushama Jose, Melissa Palmieri, Monica Borghi, Claudia Galosi, Giuseppe Paolicelli, Luigi Maiuri, Jan Fric, and Teresa Zelante

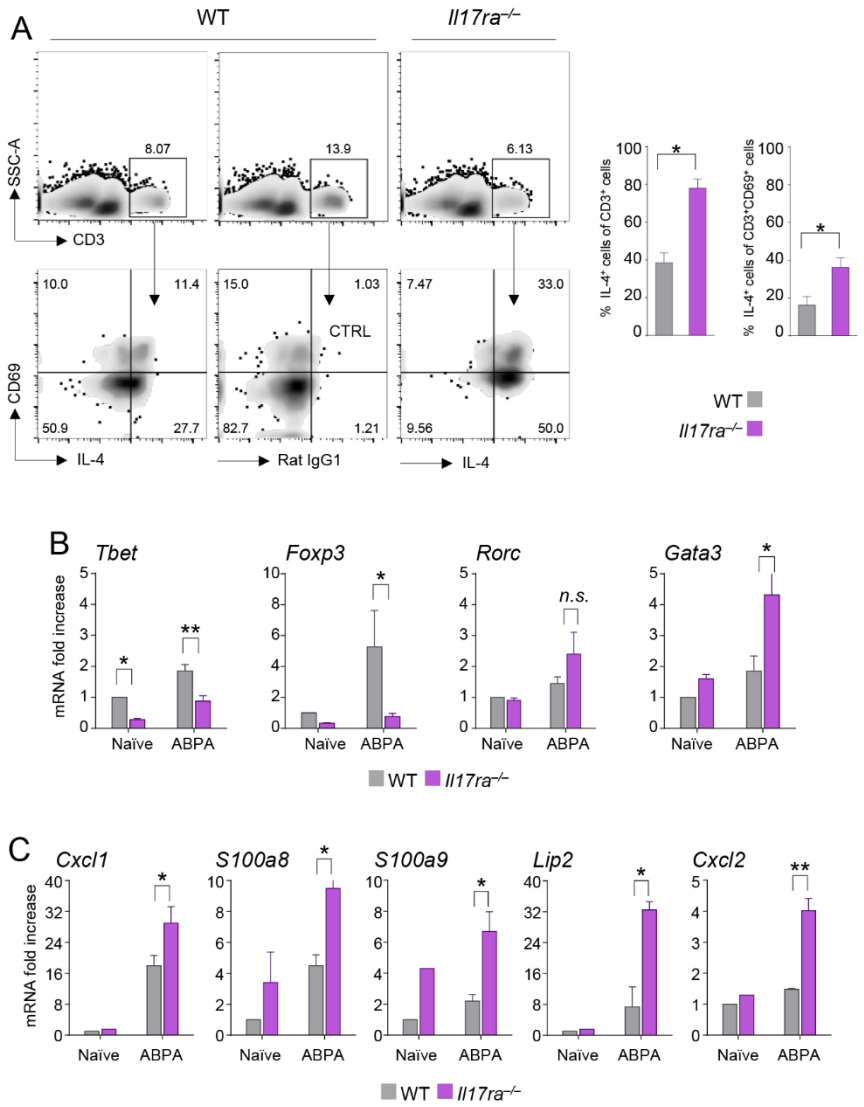

Figure S1. T-helper patterns in IL-17RA deficiency in ABPA. Related to Figure 1. A, Flow cytometry of lung and intracellular IL-4 cytokine production from WT and *Il17ra*$^{-/-}$ asthmatic mice. Flow gates indicate the percentage of CD69^{+} and CD69^{-} cells producing IL-4 on gated CD3^{+} cells. PECY7-IL-4 staining was determined using a PECY7-isotype control (CTRL) as suggested by the manufacturer. **B**, TLN relative mRNA expression assessed by RT-PCR. **C**, Lung relative mRNA expression assessed by RT-PCR. Assays were done at 5 dpi. Data pooled from three independent experiments (n = 6 mice per group); mean ± SD. *P<0.05, **P<0.01. Two-way ANOVA, Bonferroni's post hoc test.

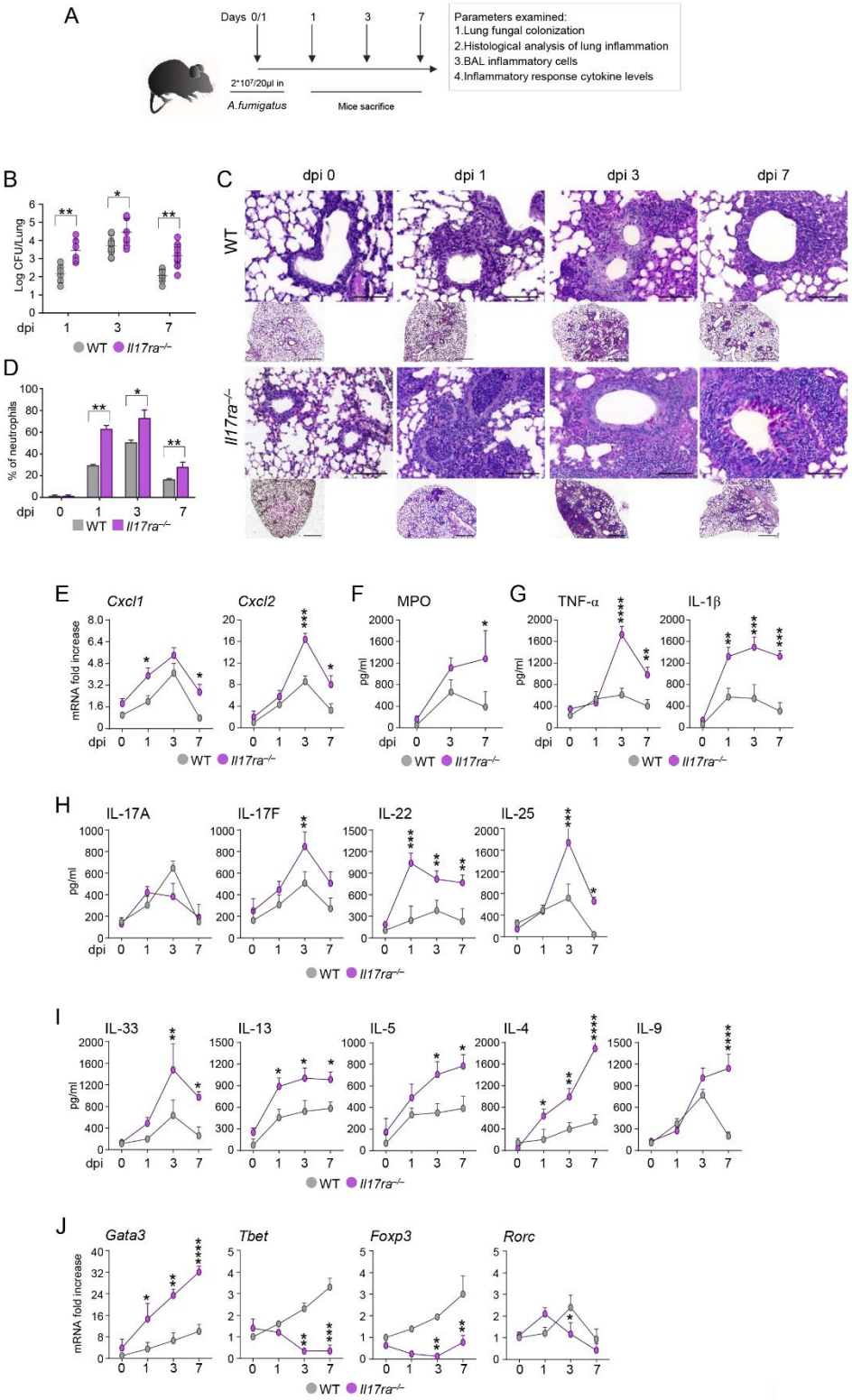

Figure S2. **IL-17RA deficiency leads to respiratory allergy during fungal infection. Related to Figure 1. A**, Schematic representation of *A. fumigatus* infection model. WT and *Il17ra*$^{-/-}$ mice were infected intranasally with live *A. fumigatus* conidia and assessed for **B**, Fungal growth (log CFU). **C**, Histological analysis of PAS-stained lung section (Scale bar 100 µm or 1 mm in inset). **D**, BAL morphometry, expresses as a percentage of neutrophils. **E-I**, Lung relative mRNA expression assessed by RT-PCR, MPO and cytokines production measured by ELISA on lung homogenates. **J**, Expression of *Gata3, Tbet, Foxp3, Rorc* gene (RT-PCR) in the TLN. Assays were done at 1, 3 and 7 dpi. Data pooled from three independent experiments (n = 6 mice per group); mean ± SD. **P*<0.05, ***P*<0.01, ****P*<0.001, *****P*<0.0001. Two-way ANOVA, Bonferroni's post hoc test.

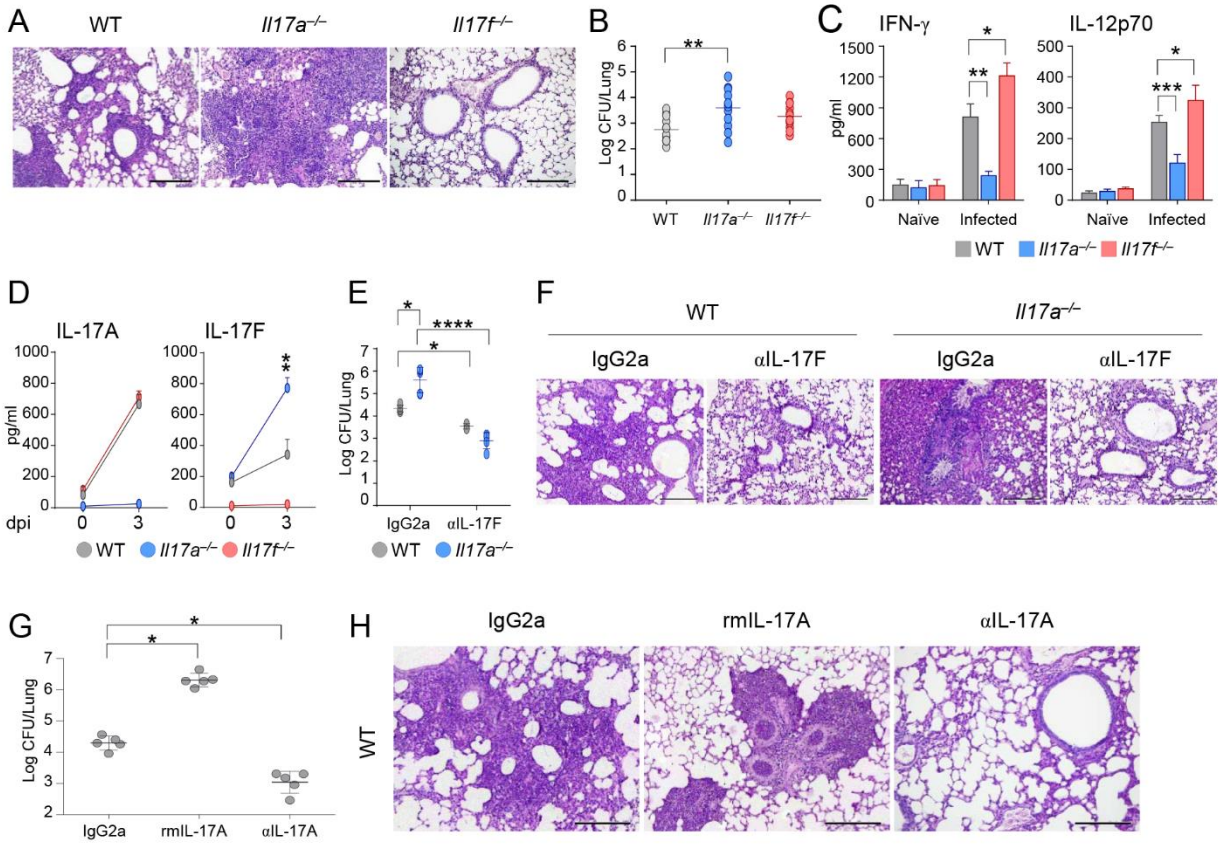

Figure S3. IL-17F contributes to susceptibility to infection. Related to Figure 2. WT, *Il17a*$^{-/-}$ and *Il17f*$^{-/-}$ mice were infected with *A. fumigatus* conidia and assessed for **A**, Histological analysis of PAS-stained lung section. (Scale bar 200 µm). **B**, Fungal growth (log CFU). **C**, ELISA in total lung homogenates at 0 and 3 dpi. **D**, IL-17A and IL-17F production (ELISA) in lung homogenates. **E-F**, Fungal growth (log CFU) in the lung (E) and lung sections from WT and *Il17ra*$^{-/-}$ *A. fumigatus*-infected mice treated with IgG2a control or anti-IL-17F blocking antibodies. (Scale bar 200 µm) (F). **G-H**, Fungal growth (log CFU) in the lung (G) and histological analysis of PAS-stained lung section from WT *A. fumigatus*-infected mice treated with IgG2a control, recombinant IL-17A or anti-IL-17A blocking antibodies (H). (Scale bar 200 µm). Assays were done at 3 dpi. Data pooled from three independent experiments (**A-D** n = 6 mice per group, **E-H** n = 3 mice per group); mean ± SD.**P*<0.05, ***P*<0.01, ****P*<0.001, *****P*<0.0001. One-way and Two-way ANOVA, Bonferroni's post hoc test.

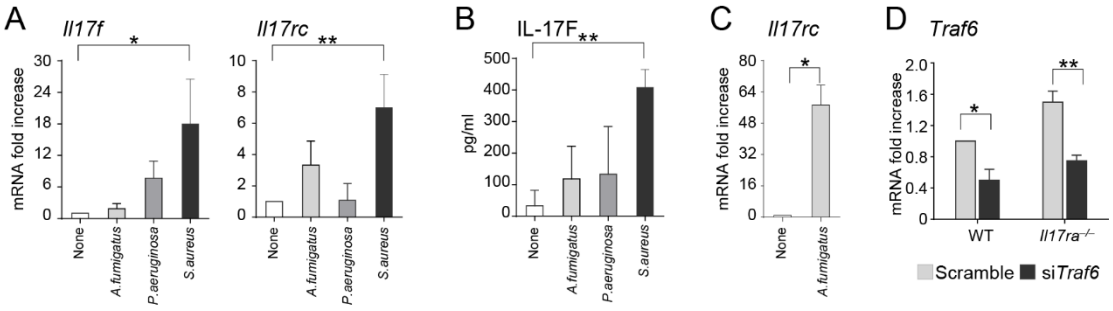

Figure S4. Pathogen differential induction of IL-17F/IL17RC axis. Related to Figure 5. A-B, Expression of *Il17f* and *Il17rc* gene (RT-PCR) (A) and production (ELISA) (B) in human bronchial epithelial cells (HBE) cultured in under ALI and stimulated with live *A. fumigatus* conidia (1:1, cells:fungi), *P. aeruginosa* or *S. aureus* (1:100, cells:bacteria) for 8 h at 37°C. **C**, Expression of *Il17rc* gene (RT-PCR) in human lung organoid stimulated with live *A. fumigatus* conidia (1:1, cells:fungi) for 8 h at 37°C. **D**, Expression of *Traf6* gene (RT-PCR) in murine lung epithelial cells from naïve WT and *Il17ra*$^{-/-}$ mice treated with specific siRNA for *Traf6* or scrambled siRNA. Data pooled from three independent experiments (n = 6 mice per group); mean ± SD. **P*<0.05, ***P*<0.01. Two-way ANOVA, Bonferroni's post hoc test.

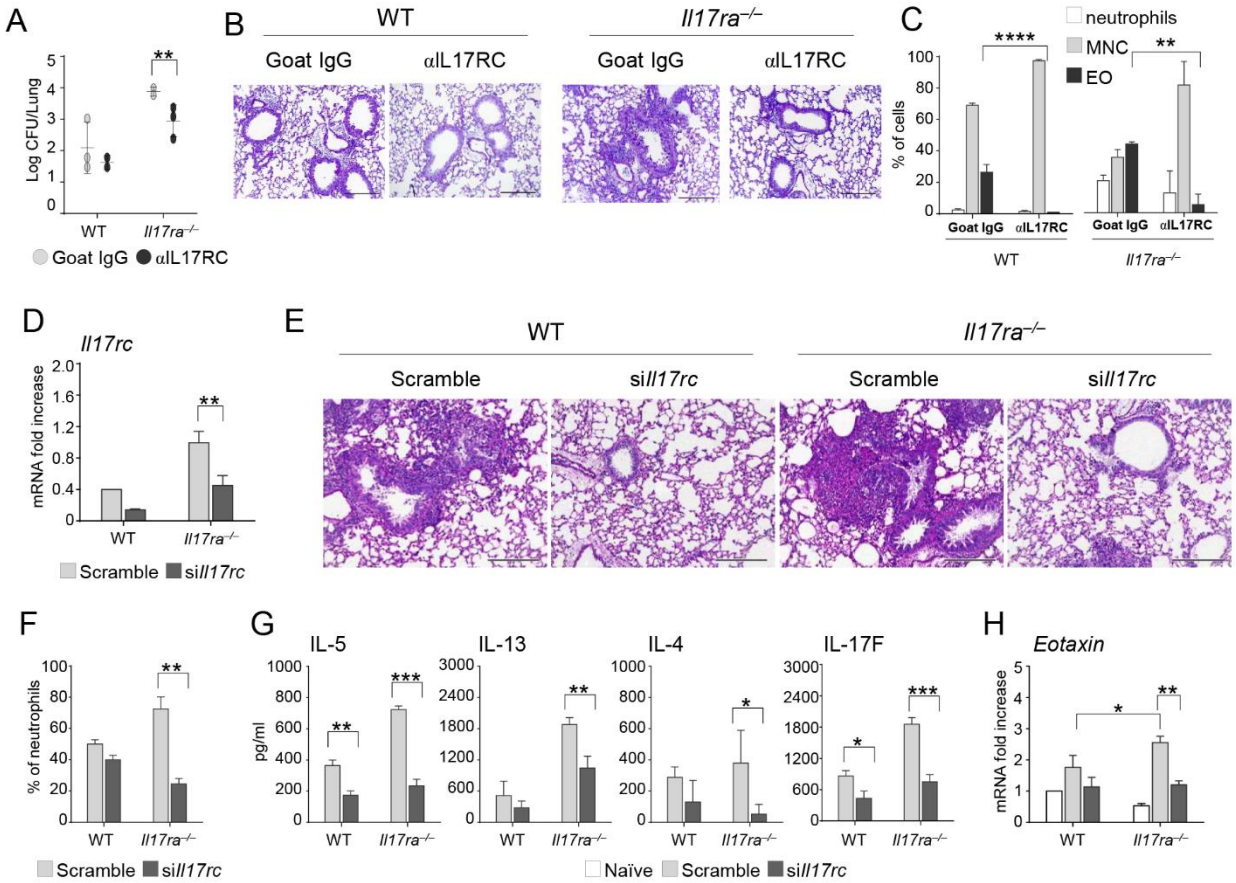

Figure S5. **IL-17F/IL-17RC pathway mediates allergic response in ABPA and to *Aspergillus* infection. Related to Figure 6.** WT and *Il17ra*$^{-/-}$ asthmatic mice were treated with isotype control mAb or IL-17RC neutralizing mAb and assessed for **A,** Fungal growth (log CFU). **B**, Lung histology (Alcian blue staining) (Scale bar 200 µm). **C**, Differential cell count of MNC, neutrophils and EOS was determined on May-Grunwald Giemsa staining. Assays were done at 5 dpi. WT and *Il17ra*$^{-/-}$ mice were infected with *A. fumigatus* conidia and were treated with specific *Il17rc* siRNA or scrambled siRNA intranasally 1 day before and 1,3 and 5 dpi and assessed for **D**, Expression of *Il17rc* gene (RT-PCR) in lung. **E**, Lung histology (PAS). (Scale bar 200 µm). **F**, BAL morphometry expressed as percentage of neutrophils. **G**, Cytokine production (ELISA); **H**, Expression of *Eotaxin* gene (RT-PCR) on lung. Assays were done at 5 or 7 dpi. Data pooled from three independent experiments (n = 6 mice per group); mean ± SD. *P<0.05, **P<0.01, ***P<0.001, ****P<0.001. Two-way ANOVA, Bonferroni's post hoc test.

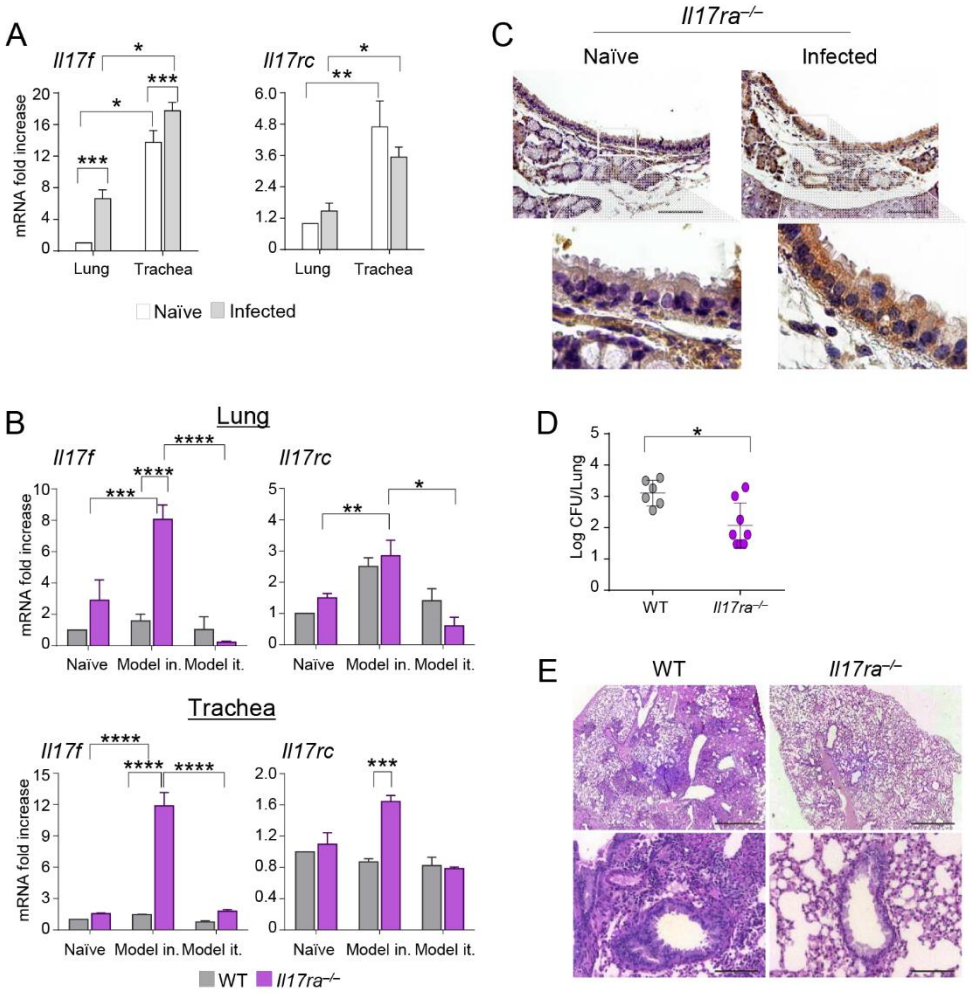

Figure S6. Intranasal and intratracheal route of infection differently activate the IL-17F/IL-17RC pathway upon fungal infection. Related to Figure 6. A, Gene expression (RT-PCR) in the lung and tracheal cells from naïve or intranasally infected *Il17ra*$^{-/-}$ mice with live *A. fumigatus* conidia at 3dpi. **B**, Gene expression (RT-PCR) in lung and trachea total cells of mice intranasally (i.n.) or intratracheally (i.t.) infected with live *A. fumigatus* conidia at 3 dpi. **C**, IL-17RC expression (stained brown) was evaluated in trachea tissue sections from *Il17ra*$^{-/-}$ mice at 3 dpi mice using immunohistochemistry. Cell nuclei were counterstained with haematoxylin. (Scale bar 100 µm or 12.5 µm in insert). **D**, Fungal growth (log CFU) and **E**, Lung PAS staining from mice it. infected with live *A. fumigatus* conidia at 3 dpi.(Scale bar 1 mm or 100 µm). Data pooled from three independent experiments (n = 6 mice per group); mean ± SD. **P*<0.05, ***P*<0.01, ****P*<0.001, *****P*<0.001. Two-way ANOVA, Bonferroni's post hoc test. Two tailed Student's, unparametric Mann-Whitney.

SUPPLEMENTARY METHODS

Infections, allergy, microbial colonization

Mice were anesthetized by intraperitoneal (i.p.) injection of 2.5% Avertin (Sigma Chemicals Co, St. Louis, MO) before intranasal instillation of 2×10^7 *A. fumigatus* (strain Af293, ATCC) resting conidia per 20µl of saline for two consecutive days, or intra-tracheal instillation of 5×10^7 resting conidia. To induce ABPA,[1] mice were sensitized by first an i.p. and then subsequently by a subcutaneous (s.c.) injection of 100 µg of *A. fumigatus* culture filtrate extract (CCFA) dissolved in incomplete Freund's adjuvant (Sigma-Aldrich) followed by two intranasal instillations, separated by two weeks, of 20 µg of CCFA in PBS. One week after the second intranasal instillation, mice received 2×10^7 resting conidia intranasally, and were evaluated for infection and immunological parameters 1 week later. For *S. aureus* and *Pseudomonas aeruginosa* infections, clinical *S. aureus* and *P. aeruginosa* strains, isolated from a patient, were obtained from the Diagnostic Unit of Microbiology from the University of Perugia. Bacteria were incubated for 3 h to establish the exponential growth phase; bacteria were then pelleted by centrifugation (2700 × g, 15 min), washed twice with sterile PBS and their density adjusted by spectrophotometry at 600 nm. The intended number of colony-forming units (CFU) was extrapolated from a standard growth curve. Appropriate dilutions with sterile PBS were made to prepare the inocula before intranasal instillation of 3×10^7 CFU/mouse. At the specified timepoints mice were assessed for microbial load (expressed as $\log_{10}$ CFU, mean ± SD) and infection-related changes to normal histology.

In vivo treatments

Mice were injected i.p. daily, from the first day of the infection up to 2 days after the infection, or 3 days after infection in the ABPA model. Doses used were: 2.5 mg/kg of anti-IL-17A, anti-IL-17F, anti-IL-17RC (R&D System). Control mice received isotype-matched control rat IgG2a or goat IgG respectively. Cytokine doses used were: 0.5 µg/mouse of recombinant murine IL-17A (rmIL-17) and IL-17F (rmIL-17F) (R&D System), all dissolved in sterile PBS. Control mice received cytokine vehicle.

Bronchoalveolar lavage

BAL was performed on sacrificed animals by cannulating the trachea and washing the airways with PBS to collect the BAL fluid. Differential cell counts were generated on BAL smears stained with May-Grünwald Giemsa reagents (Sigma-Aldrich) observed using a BX51 microscope equipped with a high-resolution DP71 camera (Olympus).

Flow cytometry

Flow cytometry was performed on a BD LSRFortessa™ cell analyzer (Becton Dickinson) with data analyzed using FlowJo software (Tree Star). For cell-surface labelling, single-cell suspensions were incubated for 20 min at 4 °C with cocktails of mAbs against CD3 (145-2C11) (Biolegend), CD69 (H1.2F3), CD90.2 (30.H12) (BD Biosciences). Mouse Lineage Cell Detection Cocktail-Biotin and Strepatvidin was purchased from Miltenyi Biotec. To detect intracellular cytokine IL-4 (eBiosciences), cell preparations were activated with PMA (Sigma-Aldrich; 10 ng/ml) and ionomycin (Sigma-Aldrich; 1 µg/ml) for 2 h before the addition of Golgi Plug (3 mM) (Becton Dickinson), to enable accumulation of intracellular proteins. Cells were then harvested and fixed for 20 min at 4 °C with 4% paraformaldehyde and subsequently permeabilized overnight at 4 °C in Perm buffer (Becton Dickinson). Intracellular IL-4 was detected using antibodies according to manufacturer's instructions (eBiosciences). State-of-the art flow cytometry analysis comprises the exclusion of autofluorescent events, dead cells and duplets.

Histological analysis

Lungs were removed and immediately fixed in 10% neutral buffered formalin (Bio-optica) for 24 h. Lungs were dehydrated, embedded in paraffin, sectioned into 3-4 µm slices and stained with Periodic Acid-Schiff (PAS), Alcian blue, or Masson's trichrome reagents (Bio-optica). Stained sections were observed using a BX51 Olympus light microscope equipped with ×4, ×20 and ×40 objective lenses, a either high-resolution DP71 camera (Olympus), and analysis image processing software (Olympus).

Cell purification and cell cultures

Lungs from C57BL/6 wild-type mice were harvested and digested with 1 mg/ml dispase (Sigma-Aldrich) in PBS washed, resuspended in prewarmed HBSS containing 0.7 mg/ml Collagenase XI (Sigma-Aldrich) and 30µg/ml DNase I (Sigma-Aldrich) and incubated at 37°C for 30 minutes for enzymatic digestion. After blocking enzymatic activity with the addition of 10% FBS, lung epithelial cells were isolated by magnetic cell sorting with CD90 Microbeads (Miltenyi Biotec). The negative fraction was seeded and only non-adherent cells were used for *in vitro* experiments. Murine enriched lung epithelial cells (1×10^6cells/well in 12-well culture plates) were incubated with 100 ng/ml rmIL-17F (R&D Systems), 100 ng/ml rmIL-17A (R&D Systems), or 50 ng/ml of rmIL-17F and 50 ng/ml of rmIL-17A, for 8 h. Murine lung epithelial cells (1×10^6cells /well in 12-well culture plates) were infected with viable resting conidia of *A. fumigatus* (1:1, cells: fungi), *P. aeruginosa* or *S. aureus* (ratio 1:100, cells: bacteria) for 8 h.

Primary HBE and ALI culture

HBE cells (Primary human bronchial epithelial cells) were obtained from lung resections of controls subject (kindly provided by L.J. Galietta, Italian Cystic Fibrosis Foundation). Polarized preparations of HBE cells were generated on the same type of Snapwell inserts as previously described[2]. In brief, cells were initially grown in flasks with LHC9/RPMI1640 serum free medium (Thermo-Fischer and Lonza, respectively) to allow the proliferation. After confluence, the cells were plated at high density on the permeable supports (500.000cells in 0.5 ml, Snapwell 3801, ~ 1 cm2, Corning). After 24hs the medium was replaced with a mixture of DMEM-Ham's F-12 medium supplemented with 2% Ultroser G (+2 mM L- Glutammine, 100 U/ml penicillin, 100 µg/ml streptomycin,Lonza) to favor the differentiation. Medium in both the apical and basolateral chambers was changed every other day. After 4-6 days the cell lines were placed in Air-Liquid-Interface (ALI) culture and the medium was changed only on basolateral compartment. The fully differentiation and polarization were obtained when the TEER reached about 800 Ω·cm2 (about 20-25days).

Maintaining iPS cells

Undifferentiated human induced pluripotent stem cells (iPSCs) iPS DF19-9-7T (WiCEll)[3] were maintained in mTESR-1 (Stemcell Technologies) media on matrigel coated tissue culture plates , according to the manufacturer's instructions.

Differentiation to Lung Organoids (LOs)

The iPSCs are differentiated into 3D-lung organoids by a three step differentiation process using modified protocol (Dye BR et al, *eLife* 2015;4:e05098 DOI: 10.7554/eLife.050). In brief: iPSCs were cultured in endoderm differentiation medium (RPMI1640 + P/S (500U/ml) + 100ng/ml Activin A and FBS with increasing concentration 0% (day 1) 0.2% (day 2) - 2% (day 3) to develop definitive endoderm. The endodermal layer is fed with foregut differentiation media daily (Advanced DMEM/F12 + N2 supplement+ B27 supplement + HEPES (15mM) + Glutamine (2.5mM) + P/S (1%) + Noggin (200ng/ml) + SB431542 (10uM)) for 4-5 days. At day 5 of foregut culture the spheroids are collected. Spheroid in matrigel are cultured using Nunc delta surface plates and fed with LO media weekly (foregut media + FGF4 (500ng/ml) + CHIR99021 (2uM) + 1% FBS). Around 15-20 days 3D-organoids are checked for expression of NKX2.1+ and FOXJ.1 and used for experiments. 10nl of the immortalized *A. fumigatus* at estimated 1 particle per cell concentration was injected into the organoids using a Sutter instruments microinjector under a stereo microscope. After triggering for 24hrs, the organoids are collected and the RNA is extracted using Qiagen RNA micro kit. The cDNA is extracted using High Capacity Rerverse Transcriptase and subsequently checked for gene expression using Taqman probes in a Roche Lightcycler 480.

ELISA and Real-time PCR

The level of murine or human cytokines and chemokines in the homogenates of lung and cell supernatants was determined by ELISA (eBioscience, R&D System and Biolegend). The detection limits of the assays were < 8 pg/ml for IL-1β, TNF-α, IL-17A and IL-22, < 4 pg/ml for IL-4, IL-5 and IL-13, < 15 pg/ml for IL-12p70, IL-17F and IFN-γ, < 30 pg/ml for IL-10, < 16 pg/ml for IL-25, < 25 pg/ml for IL-33, < 32 pg/ml for IL-9, < 20 pg/ml for MPO and < 4 ng/ml for IgE, hIL-17A: < 2pg/ml hIL-17F: < 15,5 pg/ml. Real-time PCR was performed using the iCycler iQ detection system (Bio-Rad Laboratories S.r.l. Milan, Italy) and SYBR Green chemistry (Finnzymes Oy). Cells or tissues were lysed and total RNA was extracted using RNeasy Mini Kit (QIAGEN, Milan, Italy) and reverse transcribed with Sensiscript Reverse Transcriptase (QIAGEN) according to the manufacturer's directions. The PCR primer sequences (5'-3') were as follows:

A20: AGTTGTCCCATTCGTCATTCCAGT and GCCTCATGCATGCAGCTTGTCAGT
Cxcl1: CCGCTCGCTTCTCTGTGC and CTCTGGATGTTCTTGAGGTGAATC
Cxcl2: CCAACCACCAGGCTACAG and CTTCAGGGTCAAGGCAAAC
S100a8: TCGTGACAATGCCGTCTGAACTG and TGCTACTCCTTGTGGCTGTCTTTG
S100a9: CGCAGCATAACCACCATCATC and GCCATCAGCATCATACACTCC
Lipocalin2: GGTGGTGAGTGTGGCTGAC and CCTTGGTATGGTGGCTGGTG
Cebpδ: CTGCCATGTACGACGACGAG and TTTGTGGTTGCTGTTGAAGAG
Cebpβ: CAAGCTGAGCGACGAGTACA and CAGCTGCTGCACCTTCTTCT
Traf6: CAAGTGTCGTGCCAAGTGAT and GCCCAACAGCTCCAATCC
Muc5a: CTGGACCTGGAGGTTGTATG and CAGTAGTGAGGGTTGGATGG
Il17a: GACTACCTCAACCGTTCCAC and CCTCCGCATTGACACAGC
Il17f: CCCTGGAGGATAACACTGTGAGAG and TTCCTGACCCTGGGCATTGATG
Il17rc GCCTCTCCTGCCACCTCTG and GACCACCACACGGACACG
Il33: TCCTGCCTCCCTGAGTACAT and CACCTGGTCTTGCTCTTGGT
Eotaxin GCACCCTGAAAGCCATAGTCT and ACCCACTTCTTCTTGGGGTC
Gata3: CTACCGGGTTCGGATGTAAGTCG and GTTCACACACTCCCTGCCTTCT
Foxp3: CCCAGGAAAGACAGCAACCTTTT and TTCTCACAACCAGGCCACTTG
Tbet: GGACGATCATCTGGGTCACATTGT and GCCAGGGAACCGCTTATATG

Rorc: ACAACAGCAGCAAGTGATGG and CCTGGATTTATCCCTGCTGA
hIl17f: CCTCCCCCTGGAATTACACT and TTCCTTGAGCATTGATGCAG
hIl17rc: Assay ID: Hs00994305_m1
Amplification efficiencies were validated and normalized against β-actin. The thermal profile for SYBR Green real-time PCR was at 95°C for 3 min, followed by 40 cycles of denaturation for 30 s at 95°C and an annealing/extension step of 30 sec at 60°C. Each data point was examined for integrity by analysis of the amplification plot.

Immunohistochemical labeling
Lung and trachea were removed and fixed with 10% phosphate-buffed formalin, embedded in paraffin and sectioned at 15mm. Lung and trachea sections were then incubated overnight with rabbit anti-murine polyclonal IL-17RC (Santa Cruz Biotechnology) antibodies at dilution of 1:50 followed by detection with secondary biotinylated antibodies. Cells were counterstained with hematoxylin and the images were acquired using a BX51 microscope (Olympus) equipped with 40× and 100× objective lenses and image processing software (Olympus). Quantification was performed using Cell^P Image Analysis Software (Olympus).

Western blotting
Murine lung epithelial cells were lysed in 2 × Laemmli buffer (Sigma-Aldrich) and the lysates separated on a 10% Tris/glicine SDS gel before transfer to a nitrocellulose membrane. Blots of cell lysates were incubated with rabbit anti-murine monoclonal phosphor-NF-κB (Cell Signaling Technology) followed by horseradish peroxidase-conjugated anti-rabbit IgG, as per the manufacturer's instructions (Sigma-Aldrich). Normalization was performed by probing the membrane with mouse-monoclonal anti-β actin antibody (Sigma-Aldrich). Images were acquired with LiteAblotPlus chemiluminescence substrate (Euroclone S.p.A.), using ChemiDoc XRS and Imaging system (Bio-Rad Laboratories) and quantification was achieved by densitometry image analysis using Image Lab 3.1.1 software (Bio-Rad).

SUPPLEMENTARY REFERENCES

1 Kurup, V. P. & Grunig, G. Animal models of allergic bronchopulmonary aspergillosis. *Mycopathologia* **153**, 165-177 (2002).
2 Pedemonte, N., Tomati, V., Sondo, E. & Galietta, L. J. Influence of cell background on pharmacological rescue of mutant CFTR. *Am J Physiol Cell Physiol* **298**, C866-874, doi:10.1152/ajpcell.00404.2009 (2010).
3 Yu, J. *et al.* Human induced pluripotent stem cells free of vector and transgene sequences. *Science* **324**, 797-801, doi:10.1126/science.1172482 (2009).

Article

Cell Reports

The IL-17F/IL-17RC Axis Promotes Respiratory Allergy in the Proximal Airways

Graphical Abstract

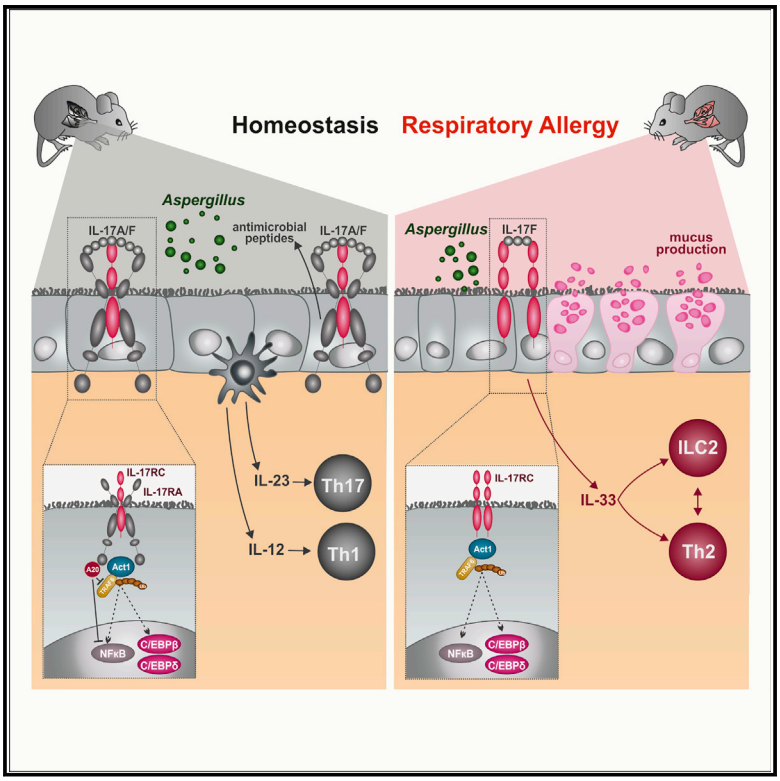

Highlights

- The IL-17F/IL-17RC axis is functional under conditions of IL-17RA deficiency
- Dysregulated signaling via IL-17RC exacerbates *Aspergillus* airway inflammation
- IL-17RC may be useful as a therapeutic target for treating respiratory allergy

Authors

Antonella De Luca, Marilena Pariano, Barbara Cellini, ..., Luigi Maiuri, Jan Fric, Teresa Zelante

Correspondence

teresa.zelante@unipg.it

In Brief

De Luca et al. reveal the complexity of IL-17 signaling in *Aspergillus* lung infection and fungal allergy. The authors describe a pathogenic loop under conditions of IL-17RA disruption and pave the way for therapeutic strategies selectively targeting the IL-17F/IL-17RC axis.

De Luca et al., 2017, Cell Reports *20*, 1667–1680
August 15, 2017 © 2017 The Author(s).
http://dx.doi.org/10.1016/j.celrep.2017.07.063

Cell Reports
Article

OPEN ACCESS
CellPress

The IL-17F/IL-17RC Axis Promotes Respiratory Allergy in the Proximal Airways

Antonella De Luca,[1] Marilena Pariano,[1] Barbara Cellini,[1] Claudio Costantini,[1] Valeria Rachela Villella,[2] Shyam Sushama Jose,[3] Melissa Palmieri,[1] Monica Borghi,[1] Claudia Galosi,[1] Giuseppe Paolicelli,[1] Luigi Maiuri,[2,4] Jan Fric,[3] and Teresa Zelante[1,5,*]
[1]Department of Experimental Medicine, University of Perugia, 06132 Perugia, Italy
[2]European Institute for Research in Cystic Fibrosis, San Raffaele Scientific Institute, Milan, Italy
[3]Center for Translational Medicine, International Clinical Research Center, St. Anne's University Hospital Brno, Czech Republic
[4]Department of Health Sciences, University of Eastern Piedmont, Novara, Italy
[5]Lead Contact
*Correspondence: teresa.zelante@unipg.it
http://dx.doi.org/10.1016/j.celrep.2017.07.063

SUMMARY

The interleukin 17 (IL-17) cytokine and receptor family is central to antimicrobial resistance and inflammation in the lung. Mice lacking IL-17A, IL-17F, or the IL-17RA subunit were compared with wild-type mice for susceptibility to airway inflammation in models of infection and allergy. Signaling through IL-17RA was required for efficient microbial clearance and prevention of allergy; in the absence of IL-17RA, signaling through IL-17RC on epithelial cells, predominantly by IL-17F, significantly exacerbated lower airway *Aspergillus* or *Pseudomonas* infection and allergic airway inflammation. In contrast, following infection with the upper respiratory pathogen *Staphylococcus aureus*, the IL-17F/IL-17RC axis mediated protection. Thus, IL-17A and IL-17F exert distinct biological effects during pulmonary infection; the IL-17F/IL-17RC signaling axis has the potential to significantly worsen pathogen-associated inflammation of the lower respiratory tract in particular, and should be investigated further as a therapeutic target for treating pathological inflammation in the lung.

INTRODUCTION

The interleukin 17 (IL-17) cytokine family is a critical component of inflammatory responses, acting on diverse cell types to induce production of pro-inflammatory cytokines, chemokines, and prostaglandins (Patel and Kuchroo, 2015). On the basis of sequence homology, a total of six IL-17 members have been described: IL-17A, IL-17B, IL-17C, IL-17D, IL-17E (also known as IL-25), and IL-17F. Of the six, IL-17A and IL-17F are best studied and most closely related. In both humans and mice, IL-17A and IL-17F can form homodimers or heterodimers (IL-17A/F) capable of ligating IL-17R subunits (Wright et al., 2007; Chang and Dong, 2007).

Signaling through IL-17R by IL-17 family members is regulated at multiple levels. The IL-17R exists as a heteromer of IL-17RA-E subunits (Moseley et al., 2003), which possess distinct biological properties and differential affinities for IL-17-family cytokines: in humans, IL-17RA binds to IL-17A with a high affinity, while IL-17RC has a high affinity for IL-17F but can also bind IL-17A (Patel and Kuchroo, 2015); in mice, IL-17RA binds both IL-17A and IL-17F, while IL-17RC binds only IL-17F (Toy et al., 2006; Krstic et al., 2015; Kuestner et al., 2007); despite having only 22% sequence homology (Haudenschild et al., 2002), the IL-17RA and IL-17RC subunits share a common ability to mediate IL-17 signaling, but disentangling the effects of signaling through each subunit has proved challenging. There is some evidence from in vitro studies that murine IL-17RA requires IL-17RC to realize its signaling potential (Toy et al., 2006), though the extent to which this is true in vivo and whether IL-17RC has a reciprocal requirement for IL-17RA remains unclear. Recent data have also uncovered a role for the intracellular ubiquitin-specific protease USP25 in negative regulation of IL-17A-mediated signaling and inflammation (Zhong et al., 2012; Ma, 2012), while earlier work found that ubiquitination of the IL-17R was triggered by IL-17F only (Rong et al., 2007). In addition, though inflammatory downstream IL-17RA signaling has been described (Conti et al., 2009), few studies have examined the potential role of IL-17RC. Thus, what is clear is that the activation of IL-17R subunits is tightly regulated; what remains unclear is how this regulation translates into significant biological effects in vivo.

The downstream effects of interactions between IL-17 and IL-17R family members are especially important for immune responses at the body's mucosal barriers: regulation of IL-17 responses is central to resolution of *Candida albicans* infection in the gut (Zelante et al., 2007; Conti and Gaffen, 2015), as well as in combating pulmonary and nasal infections (Archer et al., 2016; Rathore and Wang, 2016). However, dysregulation of the IL-17/IL-17R axis contributes to pathogenic inflammatory reactions against commensals or environmental fungi (Zelante et al., 2007), as well as to auto-immune and auto-inflammatory conditions, including asthma, psoriasis, and obesity (Endo et al., 2016; Cosmi et al., 2016; Sakkas and Bogdanos, 2016; Patel and Kuchroo, 2015), and perhaps also to cystic fibrosis (Alivand et al., 2016; McAllister et al., 2005). Of particular interest and pressing concern is the role of IL-17-mediated responses at the intersection of respiratory disease and fungal infection, such as in allergic broncho-pulmonary aspergillosis (ABPA).

This is an open access article under the CC BY-NC-ND license (http://creativecommons.org/licenses/by-nc-nd/4.0/).

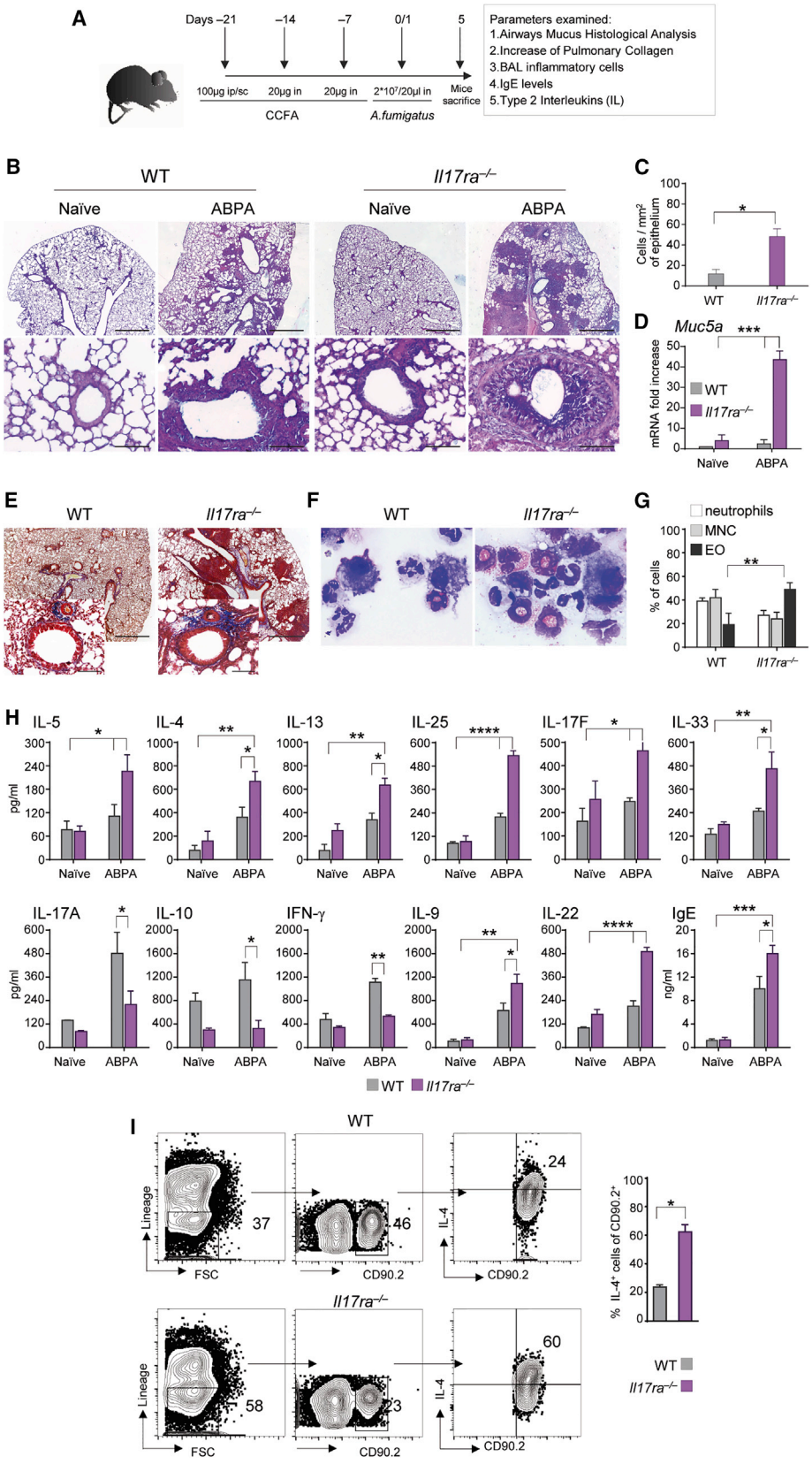

(legend on next page)

ABPA affects approximately 5 million people worldwide, causing serious recurrent respiratory impairment in immune-compromised individuals and significant exacerbations in asthma and cystic fibrosis patients (Burgel et al., 2016).

Asthma is a complex and heterogeneous disease of allergy and inflammation affecting lung functions, and there is compelling evidence for a role of the IL-17/IL-17R axis in the pathology of specific subtypes of the condition. The presence of IL-17 in asthmatic airways is significantly related to asthma severity; engineered overexpression of IL-17F results in increased inflammatory cytokine and chemokine expression and exacerbated antigen-induced goblet cell hyperplasia and pulmonary inflammation in the airways of mice (Oda et al., 2005), both hallmarks of asthma. There is also evidence that asthmatic patients express higher levels of IL-17F cytokine in the epithelial compartment compared with healthy subjects (Ota et al., 2014). A sub-group of patients with severe steroid-dependent or steroid-resistant asthma exhibit marked neutrophil recruitment and T helper 17 (Th17)-chemokine overexpression in bronchial biopsies (Fahy, 2009) and bronchoalveolar lavage (BAL) fluid (Chesné et al., 2014), sometimes with evidence of concurrent Th2 involvement (Cosmi et al., 2016). Where high levels of IL-17F, in particular, are present in the bronchial and nasal lamina propria, there is a strong association with poor lung function (Sorbello et al., 2015), but the underlying mechanisms driving IL-17-mediated exacerbation of airway inflammation remain unclear, and what, if any, role is played by IL-17 in concurrent fungal infection of these patients is unknown.

In the present study, we used genetically modified mice and models of pulmonary infection and allergy to unravel the contribution of the IL-17A/IL-17F/IL-17R pathways to microbial resistance and allergy in the lung. We found that signaling through IL-17RA was required for efficient microbial clearance and prevention of microbe-induced allergy; however, in mice lacking IL-17RA, the interaction of IL-17F with IL-17RC on epithelial cells in the upper airways contributed to inflammatory allergy, despite providing protection against local colonizers. These data shed light on the distinct roles of IL-17A and IL-17F cytokines during infection and inflammation of the lung in vivo and identify differential IL-17R subunit expression patterns within and across mucosal tissues as a potentially significant mediator of protection and pathology. Moreover, we reveal that the IL-17F/IL-17RC axis warrants further investigation as a therapeutic target for treatment of allergic inflammation of the airways.

RESULTS

Mice Lacking IL-17RA Are More Susceptible to *A. fumigatus* Infection and Allergic Inflammation

To elucidate the contribution of IL-17A or IL-17F in *Aspergillus*-induced allergic airway inflammation, we subjected wild-type (WT) and *Il17ra*$^{-/-}$ mice to experimentally induced ABPA (Figure 1A). Mice were first sensitized by injecting an adjuvanted, non-infectious mixture of *A. fumigatus* proteins and glycoproteins (crude culture filtrate antigen [CCFA]), which leads to an allergic reaction to subsequent infection with live *A. fumigatus* (Figure 1A). Alcian blue staining of lung sections indicated significant mucous cell hyperplasia in *Il17ra*$^{-/-}$ ABPA mice (Figures 1B and 1C), alongside significantly higher transcript abundance of *Muc5a* mRNA, which is associated with mucus over-production during inflammation, in *Il17ra*$^{-/-}$ ABPA mice compared with WT mice with ABPA (Figure 1D). Relative to WT mice, *Il17ra*$^{-/-}$ mice exhibited massive peri-bronchial collagen deposition (Figure 1E), significantly more BAL eosinophils (Figures 1F and 1G), and significantly higher levels of IgE protein in lung homogenates following ABPA induction (Figure 1H). Expression of type 2 cytokines (IL-5, IL-4, IL-13, IL-25, IL-33, and IL-9) and type 17 cytokines (IL-17F and IL-22) was markedly elevated in *Il17ra*$^{-/-}$ mice with ABPA compared with their naive counterparts and with WT mice as measured by ELISA (Figure 1H). Type 1 cytokine IFN-γ was downregulated in *Il17ra*$^{-/-}$ mice with ABPA as well as IL-10 (Figure 1H). Because both innate lymphoid cells type 2 (ILC2) and Th cells can expand in response to IL-33 during fungus-induced inflammation of the airways (Piehler et al., 2016), we measured the relative abundance of both these cell populations within total lung cells (Figures 1I and S1A). Lungs of *Il17ra*$^{-/-}$ mice contained higher frequencies of IL-4^{+}ILC2 (Figure 1I), IL-4^{+}CD3^{+}CD69^{+}, and IL-4^{+}CD3^{+}CD69^{-} (Figure S1A) cells during ABPA than did those of WT mice. The expansion of Th2 cells and ILC2 in the lung was further confirmed by the significantly higher abundance of *Gata3* mRNA in thoracic lymph nodes (TLNs) from *Il17ra*$^{-/-}$ mice with ABPA than in WT animals (Figure S1B). These data are consistent with published work showing that preferential expansion of IL-4^{+}ILC2 in the early phases of inflammatory responses is required to support later Th2 differentiation that is typical of asthma (Pelly et al., 2016). As expected, mRNA expression of the Th1 cytokine IFN-γ and transcription factor *Tbet* was significantly lower in *Il17ra*$^{-/-}$ mice with ABPA compared with WT; similarly, the regulatory

Figure 1. IL-17RA Deficiency Results in Higher Susceptibility to ABPA

(A) Schematic representation of ABPA model. ABPA was induced by repeated injection of mice with *A. fumigatus* culture filtrate extract dissolved in Freund's incomplete adjuvant followed by intranasal infection with resting conidia 1 week after the last injection.

(B) WT and *Il17ra*$^{-/-}$ asthmatic mice assessed for lung histology (Alcian blue staining; the scale bar represents 1 mm or 100 μm).

(C) Individual counts of lung goblet cells.

(D) Expression of *Muc5a* gene (RT-PCR) in the lung.

(E) Lung histology (Masson trichrome staining; the scale bar represents 1 mm or 100 μm in inset).

(F and G) BAL morphometry (original magnification, 100×) (F) and the differential cell count of mononuclear cells (MNC), neutrophils, and eosinophils (EO) (G) was determined on May-Grunwald Giemsa staining.

(H) IgE levels and cytokine production (ELISA) in lung homogenates.

(I) Intracellular IL-4 cytokine production was examined using flow cytometry. Flow gates indicate the percentage of CD90.2 cells producing IL-4. Pre-gate was done on total lung leukocytes; lineage marker includes anti-CD5, CD11b, CD45R, anti-7-4, anti-GR1, and anti-TER-119.

Assays were done at 5 days post-infection (dpi). Data pooled from three independent experiments (n = 6 mice per group); mean ± SD. *$p < 0.05$, **$p < 0.01$, ***$p < 0.001$, and ****$p < 0.0001$. Two-way ANOVA, Bonferroni post hoc test. Two-tailed Student's t test, nonparametric Mann-Whitney U test.

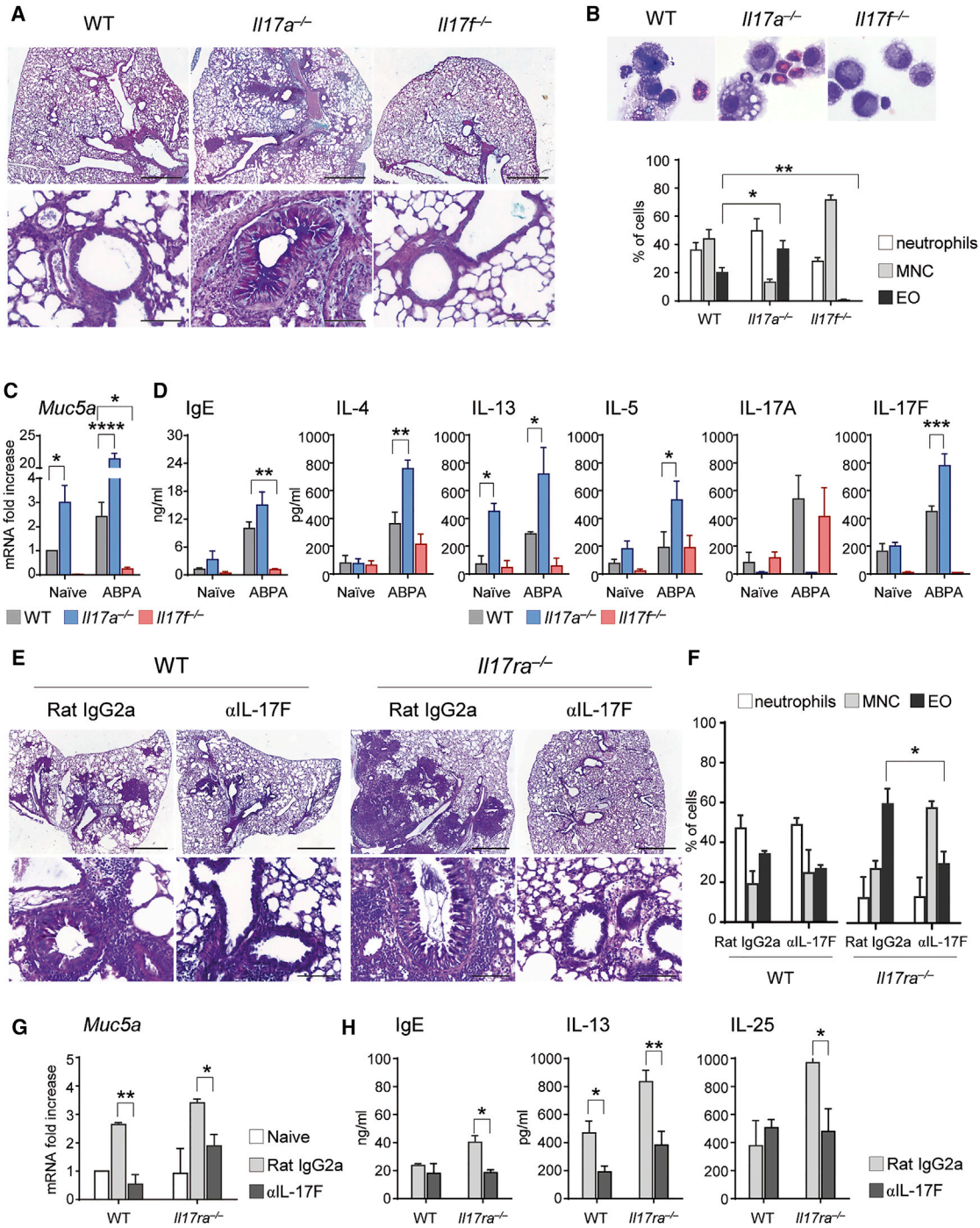

Figure 2. In ABPA, IL-17F Contributes to the Development of Allergy in IL-17RA Deficiency

(A) WT, *Il17a*$^{-/-}$, and *Il17f*$^{-/-}$ mice were sensitized and challenged with *A. fumigatus* conidia and assessed for histological analysis of Alcian blue-stained lung section (the scale bar represents 1 mm or 100 μm).

(B) BAL morphometry and differential cell count of MNC, neutrophils, and EO was determined by May-Grunwald Giemsa staining (original magnification, 100×).

(C) Expression of *Muc5a* gene (RT-PCR) in the lung.

(D) IgE levels and cytokine production (ELISA) in lung homogenates.

(E) Lung histology (Alcian blue staining; the scale bar represents 1 mm or 100 μm) of WT and *Il17ra*$^{-/-}$ asthmatic mice treated with isotype control monoclonal antibody (mAb) or IL-17F neutralizing mAb.

(F) BAL morphometry expressed as a cell percentage of mice treated as in (E).

(legend continued on next page)

cytokine IL-10 and transcription factor *Foxp3* were less abundant in *Il17ra*$^{-/-}$ mice, as was IL-17A (Figures 1H and S1B). However, despite the lack of IL-17RA, expression of genes previously identified as activated by IL-17R signaling (Conti et al., 2009) was upregulated in lung homogenates following ABPA induction (Figure S1C), although *Rorc* was not differentially expressed in *Il17ra*$^{-/-}$ mice (Figure S1B).

In summary, these data show that mice lacking the IL-17RA subunit exhibit exacerbated inflammatory responses in the lung following allergic sensitization and exposure to *A. fumigatus*; this response is characterized by excessive mucus production, aberrant collagen deposition, and the production of Th2-associated cytokines. Intriguingly, the absence of IL-17RA was associated with increased expression of IL-17R-downstream genes in ABPA. Therefore, IL-17RA is required for restraining allergic reactivity upon exposure to *A. fumigatus*, but in the absence of IL-17RA and in the context of the resultant exacerbated allergic reactivity, there is evidence of retained IL-17R signaling in these mice.

We then asked whether IL-17RA played a similar role during fungal infection of the lung as in ABPA. We previously showed that high and/or deregulated levels of IL-17A are detrimental during fungal infection (Romani et al., 2008); here we asked specifically whether mice lacking IL-17RA exhibited differential susceptibility to *Aspergillus* infection compared with WT mice. We intranasally infected *Il17ra*$^{-/-}$ mice with live *A. fumigatus* conidia and evaluated parameters of infection, inflammation and Th immunity (Figure S2A). Lungs from *Il17ra*$^{-/-}$ mice had significantly higher fungal burdens compared with WT (Figure S2B), which was associated with diffuse lung inflammation and goblet cell hyperplasia (Figure S2C), significantly higher neutrophil frequencies in BAL fluid cytospins (Figure S2D), increased mRNA expression of *Cxcl1* and *Cxcl2* in lung cells (Figure S2E), and increased MPO production from lung homogenates (Figure S2F), relative to *A. fumigatus*-infected WT mice. Protein levels of the pro-inflammatory cytokines TNF-α and IL-1β (Figure S2G), as well as IL-17F, IL-22, and IL-25, but not IL-17A (Figure S2H), were significantly more elevated in lung homogenates of *Il17ra*$^{-/-}$ mice than WT in response to *A. fumigatus* infection. In addition, type 2 cytokine and IL-9 production and *Gata3* transcription, but not *Tbet* and *Foxp3* transcription were also significantly more elevated in the lungs and TLNs, respectively, of infected IL-17RA-deficient mice (Figures S2I and S2J); taken together with the increased goblet cell mucus production (Figure S2C, inset), these findings suggesting the development of type 2 inflammation, typically characterized by Th2 adaptive response, in the airways of *Il17ra*$^{-/-}$ mice infected with *A. fumigatus*.

Considering the *A. fumigatus* infection and allergic inflammation models together, IL-17RA clearly contributes to protective antifungal responses while restraining the development of allergic lung reactivity. Mice lacking IL-17RA were also predisposed toward the production of higher levels of IL-17F and IL-25 during both ABPA (Figure 1H) and aspergillosis (Figure S2H); we therefore went on to ask what roles were played by these IL-17R-binding cytokines in experimental murine *Aspergillus* diseases.

IL-17F Contributes to Susceptibility to Infection and Allergy

Because both IL-17A and IL-17F are capable of binding to IL-17RA (Krstic et al., 2015), we used *Il17a*$^{-/-}$ and *Il17f*$^{-/-}$ mice to determine the relative contribution of each cytokine to protective IL-17RA signaling in ABPA and aspergillosis. Mice lacking IL-17A were more susceptible to ABPA, while mice lacking IL-17F were more resistant, compared with WT mice. Lung sections from *Il17a*$^{-/-}$ mice exhibited greater mucin production by goblet cells than either WT or *Il17f*$^{-/-}$ mice (Figure 2A); BAL cytospins revealed significantly higher frequencies of eosinophils in *Il17a*$^{-/-}$ mice (Figure 2B), accompanied by significantly higher spontaneous and ABPA-induced *Muc5a* mRNA expression (Figure 2C), and significantly greater production of type 2- and type 17-associated cytokines (Figure 2D) than in WT animals. In aspergillosis, we found exacerbated lung inflammatory pathology in *Il17a*$^{-/-}$ mice, compared with WT or *Il17f*$^{-/-}$ mice (Figure S3A). Accordingly, significantly greater fungal burdens were present in the lungs of *Il17a*$^{-/-}$ than in WT mice (Figure S3B), consistent with the observed attenuation in Th1-associated cytokine (IFNγ and IL-12p70) production (Figure S3C).

These results seemed to suggest that IL-17A is restraining both resistance to *Aspergillus* infection and *Aspergillus*-induced allergic responses. However, the engineered absence of IL-17A also induced significant upregulation of IL-17F expression during ABPA, while the levels of IL-17A were comparable in *Il17f*$^{-/-}$ and WT mice (Figure 2D). The same pattern was evident in aspergillosis (Figure S3D). These findings posed the question: was it the absence of IL-17A per se in *Il17a*$^{-/-}$ mice, or rather the increased levels of IL-17F, that was responsible for their increased susceptibility to *Aspergillus* diseases? We thus treated WT and *Il17ra*$^{-/-}$ mice bearing ABPA or WT and *Il17a*$^{-/-}$ bearing *Aspergillus* infection with IL-17F-neutralizing or isotype-matched control antibodies; neutralization of IL-17F induced significant reductions across all signs of mouse respiratory allergy (Figures 2E–2H), lung inflammation, and fungal colonization (Figures S3E and S3F) in infection, indicative of a pathogenic role for IL-17F in these models of *Aspergillus* allergy and infection. However, despite the high susceptibility of *Il17a*$^{-/-}$ mice to *A. fumigatus*, IL-17A administration greatly increased, while its ablation decreased, the susceptibility of WT mice to the infection (Figures S3G and S3H); conversely, the administration of IL-17F greatly exacerbated pathogenesis in WT and *Il17f*$^{-/-}$ mice bearing ABPA (Figures 3A–3D).

Taken together these findings confirm both that deregulated IL-17A production can contribute to pathology during infection (Romani et al., 2008) and that, consistent with the association of the *Il17f* gene with asthma and chronic obstructive pulmonary

(G) Expression of *Muc5a* gene (RT-PCR) in the lung.

(H) IgE levels and cytokines production (ELISA) in lung homogenates.

Assays were done at 5 dpi. Data pooled from three independent experiments (A–D, n = 6 mice per group; E–H, n = 3 mice per group); mean ± SD. *$p < 0.05$, **$p < 0.01$, ***$p < 0.001$, and ****$p < 0.0001$. Two-way ANOVA, Bonferroni post hoc test.

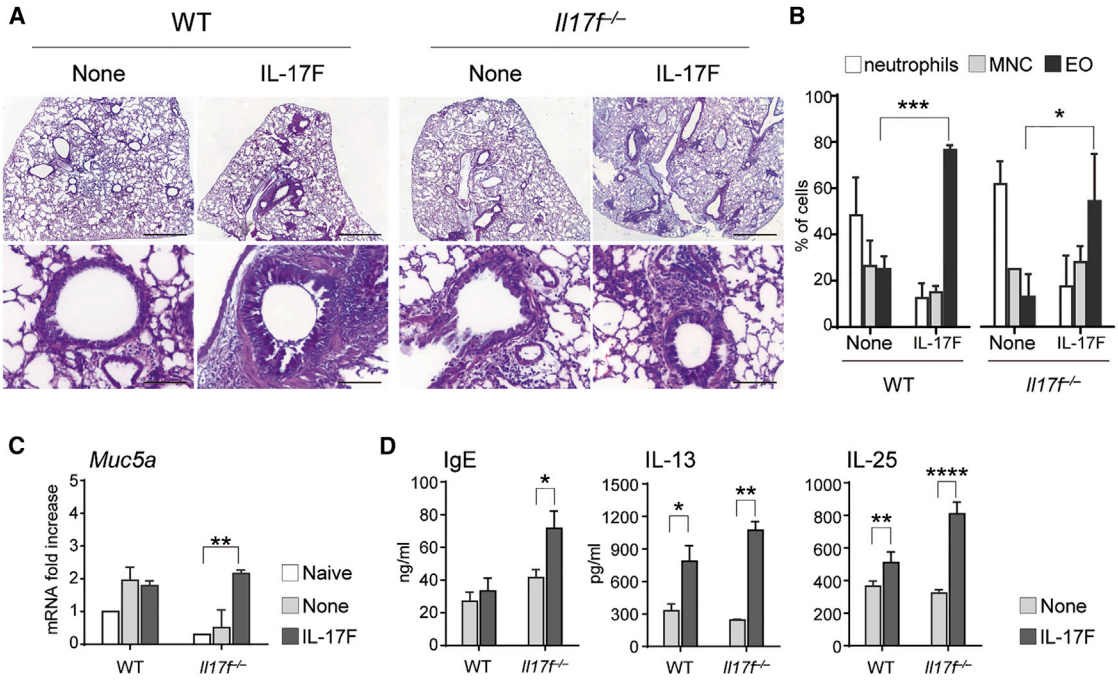

Figure 3. IL-17F Administration Exacerbates Respiratory Allergy in a Mouse Model of ABPA

(A) WT and *Il17f*$^{-/-}$ asthmatic mice were treated with murine recombinant IL-17F and assessed for histological analysis of Alcian blue-stained lung section (the scale bar represents 1 mm or 100 μm).

(B) BAL differential cell count of MNC, neutrophils, and EO.

(C) Expression of *Muc5a* gene (RT-PCR) in the lung.

(D) IgE levels and cytokines production (ELISA) in lung.

Assays were done at 5 dpi. Data pooled from three independent experiments (n = 3 mice per group); mean ± SD. *$p < 0.05$, **$p < 0.01$, ***$p < 0.001$, and ****$p < 0.0001$. Two-way ANOVA, Bonferroni post hoc test.

disease in humans (Hizawa et al., 2006), IL-17F plays a major role in driving pathological inflammation and allergy in response to *Aspergillus* in the murine lung.

IL-17F Provides Antibacterial Resistance in the Upper Airways against *S. aureus*

IL-17R signaling is also critical for pulmonary neutrophil recruitment and host defense against bacteria (Tsai et al., 2013; Gu et al., 2013); therefore to understand the broader context of our findings on the roles of the IL-17/IL-17R axis in pulmonary infections we extended our investigation to include exposure to two common bacterial pathogens. We first exposed murine lung epithelial cells from *Il17ra*$^{-/-}$ and WT mice to the upper respiratory tract colonizer *S. aureus* or the lower respiratory tract colonizers *P. aeruginosa* or *A. fumigatus* in vitro (Figure 4A). Comparative gene expression analysis revealed that the pathogens induced different levels of *Il17a* and *Il17f* transcription in both WT and *Il17ra*$^{-/-}$ epithelial cells; of particular interest, in the absence of IL-17RA, significantly higher levels of IL-17A are induced by *A. fumigatus* and *P. aeruginosa* than by *S. aureus* (Figure 4A). In contrast, significantly higher levels of IL-17F are induced by pathogens of the upper airway in *Il17ra*$^{-/-}$ lung epithelial cells. We then intranasally infected WT, *Il17f*$^{-/-}$, and *Il17ra*$^{-/-}$ mice with *S. aureus* (Figures 4B–4E) or *P. aeruginosa* (Figures 4F–4I) and measured infectious and inflammatory outcomes. These data showed that *Il17ra*$^{-/-}$ mice were as resistant as WT mice to *S. aureus* infection, as shown by lung colonization and histopathology, while in contrast, susceptibility to *S. aureus* infection was significantly higher in *Il17f*$^{-/-}$ mice (Figures 4C–4E) (lung colonization mean ± SD [log colony-forming units (CFU)]: 2.7 ± 0.24 in WT mice and 3.3 ± 0.32 in *Il17f*$^{-/-}$ mice); thus, it seems that despite its exacerbatory role in *Aspergillus* diseases, IL-17F confers antimicrobial resistance to this upper airway pathogen. This is also explained by the increased expression of IL-17F in WT epithelial cells as physiological immune protective response against *S. aureus* (Figure 4A). Conversely, and similar to our observations with *A. fumigatus* infection, *Il17ra*$^{-/-}$ mice were more susceptible to *P. aeruginosa* intranasal infection than were WT animals, exhibiting significantly higher bacterial loads in the lung (Figure 4G), significantly higher frequencies of polymorphonuclear neutrophils in BAL fluid (Figures 4H and 4I), and marked histological signs of interstitial allergic inflammation (Figure 4I). *Il17f*$^{-/-}$ mice were as resistant as WT to *P. aeruginosa* colonization (Figure 4G), neutrophil recruitment (Figures 4H and 4I), and inflammation (Figure 4I). Thus, those pathogens (*A. fumigatus* and *P. aeruginosa*) that naturally induce lower levels of *Il17f* transcription seem to become more virulent in conditions in which IL-17F release is extremely high, as seen in *Il17ra*$^{-/-}$ mice during allergic or inflammatory responses, and less virulent when IL-17F is

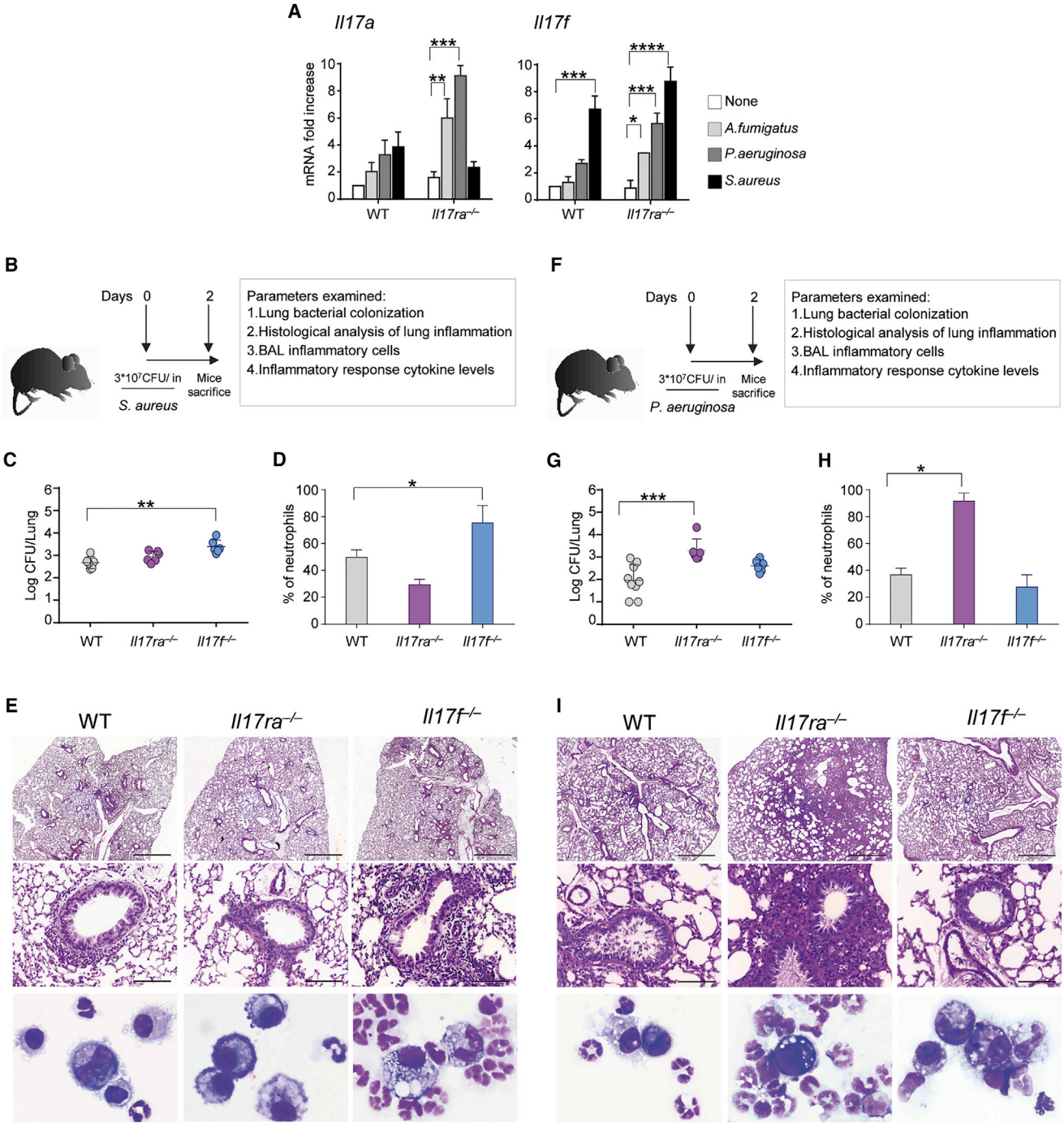

Figure 4. The IL-17F/IL17RC Pathway Provides Antibacterial Resistance in the Upper Airways

(A) Expression of *Il17a* and *Il17f* gene (RT-PCR) in WT and *Il17ra*$^{-/-}$ murine lung epithelial cells naive stimulated with live *A. fumigatus* conidia (1:1, cells/fungi), *P. aeruginosa*, or *S. aureus* (1:100, cells/bacteria) for 8 hr at 37°C.

(B) Schematic representation of *S. aureus* infection model.

(C) WT, *Il17ra*$^{-/-}$, and *Il17f*$^{-/-}$ mice were infected intranasally with live *S. aureus* and assessed for bacterial growth (log CFU).

(D) BAL morphometry, expressed as a percentage of neutrophils.

(E) Lung histology (PAS; the scale bar represents 1 mm or 100 μm) and BAL May-Grunwald Giemsa staining (original magnification, 100×).

(F) Schematic representation of *P. aeruginosa* infection model.

(G) WT, *Il17ra*$^{-/-}$, and *Il17f*$^{-/-}$ mice were infected intranasally with live *P. aeruginosa* and assessed for bacterial growth (log CFU).

(legend continued on next page)

absent, as in *Il17f*$^{-/-}$ mice. In contrast, *S. aureus*, which induces abundant *Il17f* transcription in IL-17F-competent lung epithelial cells in vitro, is rendered more virulent in the absence of IL-17F in vivo.

The IL-17F/IL-17RC Pathway in Lung Epithelial Cells Mediates Respiratory Allergy to *A. fumigatus*

The biological effects of IL-17F observed in *Il17ra*$^{-/-}$ mice led us to ask which signaling pathway was being engaged by IL-17F. Published studies show that IL-17RA only forms homodimers in the unliganded state (Kramer et al., 2006) and that both IL-17RA and IL-17RC are involved in ligand-bound IL-17R complexes (Ho et al., 2010). Given that IL-17F has a higher binding affinity for IL-17RC than IL-17RA in mice (Hu et al., 2010), we first assessed whether IL-17RC signaling was capable of mediating the downstream effects of IL-17F in conditions of IL-17RA deficiency. Comparing expression of IL-17RC protein and mRNA in epithelial cells from *A. fumigatus*-infected WT and *Il17ra*$^{-/-}$ mice revealed significant upregulation of IL-17RC in *Il17ra*$^{-/-}$ lung cells during *Aspergillus* intranasal infection (Figures 5A and 5B). In vitro, IL-17RC expression significantly increased in lung epithelial cells isolated from in *Il17ra*$^{-/-}$ mice following exposure to *A. fumigatus* and not to *P. aeruginosa* (Figure 5C), suggesting that pathogen- or fungus-specific mechanisms might be involved in driving upregulated IL-17RC expression. In addition, among the pathogens tested, only exposure to *A. fumigatus* significantly increased transcript abundance of the IL-17A or IL-17F downstream gene *Cxcl2* in *Il17ra*$^{-/-}$ epithelial cells, relative to untreated controls (Figure 5D). We also obtained a similar pattern of cytokine/cytokine receptor expression by using two different more physiological system of culture: air-liquid interface (ALI) (Figures S4A and S4B) and 3D lung organoid system of culture (Figure S4C). Further evidence that IL-17RC expressed in the context of IL-17RA deficiency was able to activate downstream signaling pathways came from detection of NF-κB phosphorylation following treatment of lung epithelial cells with IL-17A, IL-17F, or IL-17A and IL-17F (Figure 5E). In addition, a protein array analysis of murine lung epithelial cells showed that exposure to IL-17F resulted in TRAF-6-dependent phosphorylation of the IL-17R proximal signaling molecules AKT and IκBα (Figures 5F and S4D). IL-17F exposure of epithelial cells isolated from either WT or *Il17ra*$^{-/-}$ mice also resulted in significantly increased IL-33 (Figure 5G) production and of *Il17rc* expression in *Il17ra*$^{-/-}$ cells (Figure 5H). Last, in addition to NF-κB signaling IL-17RC-dependent expression of proximal signaling molecules as *Cepbβ* and *Cepbδ* transcription factors (Gaffen, 2009), which act downstream of IL-17RA proximal signaling, was evident both in vitro (Figure 5I) and in vivo (Figure 5J). These data support that following the disruption of the IL-17RA function, the remaining part of the receptor (IL-17RC) is still functional, being already demonstrated that IL-17RC may form heterodimers or homotrimers upon ligand binding (Ely et al., 2009; You et al., 2006). In this particular condition, in which IL-17RC is the only available subunit, and its expression is particularly high (Figures 5A–5C) homodimerization may eventually be favored. Therefore, we investigated whether IL-17RC, as it is lacking the distal signaling component of IL-17RA, which is essential for the activation of regulatory partners such as A20 (Garg and Gaffen, 2013), triggers a dysregulated signaling response. Thus, we exposed lung epithelial cells to IL-17A, IL-17F, or IL-17A and IL-17F (Figures 5K and 5L), and we measured *A20* expression as well as *Il33*. The results showed that only IL-17A in WT mice is able to trigger *A20* expression, while only IL-17F triggers IL-33 in IL-17RA deficiency (Figure 5L).

Thus, activation of the IL17F/IL17RC axis leadings to a positive loop because *Aspergillus* increases IL-17F expression (Figure 4A), which induces the expression of IL-33 and IL-17RC on epithelial cells, especially in IL-17RA deficiency (Figures 5G, 5H, and 5L), where A20-mediated regulation is absent (Figure 5K). In addition, IL-33 signaling is known (Hatta et al., 2017) to increase IL-17F transcription. The persistent activation of this loop may be the direct consequence of the absence of A20 induction by the IL-17RA subunits (Figure 5K).

The importance of signaling through IL-17RC in vivo was evident in both WT and *Il17ra*$^{-/-}$ mice treated with IL-17RC-specific small interfering RNA (siRNA) during ABPA induction: fungal burden (Figure 6A), inflammatory pathology (Figure 6B), eosinophil frequency in BAL fluid (Figure 6C), expression of *Il17f* and *Muc5a* (Figure 6D), production of IgE, and expression of type 2 cytokines (Figure 6E) were all markedly lower following treatment with *Il-17rc* siRNA, where a significant reduction of *Il17rc* expression was measured (Figure 6F). Similarly, use of IL-17RC=neutralizing antibody showed a reduction of ABPA pathogenesis (Figures S5A–S5C). Parallel reductions in severity of infection and inflammatory pathology upon IL-17RC siRNA treatment were also observed during *A. fumigatus* infections in vivo (Figures S5D–S5H). Interestingly, the reduction of *Il17f* with siRNA of IL-17RC suggests the existence of a positive loop of expression between IL-17RC and IL-17F (Figures 6D and S5G).

IL-17RC expression and IL-17F was increased on isolated tracheal cells compared with total lung cells and in naive or infected mice (Figure S6A) in IL-17RA deficiency, further confirming the preferential IL-17RC expression on epithelial cells. Interestingly, the tracheas of *Il17ra*$^{-/-}$ mice express higher levels of *Il17rc* then WT (Figure S6B).

Of interest, *Il17f* expression and *Il17rc* were also contingent upon the route of infection, with a higher degree in the intranasal than the intratracheal route of infection, particularly in *Il17ra*$^{-/-}$ mice (Figure S6C). In fact, although intratracheal infected WT mice showed a similar fungal load compared with the intranasal model of infection (Figures S2D and S6D), *Il17ra*$^{-/-}$ mice were more resistant upon intratracheal infection with *A. fumigatus* (Figures S6D and S6E) compared with the intranasal route (Figure S2D). Altogether, these results indicate that the expression of the IL-17F/IL-17RC axis in the upper airways may be contingent upon pathogen exposure. In the case of *Aspergillus*, the

(H) BAL morphometry, expressed as a percentage of neutrophils.

(I) Lung histology (PAS; the scale bar represents 1 mm or 100 μm) and BAL May-Grunwald Giemsa staining (original magnification, 100×).

Assays were done at 2 dpi. Data pooled from three independent experiments (n = 6 mice per group); mean ± SD. *$p < 0.05$, **$p < 0.01$, ***$p < 0.001$, and ****$p < 0.0001$. Two-way ANOVA, Bonferroni post hoc test.

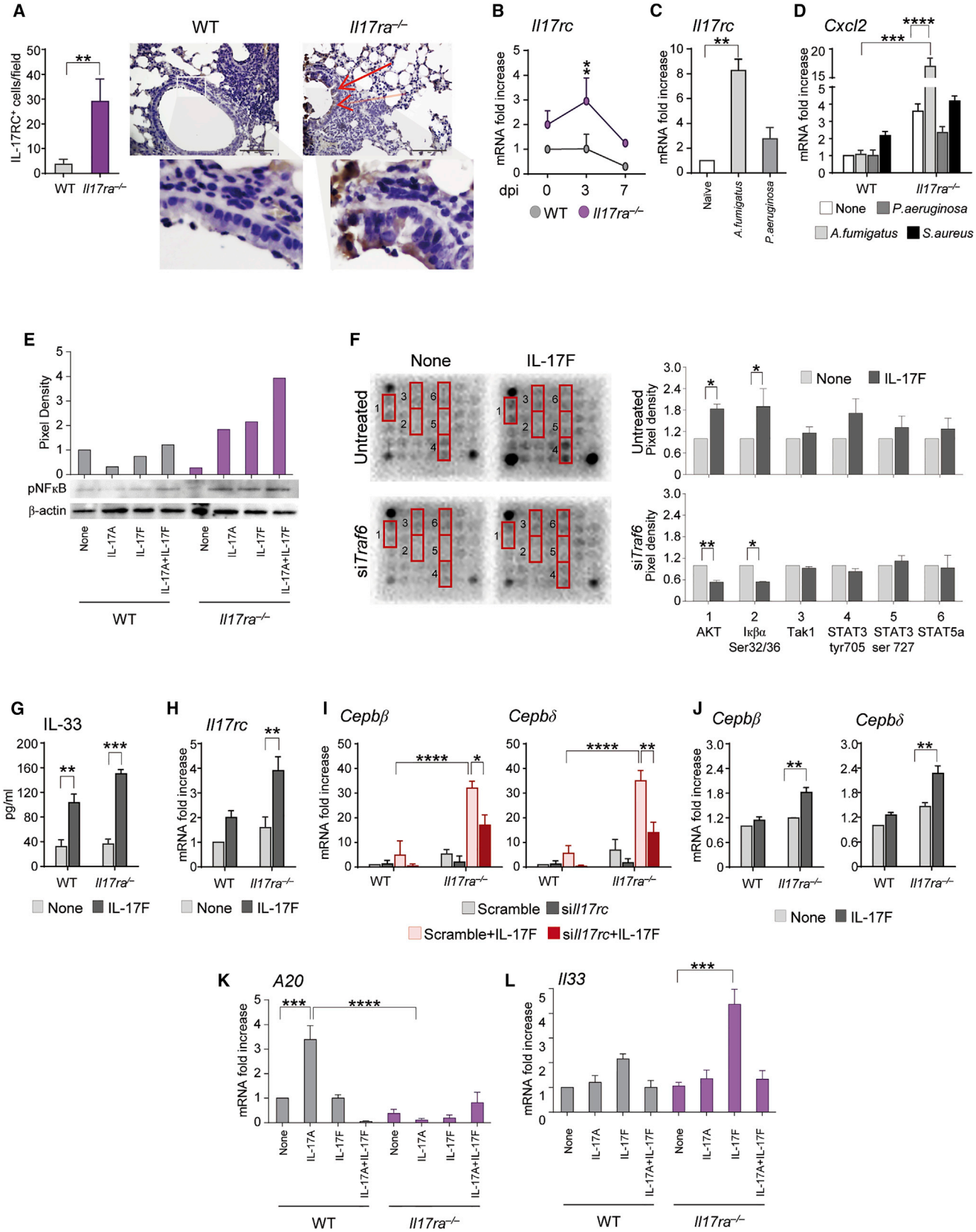

(legend on next page)

simultaneous induction of IL-17RC and IL-17F expression, the latter apparently reinforcing IL-17RC expression, points to the existence of a positive loop amplifying the allergic response to the fungus.

DISCUSSION

The complexity of the IL-17 cytokine family and its receptors shows the existence of multiple levels of regulation across space and time, designed to enable effective immunity while minimizing the risk of auto-inflammation and allergy; however, disentangling the effects of specific family members and their receptors in infection and pathologic inflammation has so far been difficult. IL-17A and IL-17F have been extensively studied in pulmonary diseases as well as in allergy (Lu et al., 2015; Fujita et al., 2012); in the case of IL-17F, there is now robust evidence of its involvement in asthma (Ota et al., 2014), with mechanistic studies uncovering induction of IL-17F production by epithelial cells in response to the Th2 cytokine IL-33, which is abundant in the asthmatic airway (Fujita et al., 2012). Our study goes on to show a plausible mechanism underlying the allergenic potential of IL-17F. By studying *Il17ra*$^{-/-}$ mice, we uncovered a pathogenic loop based on the activation of the IL-17F/IL-17RC pathway during *A. fumigatus*-linked allergy and infection; our data indicate that IL-17RA contributes to protective antifungal responses while restraining the development of allergic lung reactivity during infection; in contrast, the IL-17F/IL-17RC axis comes to predominate in conditions of IL-17RA deficiency and promotes allergy during *A. fumigatus* infection. Importantly, we have shown that exacerbation of lung pathology and allergy promotion in IL-17RA deficiency was not spontaneously developed, as the IL-17F/IL-17RC axis is induced only upon infection with specific pathogens. In addition, it can be excluded that gut or lung dysbiosis contributes to the susceptibility of *Il17ra*$^{-/-}$ mice to aspergillosis or ABPA, as naive mice do not display any spontaneous type 2 inflammation, different from atopic dermatitis as shown in double-deficient *filaggrin/Il17ra*$^{-/-}$ mice or in acute versus graft disease (Floudas et al., 2017; Varelias et al., 2017). We also observed pathogen-specific patterns of IL-17F/IL-17RC axis expression in the upper airways; *Aspergillus* and *Pseudomonas* in conditions of IL-17RA deficiency induced the simultaneous expression of IL-17RC and IL-17F, the latter apparently reinforcing IL-17RC expression, a finding highlighting the important contribution of pathogens to the generation of a positive loop amplifying the allergic response during microbial colonization and/or infection. It seems that the relative expression levels of IL-17RA and IL-17RC are key determinants of the function and overall biological activity of these cytokines in the lung: complete loss of *Il17f* resulted here in greater resistance to *A. fumigatus* infection and ABPA; likewise, silencing of IL-17RC reduced the immunopathology present in IL-17RA deficiency. These data support previous findings showing that IL-17F-deficient mice are highly resistant to acute allergic inflammation upon intranasal challenge of fungal proteinases derived from *A. oryzae* (Cheung et al., 2008). Therefore, hyperactivity of the IL-17F/IL-17RC axis can mediate allergic asthmatic disease when disruption of *Il17ra* deficiency also occurs, consistent with the increased susceptibility to fungal and bacterial infections seen in conditions of human genetic deficiency in either IL-17RA or IL-17F (Huppler et al., 2012).

It is known that IL-17RA acts as a common receptor subunit for multiple members of the IL-17 family (Ho and Gaffen, 2010), while IL-17RC recognizes only IL-17A and IL-7F (Toy et al., 2006); however, there have not been any studies on IL-17RC signaling in the absence of IL-17RA. Using *Il17ra*$^{-/-}$ mice, we provide evidence for biologically relevant IL-17RA-indepedent signaling through IL-17RC on lung epithelial cells in response to IL-17F. In our model, in infected *Il17ra*$^{-/-}$ mice, IL-17RC signaling may be due to the homodimerization of the remaining IL-17R subunit (IL-17RC), which may occur because of the increased expression of the IL-17RC subunit upon infection as well as of its ligand IL-17F. We also highlighted the potential

Figure 5. The IL-17F/IL-17RC Pathway Was Functional in IL-17RA Deficiency

(A) IL-17RC expression (stained brown) was evaluated in whole-lung tissue sections from WT and *Il17ra*$^{-/-}$ mice bearing *Aspergillus* infection at 3 dpi using immunohistochemistry. Red arrows indicate lung IL-17RC^{+} cells, quantified by individual counting at BX51 microscope (Olympus). Briefly, images were captured using bright field microscopy at 40× microscopic magnification, and the number of lung IL-17RC^{+} cells was measured in each section (n = 6 sections from ten mice per group) by an observer blinded to the treatment groups. Cell nuclei were counterstained with hematoxylin. (The scale bar represents 100 μm or 12.5 μm in insert).

(B and C) Expression of *Il17rc* gene (RT-PCR) in lung infected at 3 and 7 dpi (B) and murine lung epithelial cells, isolated from *Il17ra*$^{-/-}$ mice, stimulated with live *A. fumigatus* conidia (1:1, cells/fungi) or *P. aeruginosa* (1:100, cells/bacteria) for 8 hr at 37°C (C).

(D) Expression of *Cxcl2* gene (RT-PCR) in murine lung epithelial cells stimulated with live *A. fumigatus* conidia (1:1, cells/fungi), *P. aeruginosa*, or *S. aureus* (1:100, cells/bacteria) for 8 hr at 37°C.

(E) Phospho(p)NF-κB protein expression in murine lung epithelial cells stimulated with recombinant IL-17A and/or IL-17F. Expression of pNF-κB was normalized against the corresponding β-actin.

(F) Activation of distinct intracellular kinases in murine lung epithelial cells from naive *Il17ra*$^{-/-}$ mice using the PathScan immune cell signaling antibody array kit, exposed to 100 ng/ml IL-17F for 15 min and pretreated with specific siRNA for *Traf6*.

(G and H) ELISA of IL-33 (G) and expression of *Il17rc* gene (H) (RT-PCR) under exposure of 100 ng of IL-17F for 8 hr on murine lung epithelial cells.

(I) Expression of *Cepbβ* and *Cepbδ* genes (RT-PCR) in murine lung epithelial cells from naive WT and *Il17ra*$^{-/-}$ mice exposed to 100 ng/ml IL-17F for 8 hr and pretreated with specific siRNA for *Il17rc* or scrambled siRNA.

(J) WT and *Il17ra*$^{-/-}$ asthmatic mice were treated with murine recombinant IL-17F and assessed for expression of *Cepbβ* and *Cepbδ* genes (RT-PCR) in murine lung cells.

(K and L) Expression of *A20* (K) and *Il33* (L) genes (RT-PCR) in murine lung epithelial cells from naive WT and *Il17ra*$^{-/-}$ mice stimulated with recombinant IL-17A and/or IL-17F for 8 hr at 37°C.

Data pooled from three independent experiments (n = 6 mice per group); mean ± SD. *$p < 0.05$, **$p < 0.01$, ***$p < 0.001$, and ****$p < 0.0001$. One-way and two-way ANOVA, Bonferroni post hoc test.

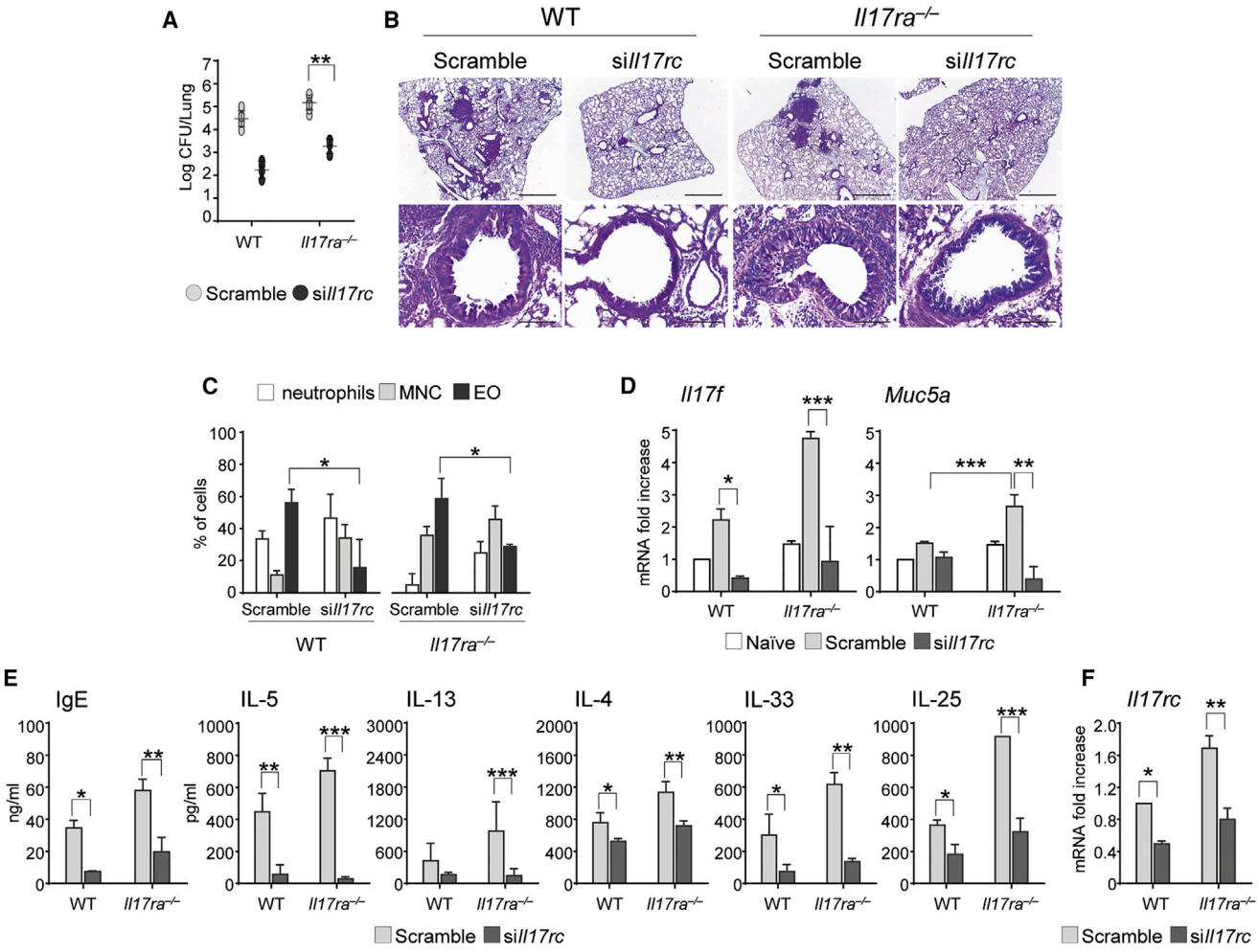

Figure 6. The IL-17F/IL-17RC Pathway Mediates Allergic Response in ABPA

(A) WT and *Il17ra*$^{-/-}$ asthmatic mice were given *Il17rc* siRNA or scrambled siRNA intranasally 1 day before and 1 and 3 days after the infection and assessed for fungal growth (log CFU).

(B) Lung histology (Alcian blue; the scale bar represents 1 mm or 100 μm).

(C) BAL morphometry expressed as percentages of MNC, neutrophils, and EO.

(D) Expression of *Il17f* and *Muc5a* genes (RT-PCR) in the lung.

(E) IgE levels and cytokines production (ELISA) in lung homogenates.

(F) Expression of *Il17rc* gene (RT-PCR) in the lung.

Assays were done at 5 dpi. Data pooled from three independent experiments (n = 3 mice per group); mean ± SD. *$p < 0.05$, **$p < 0.01$, and ***$p < 0.001$. Two-way ANOVA, Bonferroni post hoc test.

significance of compartmentalized expression of IL-17R subunits in the airways, finding indications that the IL-17F/IL-17RC axis is more active in the upper airways rather than the lower. This may also partly explain the relative pathogen specificity of IL-17F/IL-17RC expression; it is plausibly adaptive that the IL-17F/IL-17RC pathway was both more highly induced and overtly protective against *S. aureus,* an upper respiratory tract pathogen, while the IL-17A/IL-17RA pathway was both more stimulated by, and required for protection from, *Aspergillus* diseases of the lower airways. It will be interesting in future studies to understand whether the same pattern is generalized to other pathogens of specific regions of the airways and indeed to other mucosal sites. In addition, the discovery of a pathogenic loop in conditions of IL-17RA disruption may eventually pave the way for therapeutic strategies based on the use of neutralizing antibodies. Interestingly, the most direct evidence for a role in Th17 immunity in human fungal infections comes from cases of IL-17RA or IL-17RC mutations (Ling et al., 2015; Puel et al., 2011).

Moreover, hyperexpression of *Il-17f* gene in the airway of mice has been demonstrated to increase airway neutrophilia, airway hyperreactivity, and mucus hypersecretion (Kawaguchi et al., 2009). Therefore, the use of antibodies against IL-17RC or IL-17F may have important therapeutic implications in asthma. Importantly, targeting IL-17 is an effective therapy for several specific conditions, although the clinical use revealed different

essential aspects of Th17 to be considered in therapy. Indeed, clinical trial using antibodies targeting IL-17RA (brodalumab [anti-IL-17RA]) in Crohn's disease were terminated early because of exacerbation of the disease in the treatment group (Targan et al., 2016). Also, in the context of persistent asthma, it has been demonstrated a failure in the treatment of patient with brodalumab (Busse et al., 2013). In this regard, our study highlights an important aspect of IL-17R biology, which may eventually explain the failure of targeted therapy following neutralization of IL-17RA proteins. Definitively, neutralization of IL-17RA may have a strong impact on IL-17RC signaling dysregulation.

In conclusion, IL-17F/IL-17RC axis dysregulation predisposing to allergic inflammation, as highlighted here, would argue against these therapeutics in the context of asthma, while antibodies neutralizing IL-17F may represent a better option in the future.

EXPERIMENTAL PROCEDURES

Animals

Female C57BL/6 8- to 10-week-old mice were purchased from Charles River. Homozygous female 8- to 10-week-old *Il17ra*$^{-/-}$, *Il17a*$^{-/-}$, and *Il17f*$^{-/-}$ mice on a C57BL/6 background were bred under specific pathogen-free conditions in the animal facility at the University of Perugia. The animal studies described here were performed in accordance with the Italian Approved Animal Welfare Authorization 360/2015-PR and Legislative Decree #26/2014, which provided ad hoc clearance by the Italian Ministry of Health over a 5-year period (2015–2020). Animals were assessed twice daily for physical conditions and behavior. Animals ranked as moribund were humanely euthanized by CO_2 asphyxiation.

siRNA Design and Delivery

The Integrated DNA Technologies pool duplexes of predesigned siRNA IL-17RC (MMC.RNAI.N134159.12.1) were purchased from Integrated DNA Technologies (IDT, TEMA Ricerca) and siRNA against TRAF6 from Eurofins. For in vivo studies, each mouse was lightly anesthetized by inhaled ether, then given unmodified siRNA (10 mg/kg), or equivalent doses of nonspecific control siRNA duplex, intranasally in a volume of 20 μl of duplex buffer (IDT, TEMA Ricerca). This procedure was repeated four times 1 day before the infection and on days 1, 3, and 5 after infection in the infection model; in ABPA 1 day before the infection and on days 1 and 3. For in vitro studies, specific predesigned siRNA targeting TRAF6 was transfected into murine lung epithelial cells using Lipofectamine 2000 (Invitrogen) before incubation for 24 hr at 37°C in 5% CO_2. The efficiency of gene silencing was assessed by RT-PCR at 48 hr after the last siRNA injection in total lung cells, for in vitro studies after 24 hr of culture.

Cell Signaling Array

Murine lung epithelial cells were exposed to 100 ng/ml of IL-17F for 15 min. The detection of 18 well-characterized signaling molecules when phosphorylated or cleaved was performed using the PathScan Intracellular Signaling Array Kit (Chemiluminescent Readout; Cell Signaling): cell lysate was incubated on the slide followed by application of a biotinylated detection antibody cocktail; streptavidin-conjugated HRP and LumiGLO reagent were then used to visualize the bound detection antibody by chemiluminescence. Images of the slides were captured with either a digital imaging system using ChemiDoc XRS, or the Bio-Rad imaging system (Bio-Rad) and quantification achieved by densitometry image analysis using Image Lab 3.1.1 software (Bio-Rad).

Statistical Analysis

Data are expressed as mean ± SD. Horizontal bars in figures indicate means. Statistical significance was calculated using one- or two-way ANOVA (Bonferroni post hoc test) for multiple comparisons and using a two-tailed Student's t test for single comparison. The data reported either are from one representative experiment out of three to five independent experiments (western blotting) or are pooled from three to five experiments. The in vivo groups consisted of three to six mice per group. Statistical analysis was performed with Prism 6 software (GraphPad Software).

ACCESSION NUMBERS

The accession numbers for flow cytometry data reported in this paper are Flow Repository: FR-FCM-ZY83 and FR-FCM-ZY85.

SUPPLEMENTAL INFORMATION

Supplemental Information includes Supplemental Experimental Procedures and six figures and can be found with this article online at http://dx.doi.org/10.1016/j.celrep.2017.07.063.

AUTHOR CONTRIBUTIONS

A.D.L. conducted, designed, and analyzed experiments. M. Pariano did immunohistochemistry and western blotting. B.C. and C.C. revised the manuscript and performed data analysis. V.R.V. and L.M. performed and designed ALI experiments. S.S.J. and J.F. designed and performed experiments with lung organoids. M. Palmieri conducted bacterial infection experiments. M.B. performed histological analysis. C.G. and G.P. analyzed qPCR data. T.Z. wrote the manuscript and coordinated the project.

ACKNOWLEDGMENTS

This study was supported by an Italian grant funded by the Italian Cystic Fibrosis Research Foundation (Research Project FFC#22/2014), the Specific Targeted Research Project FunMeta (ERC-2011-AdG-293714), Italian grant "Programma per Giovani Ricercatori—Rita Levi Montalcini 2013," the European Social Fund, the European Regional Development Fund, Project MAGNET (CZ.02.1.01/0.0/0.0/15_003/0000492), and the European Regional Development Fund for the project Kompetenzzentrum MechanoBiologie (ATCZ133) in the Interreg V-A Austria–Czech Republic program. We thank Dr. Lucy Robinson of Insight Editing London for her assistance in the preparation of the text and Dr. Cristina Massi-Benedetti for digital art and editorial assistance.

Received: March 6, 2017
Revised: June 17, 2017
Accepted: July 23, 2017
Published: August 15, 2017

REFERENCES

Alivand, M.R., Sabouni, F., and Soheili, Z.S. (2016). Probable chemical hypoxia effects on progress of CNV through induction of promoter CpG demethylation and overexpression of IL17RC in human RPE cells. Curr. Eye Res. *41*, 1245–1254.

Archer, N.K., Adappa, N.D., Palmer, J.N., Cohen, N.A., Harro, J.M., Lee, S.K., Miller, L.S., and Shirtliff, M.E. (2016). IL-17A and IL-17F are critical for antimicrobial peptide production and clearance of *Staphylococcus aureus* nasal colonization. Infect. Immun. *84*, 3575–3583.

Burgel, P.R., Paugam, A., Hubert, D., and Martin, C. (2016). *Aspergillus fumigatus* in the cystic fibrosis lung: pros and cons of azole therapy. Infect. Drug Resist. *9*, 229–238.

Busse, W.W., Holgate, S., Kerwin, E., Chon, Y., Feng, J., Lin, J., and Lin, S.L. (2013). Randomized, double-blind, placebo-controlled study of brodalumab, a human anti-IL-17 receptor monoclonal antibody, in moderate to severe asthma. Am. J. Respir. Crit. Care Med. *188*, 1294–1302.

Chang, S.H., and Dong, C. (2007). A novel heterodimeric cytokine consisting of IL-17 and IL-17F regulates inflammatory responses. Cell Res. *17*, 435–440.

Chesné, J., Braza, F., Mahay, G., Brouard, S., Aronica, M., and Magnan, A. (2014). IL-17 in severe asthma. Where do we stand? Am. J. Respir. Crit. Care Med. *190*, 1094–1101.

Cheung, P.F., Wong, C.K., and Lam, C.W. (2008). Molecular mechanisms of cytokine and chemokine release from eosinophils activated by IL-17A, IL-17F, and IL-23: implication for Th17 lymphocytes-mediated allergic inflammation. J. Immunol. *180*, 5625–5635.

Conti, H.R., and Gaffen, S.L. (2015). IL-17-mediated immunity to the opportunistic fungal pathogen *Candida albicans*. J. Immunol. *195*, 780–788.

Conti, H.R., Shen, F., Nayyar, N., Stocum, E., Sun, J.N., Lindemann, M.J., Ho, A.W., Hai, J.H., Yu, J.J., Jung, J.W., et al. (2009). Th17 cells and IL-17 receptor signaling are essential for mucosal host defense against oral candidiasis. J. Exp. Med. *206*, 299–311.

Cosmi, L., Liotta, F., and Annunziato, F. (2016). Th17 regulating lower airway disease. Curr. Opin. Allergy Clin. Immunol. *16*, 1–6.

Ely, L.K., Fischer, S., and Garcia, K.C. (2009). Structural basis of receptor sharing by interleukin 17 cytokines. Nat. Immunol. *10*, 1245–1251.

Endo, Y., Yokote, K., and Nakayama, T. (2016). The obesity-related pathology and Th17 cells. Cell. Mol. Life Sci. *74*, 1231–1245.

Fahy, J.V. (2009). Eosinophilic and neutrophilic inflammation in asthma: insights from clinical studies. Proc. Am. Thorac. Soc. *6*, 256–259.

Floudas, A., Saunders, S.P., Moran, T., Schwartz, C., Hams, E., Fitzgerald, D.C., Johnston, J.A., Ogg, G.S., Mckenzie, A.N., Walsh, P.T., and Fallon, P.G. (2017). IL-17 receptor A maintains and protects the skin barrier to prevent allergic skin inflammation. J. Immunol. *199*, 707–717.

Fujita, J., Kawaguchi, M., Kokubu, F., Ohara, G., Ota, K., Huang, S.K., Morishima, Y., Ishii, Y., Satoh, H., Sakamoto, T., and Hizawa, N. (2012). Interleukin-33 induces interleukin-17F in bronchial epithelial cells. Allergy *67*, 744–750.

Gaffen, S.L. (2009). Structure and signalling in the IL-17 receptor family. Nat. Rev. Immunol. *9*, 556–567.

Garg, A.V., and Gaffen, S.L. (2013). IL-17 signaling and A20: a balancing act. Cell Cycle *12*, 3459–3460.

Gu, C., Wu, L., and Li, X. (2013). IL-17 family: cytokines, receptors and signaling. Cytokine *64*, 477–485.

Hatta, M., Surachmanto, E.E., Islam, A.A., and Wahid, S. (2017). Expression of mRNA IL-17F and sIL-17F in atopic asthma patients. BMC Res. Notes *10*, 202.

Haudenschild, D., Moseley, T., Rose, L., and Reddi, A.H. (2002). Soluble and transmembrane isoforms of novel interleukin-17 receptor-like protein by RNA splicing and expression in prostate cancer. J. Biol. Chem. *277*, 4309–4316.

Hizawa, N., Kawaguchi, M., Huang, S.K., and Nishimura, M. (2006). Role of interleukin-17F in chronic inflammatory and allergic lung disease. Clin. Exp. Allergy *36*, 1109–1114.

Ho, A.W., and Gaffen, S.L. (2010). IL-17RC: a partner in IL-17 signaling and beyond. Semin. Immunopathol. *32*, 33–42.

Ho, A.W., Shen, F., Conti, H.R., Patel, N., Childs, E.E., Peterson, A.C., Hernández-Santos, N., Kolls, J.K., Kane, L.P., Ouyang, W., and Gaffen, S.L. (2010). IL-17RC is required for immune signaling via an extended SEF/IL-17R signaling domain in the cytoplasmic tail. J. Immunol. *185*, 1063–1070.

Hu, Y., Ota, N., Peng, I., Refino, C.J., Danilenko, D.M., Caplazi, P., and Ouyang, W. (2010). IL-17RC is required for IL-17A- and IL-17F-dependent signaling and the pathogenesis of experimental autoimmune encephalomyelitis. J. Immunol. *184*, 4307–4316.

Huppler, A.R., Bishu, S., and Gaffen, S.L. (2012). Mucocutaneous candidiasis: the IL-17 pathway and implications for targeted immunotherapy. Arthritis Res. Ther. *14*, 217.

Kawaguchi, M., Kokubu, F., Fujita, J., Huang, S.K., and Hizawa, N. (2009). Role of interleukin-17F in asthma. Inflamm. Allergy Drug Targets *8*, 383–389.

Kramer, J.M., Yi, L., Shen, F., Maitra, A., Jiao, X., Jin, T., and Gaffen, S.L. (2006). Evidence for ligand-independent multimerization of the IL-17 receptor. J. Immunol. *176*, 711–715.

Krstic, J., Obradovic, H., Kukolj, T., Mojsilovic, S., Okic-Dordevic, I., Bugarski, D., and Santibanez, J.F. (2015). An overview of interleukin-17A and interleukin-17 receptor A structure, interaction and signaling. Protein Pept. Lett. *22*, 570–578.

Kuestner, R.E., Taft, D.W., Haran, A., Brandt, C.S., Brender, T., Lum, K., Harder, B., Okada, S., Ostrander, C.D., Kreindler, J.L., et al. (2007). Identification of the IL-17 receptor related molecule IL-17RC as the receptor for IL-17F. J. Immunol. *179*, 5462–5473.

Ling, Y., Cypowyj, S., Aytekin, C., Galicchio, M., Camcioglu, Y., Nepesov, S., Ikinciogullari, A., Dogu, F., Belkadi, A., Levy, R., et al. (2015). Inherited IL-17RC deficiency in patients with chronic mucocutaneous candidiasis. J. Exp. Med. *212*, 619–631.

Lu, S., Li, H., Gao, R., Gao, X., Xu, F., Wang, Q., Lu, G., Xia, D., and Zhou, J. (2015). IL-17A, but not IL-17F, is indispensable for airway vascular remodeling induced by exaggerated Th17 cell responses in prolonged ovalbumin-challenged mice. J. Immunol. *194*, 3557–3566.

Ma, A.I. (2012). The ubiquitous nature of IL-17. Nat. Immunol. *13*, 1034–1035.

McAllister, F., Henry, A., Kreindler, J.L., Dubin, P.J., Ulrich, L., Steele, C., Finder, J.D., Pilewski, J.M., Carreno, B.M., Goldman, S.J., et al. (2005). Role of IL-17A, IL-17F, and the IL-17 receptor in regulating growth-related oncogene-alpha and granulocyte colony-stimulating factor in bronchial epithelium: implications for airway inflammation in cystic fibrosis. J. Immunol. *175*, 404–412.

Moseley, T.A., Haudenschild, D.R., Rose, L., and Reddi, A.H. (2003). Interleukin-17 family and IL-17 receptors. Cytokine Growth Factor Rev. *14*, 155–174.

Oda, N., Canelos, P.B., Essayan, D.M., Plunkett, B.A., Myers, A.C., and Huang, S.K. (2005). Interleukin-17F induces pulmonary neutrophilia and amplifies antigen-induced allergic response. Am. J. Respir. Crit. Care Med. *171*, 12–18.

Ota, K., Kawaguchi, M., Matsukura, S., Kurokawa, M., Kokubu, F., Fujita, J., Morishima, Y., Huang, S.K., Ishii, Y., Satoh, H., and Hizawa, N. (2014). Potential involvement of IL-17F in asthma. J. Immunol. Res. *2014*, 602846.

Patel, D.D., and Kuchroo, V.K. (2015). Th17 cell pathway in human immunity: lessons from genetics and therapeutic interventions. Immunity *43*, 1040–1051.

Pelly, V.S., Kannan, Y., Coomes, S.M., Entwistle, L.J., Rückerl, D., Seddon, B., MacDonald, A.S., McKenzie, A., and Wilson, M.S. (2016). IL-4-producing ILC2s are required for the differentiation of TH2 cells following Heligmosomoides polygyrus infection. Mucosal Immunol. *9*, 1407–1417.

Piehler, D., Eschke, M., Schulze, B., Protschka, M., Müller, U., Grahnert, A., Richter, T., Heyen, L., Köhler, G., Brombacher, F., and Alber, G. (2016). The IL-33 receptor (ST2) regulates early IL-13 production in fungus-induced allergic airway inflammation. Mucosal Immunol. *9*, 937–949.

Puel, A., Cypowyj, S., Bustamante, J., Wright, J.F., Liu, L., Lim, H.K., Migaud, M., Israel, L., Chrabieh, M., Audry, M., et al. (2011). Chronic mucocutaneous candidiasis in humans with inborn errors of interleukin-17 immunity. Science *332*, 65–68.

Rathore, J.S., and Wang, Y. (2016). Protective role of Th17 cells in pulmonary infection. Vaccine *34*, 1504–1514.

Romani, L., Fallarino, F., De Luca, A., Montagnoli, C., D'Angelo, C., Zelante, T., Vacca, C., Bistoni, F., Fioretti, M.C., Grohmann, U., et al. (2008). Defective tryptophan catabolism underlies inflammation in mouse chronic granulomatous disease. Nature *451*, 211–215.

Rong, Z., Cheng, L., Ren, Y., Li, Z., Li, Y., Li, X., Li, H., Fu, X.Y., and Chang, Z. (2007). Interleukin-17F signaling requires ubiquitination of interleukin-17 receptor via TRAF6. Cell. Signal. *19*, 1514–1520.

Sakkas, L.I., and Bogdanos, D.P. (2016). Are psoriasis and psoriatic arthritis the same disease? The IL-23/IL-17 axis data. Autoimmun. Rev. *16*, 10–15.

Sorbello, V., Ciprandi, G., Di Stefano, A., Massaglia, G.M., Favatà, G., Conticello, S., Malerba, M., Folkerts, G., Profita, M., Rolla, G., and Ricciardolo, F.L. (2015). Nasal IL-17F is related to bronchial IL-17F/neutrophilia and exacerbations in stable atopic severe asthma. Allergy *70*, 236–240.

Targan, S.R., Feagan, B., Vermeire, S., Panaccione, R., Melmed, G.Y., Landers, C., Li, D., Russell, C., Newmark, R., Zhang, N., et al. (2016). A randomized, double-blind, placebo-controlled phase 2 study of brodalumab in

patients with moderate-to-severe Crohn's disease. Am. J. Gastroenterol. *111*, 1599–1607.

Toy, D., Kugler, D., Wolfson, M., Vanden Bos, T., Gurgel, J., Derry, J., Tocker, J., and Peschon, J. (2006). Cutting edge: interleukin 17 signals through a heteromeric receptor complex. J. Immunol. *177*, 36–39.

Tsai, H.C., Velichko, S., Hung, L.Y., and Wu, R. (2013). IL-17A and Th17 cells in lung inflammation: an update on the role of Th17 cell differentiation and IL-17R signaling in host defense against infection. Clin. Dev. Immunol. *2013*, 267971.

Varelias, A., Ormerod, K.L., Bunting, M.D., Koyama, M., Gartlan, K.H., Kuns, R.D., Lachner, N., Locke, K.R., Lim, C.Y., Henden, A.S., et al. (2017). Acute graft-versus-host disease is regulated by an IL-17-sensitive microbiome. Blood *129*, 2172–2185.

Wright, J.F., Guo, Y., Quazi, A., Luxenberg, D.P., Bennett, F., Ross, J.F., Qiu, Y., Whitters, M.J., Tomkinson, K.N., Dunussi-Joannopoulos, K., et al. (2007). Identification of an interleukin 17F/17A heterodimer in activated human CD4+ T cells. J. Biol. Chem. *282*, 13447–13455.

You, Z., Shi, X.B., DuRaine, G., Haudenschild, D., Tepper, C.G., Lo, S.H., Gandour-Edwards, R., de Vere White, R.W., and Reddi, A.H. (2006). Interleukin-17 receptor-like gene is a novel antiapoptotic gene highly expressed in androgen-independent prostate cancer. Cancer Res. *66*, 175–183.

Zelante, T., De Luca, A., Bonifazi, P., Montagnoli, C., Bozza, S., Moretti, S., Belladonna, M.L., Vacca, C., Conte, C., Mosci, P., et al. (2007). IL-23 and the Th17 pathway promote inflammation and impair antifungal immune resistance. Eur. J. Immunol. *37*, 2695–2706.

Zhong, B., Liu, X., Wang, X., Chang, S.H., Liu, X., Wang, A., Reynolds, J.M., and Dong, C. (2012). Negative regulation of IL-17-mediated signaling and inflammation by the ubiquitin-specific protease USP25. Nat. Immunol. *13*, 1110–1117.

Cell Reports, Volume *20*

Supplemental Information

The IL-17F/IL-17RC Axis Promotes Respiratory Allergy in the Proximal Airways

Antonella De Luca, Marilena Pariano, Barbara Cellini, Claudio Costantini, Valeria Rachela Villella, Shyam Sushama Jose, Melissa Palmieri, Monica Borghi, Claudia Galosi, Giuseppe Paolicelli, Luigi Maiuri, Jan Fric, and Teresa Zelante

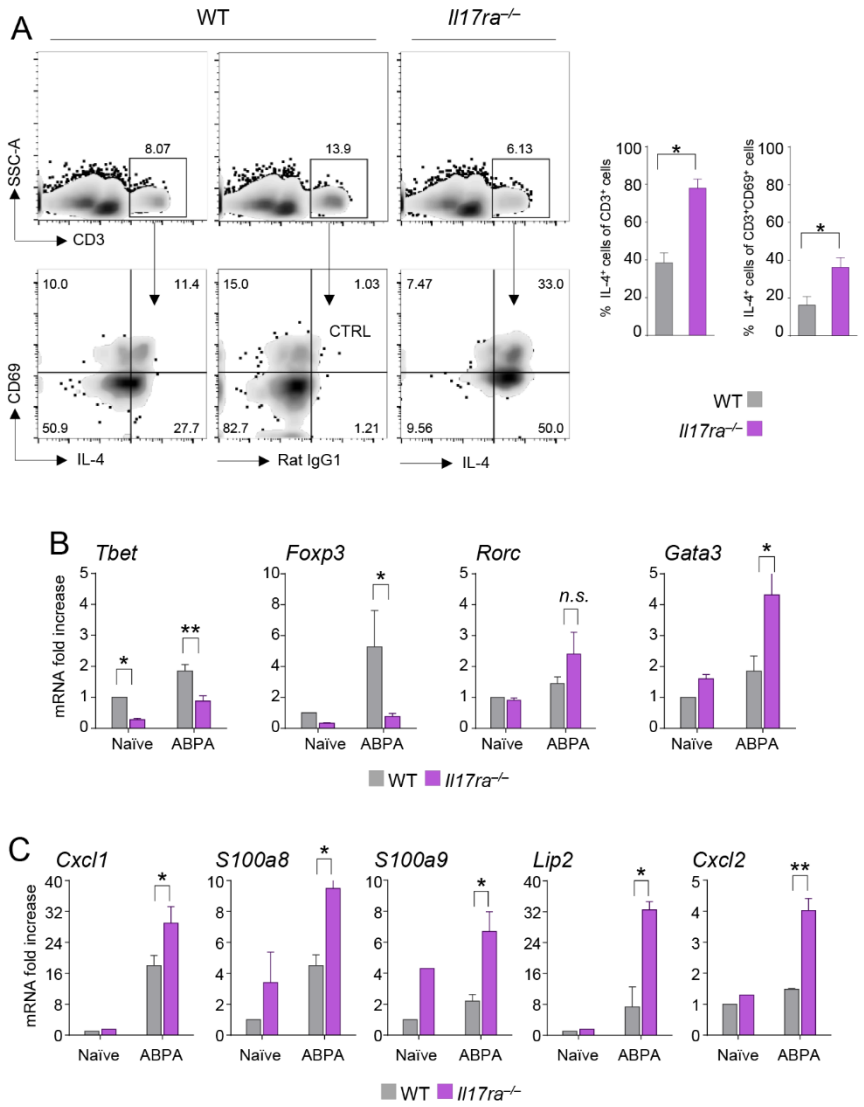

Figure S1. T-helper patterns in IL-17RA deficiency in ABPA. Related to Figure 1. A, Flow cytometry of lung and intracellular IL-4 cytokine production from WT and *Il17ra*$^{-/-}$ asthmatic mice. Flow gates indicate the percentage of CD69^{+} and CD69^{-} cells producing IL-4 on gated CD3^{+} cells. PECY7-IL-4 staining was determined using a PECY7-isotype control (CTRL) as suggested by the manufacturer. **B**, TLN relative mRNA expression assessed by RT-PCR. **C**, Lung relative mRNA expression assessed by RT-PCR. Assays were done at 5 dpi. Data pooled from three independent experiments (n = 6 mice per group); mean ± SD. *P<0.05, **P<0.01. Two-way ANOVA, Bonferroni's post hoc test.

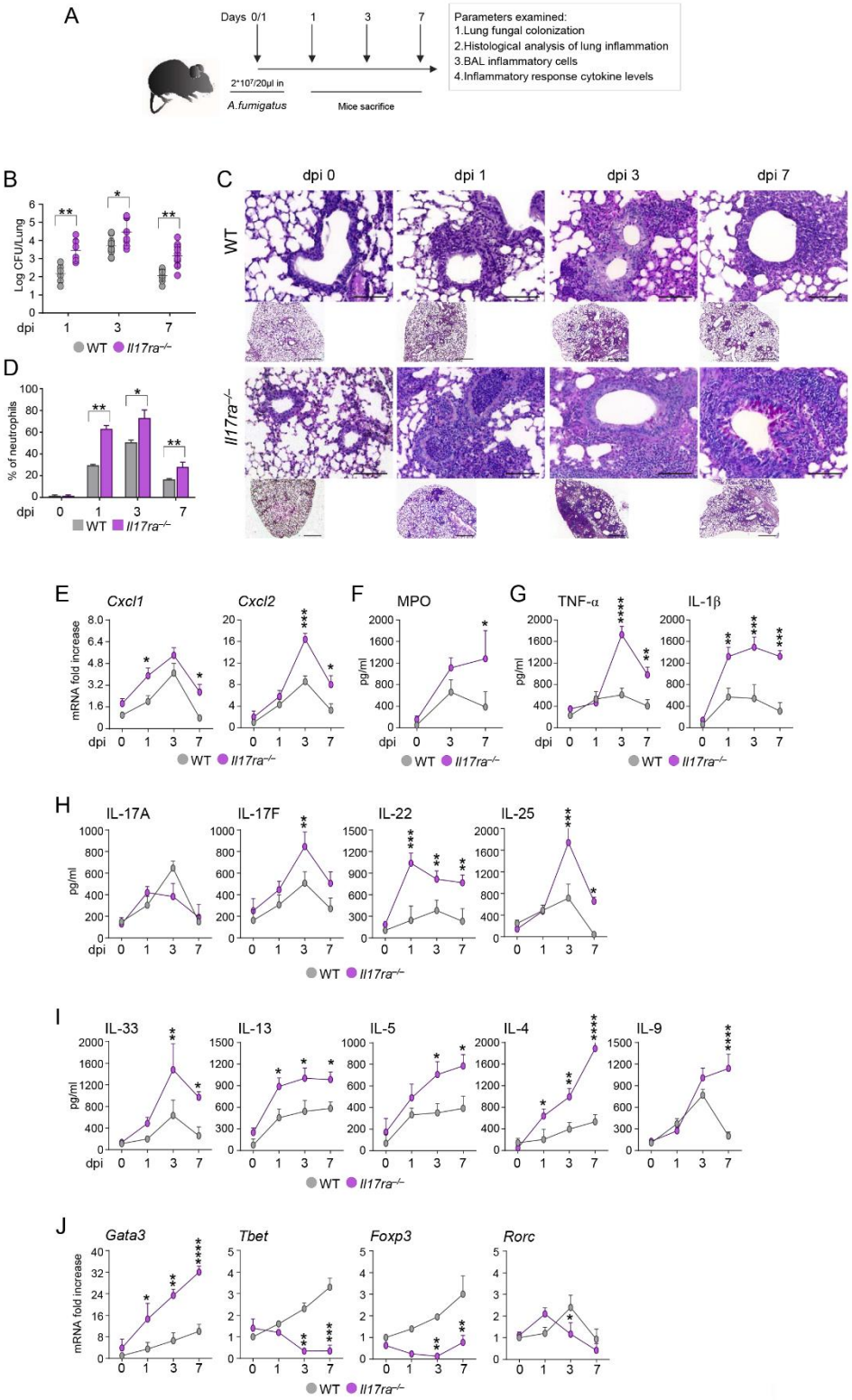

Figure S2. **IL-17RA deficiency leads to respiratory allergy during fungal infection. Related to Figure 1. A**, Schematic representation of *A. fumigatus* infection model. WT and *Il17ra*$^{-/-}$ mice were infected intranasally with live *A. fumigatus* conidia and assessed for **B**, Fungal growth (log CFU). **C**, Histological analysis of PAS-stained lung section (Scale bar 100 µm or 1 mm in inset). **D**, BAL morphometry, expresses as a percentage of neutrophils. **E-I**, Lung relative mRNA expression assessed by RT-PCR, MPO and cytokines production measured by ELISA on lung homogenates. **J**, Expression of *Gata3, Tbet, Foxp3, Rorc* gene (RT-PCR) in the TLN. Assays were done at 1, 3 and 7 dpi. Data pooled from three independent experiments (n = 6 mice per group); mean ± SD. **P*<0.05, ***P*<0.01, ****P*<0.001, *****P*<0.0001. Two-way ANOVA, Bonferroni's post hoc test.

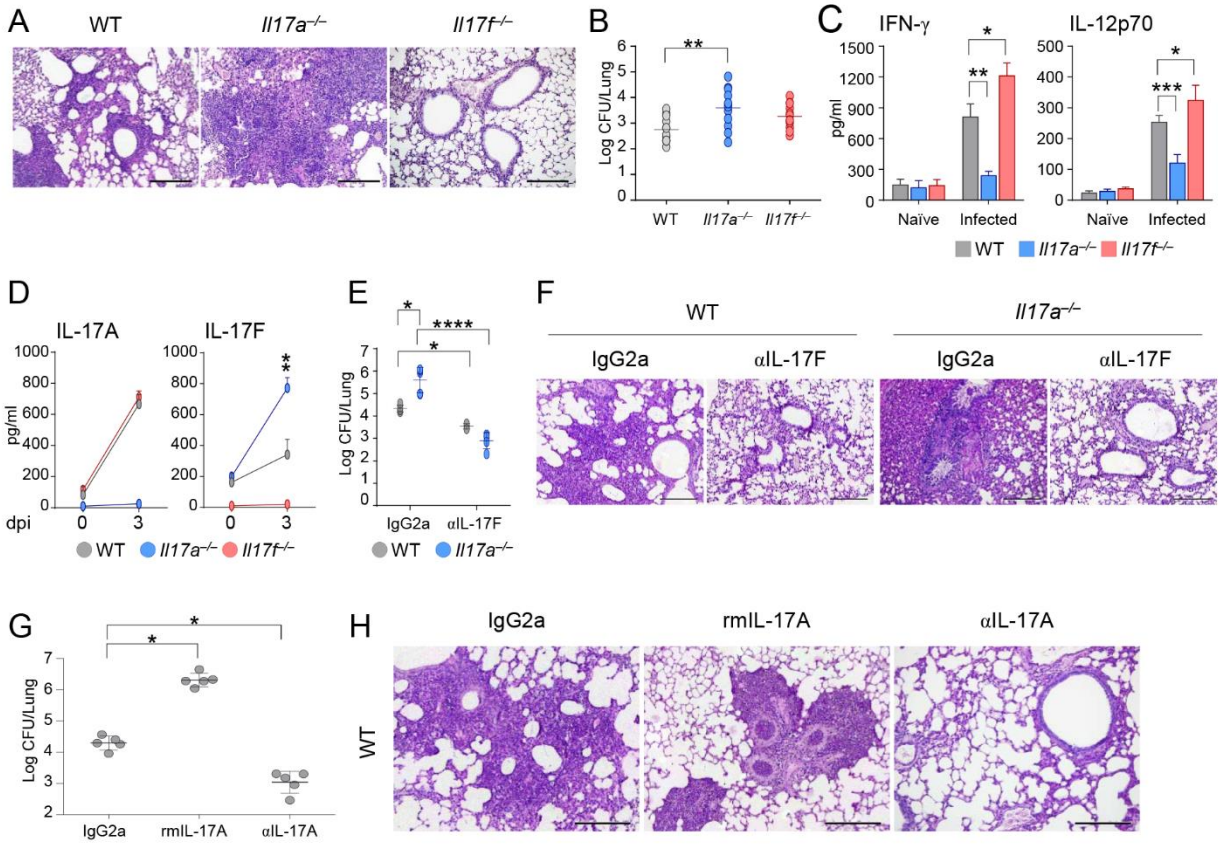

Figure S3. IL-17F contributes to susceptibility to infection. Related to Figure 2. WT, *Il17a*$^{-/-}$ and *Il17f*$^{-/-}$ mice were infected with *A. fumigatus* conidia and assessed for **A**, Histological analysis of PAS-stained lung section. (Scale bar 200 µm). **B**, Fungal growth (log CFU). **C**, ELISA in total lung homogenates at 0 and 3 dpi. **D**, IL-17A and IL-17F production (ELISA) in lung homogenates. **E-F**, Fungal growth (log CFU) in the lung (E) and lung sections from WT and *Il17ra*$^{-/-}$ *A. fumigatus*-infected mice treated with IgG2a control or anti-IL-17F blocking antibodies. (Scale bar 200 µm) (F). **G-H**, Fungal growth (log CFU) in the lung (G) and histological analysis of PAS-stained lung section from WT *A. fumigatus*-infected mice treated with IgG2a control, recombinant IL-17A or anti-IL-17A blocking antibodies (H). (Scale bar 200 µm). Assays were done at 3 dpi. Data pooled from three independent experiments (**A-D** n = 6 mice per group, **E-H** n = 3 mice per group); mean ± SD.**P*<0.05, ***P*<0.01, ****P*<0.001, *****P*<0.0001. One-way and Two-way ANOVA, Bonferroni's post hoc test.

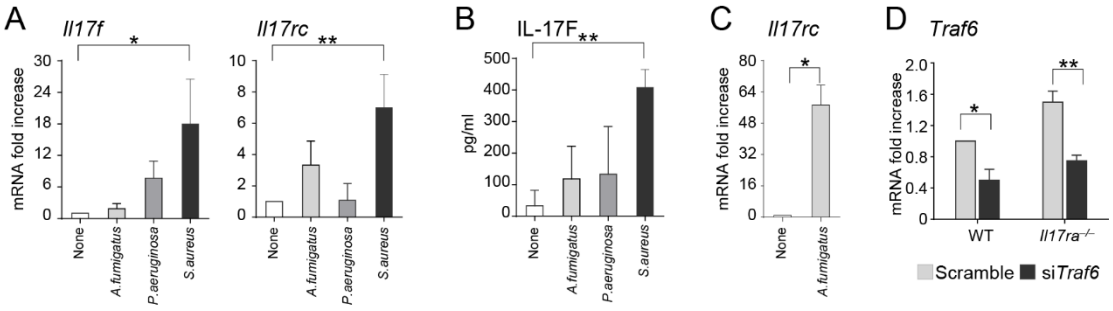

Figure S4. Pathogen differential induction of IL-17F/IL17RC axis. Related to Figure 5. A-B, Expression of *Il17f* and *Il17rc* gene (RT-PCR) (A) and production (ELISA) (B) in human bronchial epithelial cells (HBE) cultured in under ALI and stimulated with live *A. fumigatus* conidia (1:1, cells:fungi), *P. aeruginosa* or *S. aureus* (1:100, cells:bacteria) for 8 h at 37°C. **C**, Expression of *Il17rc* gene (RT-PCR) in human lung organoid stimulated with live *A. fumigatus* conidia (1:1, cells:fungi) for 8 h at 37°C. **D**, Expression of *Traf6* gene (RT-PCR) in murine lung epithelial cells from naïve WT and *Il17ra*$^{-/-}$ mice treated with specific siRNA for *Traf6* or scrambled siRNA. Data pooled from three independent experiments (n = 6 mice per group); mean ± SD. **P*<0.05, ***P*<0.01. Two-way ANOVA, Bonferroni's post hoc test.

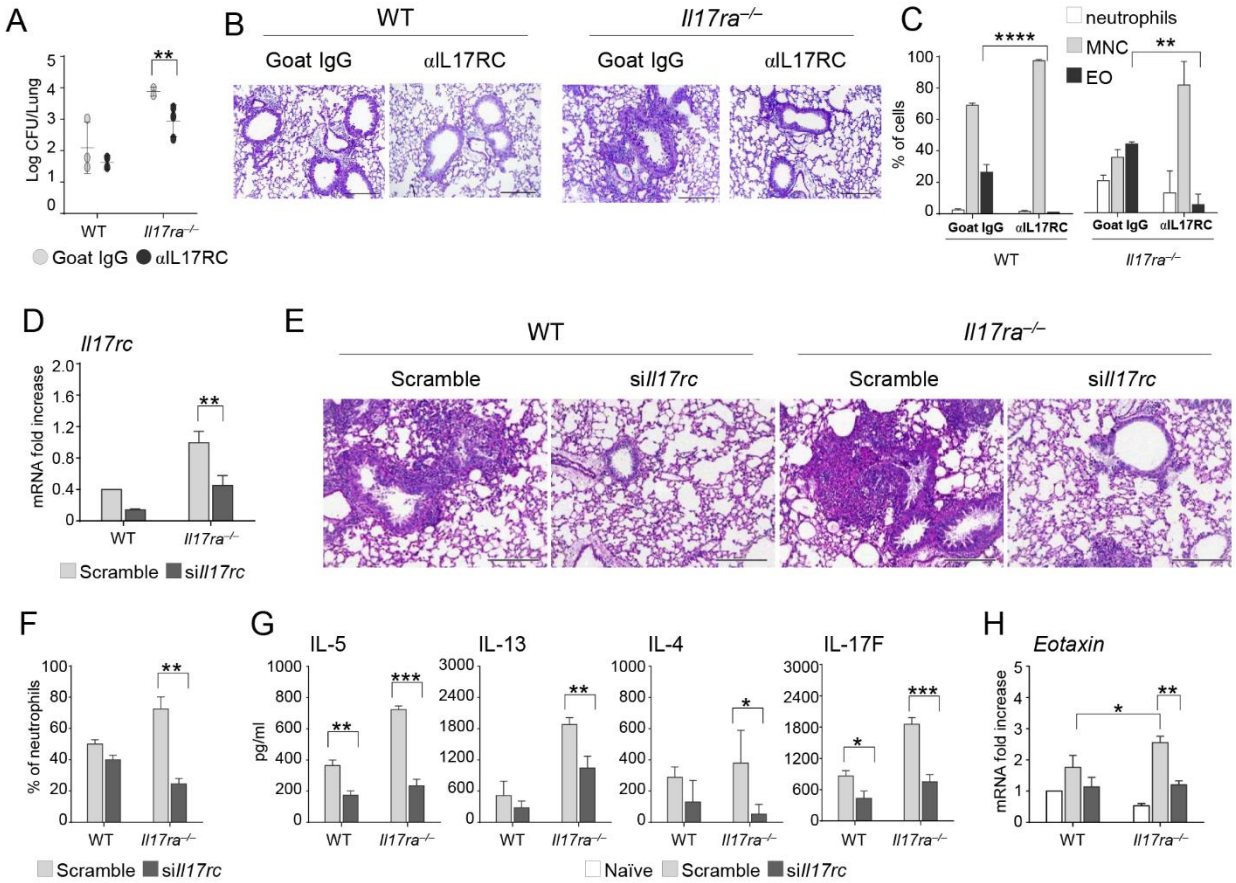

Figure S5. **IL-17F/IL-17RC pathway mediates allergic response in ABPA and to *Aspergillus* infection. Related to Figure 6.** WT and *Il17ra*$^{-/-}$ asthmatic mice were treated with isotype control mAb or IL-17RC neutralizing mAb and assessed for **A,** Fungal growth (log CFU). **B**, Lung histology (Alcian blue staining) (Scale bar 200 µm). **C**, Differential cell count of MNC, neutrophils and EOS was determined on May-Grunwald Giemsa staining. Assays were done at 5 dpi. WT and *Il17ra*$^{-/-}$ mice were infected with *A. fumigatus* conidia and were treated with specific *Il17rc* siRNA or scrambled siRNA intranasally 1 day before and 1,3 and 5 dpi and assessed for **D**, Expression of *Il17rc* gene (RT-PCR) in lung. **E**, Lung histology (PAS). (Scale bar 200 µm). **F**, BAL morphometry expressed as percentage of neutrophils. **G**, Cytokine production (ELISA); **H**, Expression of *Eotaxin* gene (RT-PCR) on lung. Assays were done at 5 or 7 dpi. Data pooled from three independent experiments (n = 6 mice per group); mean ± SD. *P<0.05, **P<0.01, ***P<0.001, ****P<0.001. Two-way ANOVA, Bonferroni's post hoc test.

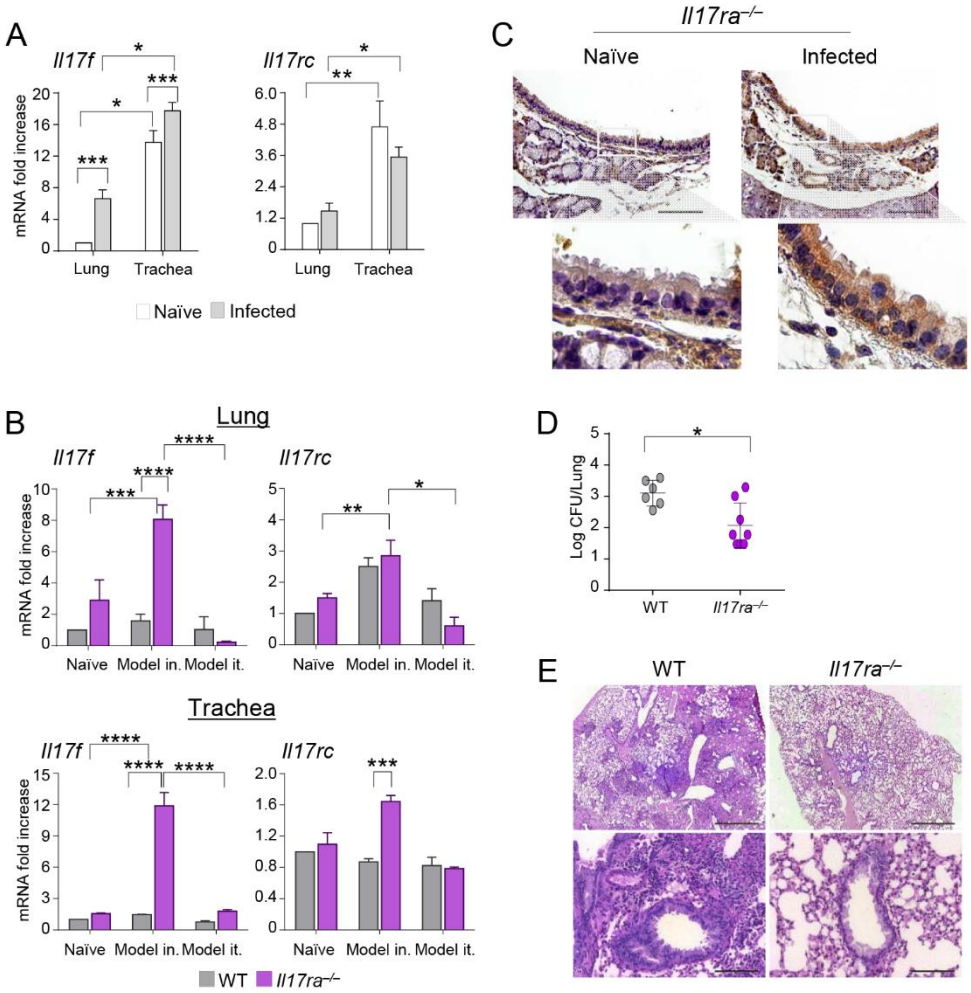

Figure S6. Intranasal and intratracheal route of infection differently activate the IL-17F/IL-17RC pathway upon fungal infection. Related to Figure 6. A, Gene expression (RT-PCR) in the lung and tracheal cells from naïve or intranasally infected *Il17ra*$^{-/-}$ mice with live *A. fumigatus* conidia at 3dpi. **B**, Gene expression (RT-PCR) in lung and trachea total cells of mice intranasally (i.n.) or intratracheally (i.t.) infected with live *A. fumigatus* conidia at 3 dpi. **C**, IL-17RC expression (stained brown) was evaluated in trachea tissue sections from *Il17ra*$^{-/-}$ mice at 3 dpi mice using immunohistochemistry. Cell nuclei were counterstained with haematoxylin. (Scale bar 100 µm or 12.5 µm in insert). **D**, Fungal growth (log CFU) and **E**, Lung PAS staining from mice it. infected with live *A. fumigatus* conidia at 3 dpi.(Scale bar 1 mm or 100 µm). Data pooled from three independent experiments (n = 6 mice per group); mean ± SD. **P*<0.05, ***P*<0.01, ****P*<0.001, *****P*<0.001. Two-way ANOVA, Bonferroni's post hoc test. Two tailed Student's, unparametric Mann-Whitney.

SUPPLEMENTARY METHODS

Infections, allergy, microbial colonization

Mice were anesthetized by intraperitoneal (i.p.) injection of 2.5% Avertin (Sigma Chemicals Co, St. Louis, MO) before intranasal instillation of 2×10^7 *A. fumigatus* (strain Af293, ATCC) resting conidia per 20µl of saline for two consecutive days, or intra-tracheal instillation of 5×10^7 resting conidia. To induce ABPA,[1] mice were sensitized by first an i.p. and then subsequently by a subcutaneous (s.c.) injection of 100 µg of *A. fumigatus* culture filtrate extract (CCFA) dissolved in incomplete Freund's adjuvant (Sigma-Aldrich) followed by two intranasal instillations, separated by two weeks, of 20 µg of CCFA in PBS. One week after the second intranasal instillation, mice received 2×10^7 resting conidia intranasally, and were evaluated for infection and immunological parameters 1 week later. For *S. aureus* and *Pseudomonas aeruginosa* infections, clinical *S. aureus* and *P. aeruginosa* strains, isolated from a patient, were obtained from the Diagnostic Unit of Microbiology from the University of Perugia. Bacteria were incubated for 3 h to establish the exponential growth phase; bacteria were then pelleted by centrifugation (2700 × g, 15 min), washed twice with sterile PBS and their density adjusted by spectrophotometry at 600 nm. The intended number of colony-forming units (CFU) was extrapolated from a standard growth curve. Appropriate dilutions with sterile PBS were made to prepare the inocula before intranasal instillation of 3×10^7 CFU/mouse. At the specified timepoints mice were assessed for microbial load (expressed as $\log_{10}$ CFU, mean ± SD) and infection-related changes to normal histology.

In vivo treatments

Mice were injected i.p. daily, from the first day of the infection up to 2 days after the infection, or 3 days after infection in the ABPA model. Doses used were: 2.5 mg/kg of anti-IL-17A, anti-IL-17F, anti-IL-17RC (R&D System). Control mice received isotype-matched control rat IgG2a or goat IgG respectively. Cytokine doses used were: 0.5 µg/mouse of recombinant murine IL-17A (rmIL-17) and IL-17F (rmIL-17F) (R&D System), all dissolved in sterile PBS. Control mice received cytokine vehicle.

Bronchoalveolar lavage

BAL was performed on sacrificed animals by cannulating the trachea and washing the airways with PBS to collect the BAL fluid. Differential cell counts were generated on BAL smears stained with May-Grünwald Giemsa reagents (Sigma-Aldrich) observed using a BX51 microscope equipped with a high-resolution DP71 camera (Olympus).

Flow cytometry

Flow cytometry was performed on a BD LSRFortessa™ cell analyzer (Becton Dickinson) with data analyzed using FlowJo software (Tree Star). For cell-surface labelling, single-cell suspensions were incubated for 20 min at 4 °C with cocktails of mAbs against CD3 (145-2C11) (Biolegend), CD69 (H1.2F3), CD90.2 (30.H12) (BD Biosciences). Mouse Lineage Cell Detection Cocktail-Biotin and Strepatvidin was purchased from Miltenyi Biotec. To detect intracellular cytokine IL-4 (eBiosciences), cell preparations were activated with PMA (Sigma-Aldrich; 10 ng/ml) and ionomycin (Sigma-Aldrich; 1 µg/ml) for 2 h before the addition of Golgi Plug (3 mM) (Becton Dickinson), to enable accumulation of intracellular proteins. Cells were then harvested and fixed for 20 min at 4 °C with 4% paraformaldehyde and subsequently permeabilized overnight at 4 °C in Perm buffer (Becton Dickinson). Intracellular IL-4 was detected using antibodies according to manufacturer's instructions (eBiosciences). State-of-the art flow cytometry analysis comprises the exclusion of autofluorescent events, dead cells and duplets.

Histological analysis

Lungs were removed and immediately fixed in 10% neutral buffered formalin (Bio-optica) for 24 h. Lungs were dehydrated, embedded in paraffin, sectioned into 3-4 µm slices and stained with Periodic Acid-Schiff (PAS), Alcian blue, or Masson's trichrome reagents (Bio-optica). Stained sections were observed using a BX51 Olympus light microscope equipped with ×4, ×20 and ×40 objective lenses, a either high-resolution DP71 camera (Olympus), and analysis image processing software (Olympus).

Cell purification and cell cultures

Lungs from C57BL/6 wild-type mice were harvested and digested with 1 mg/ml dispase (Sigma-Aldrich) in PBS washed, resuspended in prewarmed HBSS containing 0.7 mg/ml Collagenase XI (Sigma-Aldrich) and 30µg/ml DNase I (Sigma-Aldrich) and incubated at 37°C for 30 minutes for enzymatic digestion. After blocking enzymatic activity with the addition of 10% FBS, lung epithelial cells were isolated by magnetic cell sorting with CD90 Microbeads (Miltenyi Biotec). The negative fraction was seeded and only non-adherent cells were used for *in vitro* experiments. Murine enriched lung epithelial cells (1×10^6cells/well in 12-well culture plates) were incubated with 100 ng/ml rmIL-17F (R&D Systems), 100 ng/ml rmIL-17A (R&D Systems), or 50 ng/ml of rmIL-17F and 50 ng/ml of rmIL-17A, for 8 h. Murine lung epithelial cells (1×10^6cells /well in 12-well culture plates) were infected with viable resting conidia of *A. fumigatus* (1:1, cells: fungi), *P. aeruginosa* or *S. aureus* (ratio 1:100, cells: bacteria) for 8 h.

Primary HBE and ALI culture

HBE cells (Primary human bronchial epithelial cells) were obtained from lung resections of controls subject (kindly provided by L.J. Galietta, Italian Cystic Fibrosis Foundation). Polarized preparations of HBE cells were generated on the same type of Snapwell inserts as previously described[2]. In brief, cells were initially grown in flasks with LHC9/RPMI1640 serum free medium (Thermo-Fischer and Lonza, respectively) to allow the proliferation. After confluence, the cells were plated at high density on the permeable supports (500.000cells in 0.5 ml, Snapwell 3801, ~ 1 cm2, Corning). After 24hs the medium was replaced with a mixture of DMEM-Ham's F-12 medium supplemented with 2% Ultroser G (+2 mM L- Glutammine, 100 U/ml penicillin, 100 µg/ml streptomycin,Lonza) to favor the differentiation. Medium in both the apical and basolateral chambers was changed every other day. After 4-6 days the cell lines were placed in Air-Liquid-Interface (ALI) culture and the medium was changed only on basolateral compartment. The fully differentiation and polarization were obtained when the TEER reached about 800 Ω·cm2 (about 20-25days).

Maintaining iPS cells

Undifferentiated human induced pluripotent stem cells (iPSCs) iPS DF19-9-7T (WiCEll)[3] were maintained in mTESR-1 (Stemcell Technologies) media on matrigel coated tissue culture plates , according to the manufacturer's instructions.

Differentiation to Lung Organoids (LOs)

The iPSCs are differentiated into 3D-lung organoids by a three step differentiation process using modified protocol (Dye BR et al, *eLife* 2015;4:e05098 DOI: 10.7554/eLife.050). In brief: iPSCs were cultured in endoderm differentiation medium (RPMI1640 + P/S (500U/ml) + 100ng/ml Activin A and FBS with increasing concentration 0% (day 1) 0.2% (day 2) - 2% (day 3) to develop definitive endoderm. The endodermal layer is fed with foregut differentiation media daily (Advanced DMEM/F12 + N2 supplement+ B27 supplement + HEPES (15mM) + Glutamine (2.5mM) + P/S (1%) + Noggin (200ng/ml) + SB431542 (10uM)) for 4-5 days. At day 5 of foregut culture the spheroids are collected. Spheroid in matrigel are cultured using Nunc delta surface plates and fed with LO media weekly (foregut media + FGF4 (500ng/ml) + CHIR99021 (2uM) + 1% FBS). Around 15-20 days 3D-organoids are checked for expression of NKX2.1+ and FOXJ.1 and used for experiments. 10nl of the immortalized *A. fumigatus* at estimated 1 particle per cell concentration was injected into the organoids using a Sutter instruments microinjector under a stereo microscope. After triggering for 24hrs, the organoids are collected and the RNA is extracted using Qiagen RNA micro kit. The cDNA is extracted using High Capacity Rerverse Transcriptase and subsequently checked for gene expression using Taqman probes in a Roche Lightcycler 480.

ELISA and Real-time PCR

The level of murine or human cytokines and chemokines in the homogenates of lung and cell supernatants was determined by ELISA (eBioscience, R&D System and Biolegend). The detection limits of the assays were < 8 pg/ml for IL-1β, TNF-α, IL-17A and IL-22, < 4 pg/ml for IL-4, IL-5 and IL-13, < 15 pg/ml for IL-12p70, IL-17F and IFN-γ, < 30 pg/ml for IL-10, < 16 pg/ml for IL-25, < 25 pg/ml for IL-33, < 32 pg/ml for IL-9, < 20 pg/ml for MPO and < 4 ng/ml for IgE, hIL-17A: < 2pg/ml hIL-17F: < 15,5 pg/ml. Real-time PCR was performed using the iCycler iQ detection system (Bio-Rad Laboratories S.r.l. Milan, Italy) and SYBR Green chemistry (Finnzymes Oy). Cells or tissues were lysed and total RNA was extracted using RNeasy Mini Kit (QIAGEN, Milan, Italy) and reverse transcribed with Sensiscript Reverse Transcriptase (QIAGEN) according to the manufacturer's directions. The PCR primer sequences (5'-3') were as follows:

A20: AGTTGTCCCATTCGTCATTCCAGT and GCCTCATGCATGCAGCTTGTCAGT
Cxcl1: CCGCTCGCTTCTCTGTGC and CTCTGGATGTTCTTGAGGTGAATC
Cxcl2: CCAACCACCAGGCTACAG and CTTCAGGGTCAAGGCAAAC
S100a8: TCGTGACAATGCCGTCTGAACTG and TGCTACTCCTTGTGGCTGTCTTTG
S100a9: CGCAGCATAACCACCATCATC and GCCATCAGCATCATACACTCC
Lipocalin2: GGTGGTGAGTGTGGCTGAC and CCTTGGTATGGTGGCTGGTG
Cebpδ: CTGCCATGTACGACGACGAG and TTTGTGGTTGCTGTTGAAGAG
Cebpβ: CAAGCTGAGCGACGAGTACA and CAGCTGCTGCACCTTCTTCT
Traf6: CAAGTGTCGTGCCAAGTGAT and GCCCAACAGCTCCAATCC
Muc5a: CTGGACCTGGAGGTTGTATG and CAGTAGTGAGGGTTGGATGG
Il17a: GACTACCTCAACCGTTCCAC and CCTCCGCATTGACACAGC
Il17f: CCCTGGAGGATAACACTGTGAGAG and TTCCTGACCCTGGGCATTGATG
Il17rc GCCTCTCCTGCCACCTCTG and GACCACCACACGGACACG
Il33: TCCTGCCTCCCTGAGTACAT and CACCTGGTCTTGCTCTTGGT
Eotaxin GCACCCTGAAAGCCATAGTCT and ACCCACTTCTTCTTGGGGTC
Gata3: CTACCGGGTTCGGATGTAAGTCG and GTTCACACACTCCCTGCCTTCT
Foxp3: CCCAGGAAAGACAGCAACCTTTT and TTCTCACAACCAGGCCACTTG
Tbet: GGACGATCATCTGGGTCACATTGT and GCCAGGGAACCGCTTATATG

Rorc: ACAACAGCAGCAAGTGATGG and CCTGGATTTATCCCTGCTGA
hIl17f: CCTCCCCCTGGAATTACACT and TTCCTTGAGCATTGATGCAG
hIl17rc: Assay ID: Hs00994305_m1
Amplification efficiencies were validated and normalized against β-actin. The thermal profile for SYBR Green real-time PCR was at 95°C for 3 min, followed by 40 cycles of denaturation for 30 s at 95°C and an annealing/extension step of 30 sec at 60°C. Each data point was examined for integrity by analysis of the amplification plot.

Immunohistochemical labeling
Lung and trachea were removed and fixed with 10% phosphate-buffed formalin, embedded in paraffin and sectioned at 15mm. Lung and trachea sections were then incubated overnight with rabbit anti-murine polyclonal IL-17RC (Santa Cruz Biotechnology) antibodies at dilution of 1:50 followed by detection with secondary biotinylated antibodies. Cells were counterstained with hematoxylin and the images were acquired using a BX51 microscope (Olympus) equipped with 40× and 100× objective lenses and image processing software (Olympus). Quantification was performed using Cell^P Image Analysis Software (Olympus).

Western blotting
Murine lung epithelial cells were lysed in 2 × Laemmli buffer (Sigma-Aldrich) and the lysates separated on a 10% Tris/glicine SDS gel before transfer to a nitrocellulose membrane. Blots of cell lysates were incubated with rabbit anti-murine monoclonal phosphor-NF-κB (Cell Signaling Technology) followed by horseradish peroxidase-conjugated anti-rabbit IgG, as per the manufacturer's instructions (Sigma-Aldrich). Normalization was performed by probing the membrane with mouse-monoclonal anti-β actin antibody (Sigma-Aldrich). Images were acquired with LiteAblotPlus chemiluminescence substrate (Euroclone S.p.A.), using ChemiDoc XRS and Imaging system (Bio-Rad Laboratories) and quantification was achieved by densitometry image analysis using Image Lab 3.1.1 software (Bio-Rad).

SUPPLEMENTARY REFERENCES

1 Kurup, V. P. & Grunig, G. Animal models of allergic bronchopulmonary aspergillosis. *Mycopathologia* **153**, 165-177 (2002).
2 Pedemonte, N., Tomati, V., Sondo, E. & Galietta, L. J. Influence of cell background on pharmacological rescue of mutant CFTR. *Am J Physiol Cell Physiol* **298**, C866-874, doi:10.1152/ajpcell.00404.2009 (2010).
3 Yu, J. *et al.* Human induced pluripotent stem cells free of vector and transgene sequences. *Science* **324**, 797-801, doi:10.1126/science.1172482 (2009).